BITTER-SWEET PROGRESSION: O-GLCNACYLATION IS REQUIRED FOR MUTANT KRAS-INDUCED LUNG TUMORIGENESIS

by
Kekoa A. Taparra

A dissertation submitted to Johns Hopkins University in conformity with the requirements for the degree of Doctor of Philosophy

Baltimore, Maryland
June, 2016

© 2016 Kekoa A. Taparra
All Rights Reserved

Abstract

Lung cancer is the deadliest and most common malignancy worldwide. Tumor invasion and metastasis influence the dismal 16% overall 5-year survival. Evidence suggests that malignancies commandeer epithelial plasticity programs (*i.e.* the epithelial-mesenchymal transition [EMT]) to promote tumorigenesis, tumor progression, and metastasis. However, recent evidence suggests there may be diverse roles of EMT beyond metastasis, such as chemoresistance. Furthermore, EMT may orchestrate cancer metabolic reprogramming, engendering adaptation to environmental stress while supporting the macromolecular demand of the cancer cell's rapid proliferation. Specifically, the role of protein glycosylation in cancer is becoming of increased interest, as novel technologies are being developed to study these unique post-translational modifications. Understanding these modifications in cancer provides more insight into mechanisms of the disease, complementing our existing knowledge of the genomic and proteomic alterations of cancer.

SNAI1 and TWIST1 are two master EMT regulators and are often aberrantly overexpressed in many cancers. To investigate the role of EMT in tumorigenesis, we created novel inducible autochthonous mouse models. Our models reveal that EMT-driven mutant *Kras* mice generate tumors more rapidly than mice overexpressing mutant *Kras* alone. With these useful models, we identified significantly altered gene signatures related to metabolic reprogramming driven by the EMT. Specifically, EMT upregulates the hexosamine biosynthetic pathway (HBP) in mutant *Kras*-driven mouse lung tumors. Here we show EMT promotes flux through the HBP to promote increased total levels of

O-GlcNAcylated proteins in lung tumors *in vivo*. The role of O-GlcNAcylation in tumorigenesis has recently been gaining traction, as half of the body of literature on O-GlcNAcylation and cancer has been published in the past three years. Together, the data in this thesis suggest a novel EMT-HBP axis that elevates the levels of protein O-GlcNAcylation to accelerate mutant *Kras*-induced lung tumorigenesis and progression.

Readers

Phuoc T. Tran, M.D., Ph.D.

Fred Bunz, M.D., Ph.D.

Dissertation Committee

Phuoc T. Tran, M.D., Ph.D. (Principal Investigator)

Fred Bunz, M.D., Ph.D. (Chair)

Dean Felsher, M.D., Ph.D.

Acknowledgements

First and foremost I would like to thank my thesis advisor, Dr. Phuoc Tran. Throughout my years in Dr. Tran's lab, he demonstrated himself to be an incredibly knowledgeable leader and mentor. He provided me with so many tools to help me succeed in my academic, professional, and personal life. I can honestly say that without Dr. Tran, the academic achievements as well as my path into medical school would be non-existent. From his encouragement in the lab and the clinic, he represents a role model in my life that I strive to become in the future. Despite his young age, he has served not only as a mentor, but a fatherly figure for me, guiding my professional and personal life in the best direction possible. I cannot thank him enough for all of those times he would work with me over the phone or e-mail well beyond midnight. Although it was incredibly tough at times, Dr. Tran made it his mission to push me to become a better scientist and person and I will be indebted to him for all the life lessons he instilled in me.

In addition to having the guidance of Dr. Tran, I was absolutely fortunate to have a world expert in glycobiology by my side to help me throughout my thesis. Dr. Natasha Zachara was incredible to work with as she pushed my knowledge and got me interested in a new field beyond my comfort zone. The field of glycobiology scares away many students, including myself, however Dr. Zachara taught it to me in such a way that I became fascinated by the field and grew to love it very much. I am very grateful for all of her time and thousands of dollars' worth of reagents. Having trained under the scientist who discovered O-GlcNAcylation at Johns Hopkins three decades ago, Dr. Zachara reminded me how much of a privilege it is to train at this institution. It was incredible that early in

my research, I found the subject I wanted to study was conveniently discovered on this very campus. There literally could have been no other place for me to stumble upon this field.

I also would like to thank all my many lab mates both past and present for helping me with the technical aspects of my experiments and moral support. My lab mates, Dr. Hailun Wang and Dr. Reem Malek, in particular have been with me from the very beginning and have endured many hours answering all of my many questions. Without these two, I could not have been able to build my academic niche and life would definitely not have been as entertaining. Their friendship and camaraderie was critical to my success throughout this entire process.

Additionally, my research ideas would not have been possible without the direction of my thesis committee. Dr. Fred Bunz was there for me before I had even started my thesis project as he helped guide me during my difficult graduate board oral exam process. I am very grateful for his support and mentorship throughout the years. Dr. Dean Felsher has likewise provided great insight on my project. His depth of knowledge and keen eye for innovative science were invaluable for my research experience. I thank him for his expertise and wisdom as he also endured early morning thesis meetings via Skype in his California time zone.

I consider it a privilege to have the opportunity to train at the Johns Hopkins University School of Medicine and I am very grateful for the Cellular and Molecular Medicine PhD

Program. Thank you to Colleen Graham, Leslie Lichter, Rajni Rao and Robert Casero. Thank you for giving me the special interview day and convincing me to visit Hopkins when I couldn't make either of the two interview days. Without the personalized support, I would have missed something very special. To all my classmates, I thank them for their support over the years and for helping me when I was clueless.

I would like to thank all the members of the Radiation Oncology department for providing me the opportunity to present my work and providing new insight to my project over the years. I also would like to make a special acknowledgement and express my gratitude for the National Institutes of Health, National Cancer Institute, and the National Research Service Award (NRSA) Pre-doctoral Training Program for funding my education during my time at Hopkins.

Both in and out of the lab, I also would like to thank my partner in crime, Katie Nugent. Over the past three years we have shared so many hours together, many of which were in the lab. Katie spent endless hours genotyping and organizing the mouse colonies over the years of my research. Beyond lab we grew up together and she has taught me much about myself and has ultimately made me a better person. I can't thank her enough for all of those times she would fall asleep on the couch in CRB while I worked in lab until 3:00 AM. She made many sacrifices being by my side over the past three years and I am excited for what the future holds for the both of us. I am very proud of her as she continues to excel at Johns Hopkins University School of Nursing.

Lastly, to my mother and father, Judy and Tony Taparra, as well as my entire family, I thank them for all of the support over the years. They are the reason why I do what I do. From my early years, my parents gave me the confidence to always try my best and push myself. Along with my sister, Kiane, these three were always there with me during my ups and downs over the past four years, unconditionally supportive. Despite not really knowing what this whole PhD journey was all about, they stuck by my decision to get a PhD and provided endless encouragement and love throughout these years, as well as throughout my entire life. I am incredibly fortunate to have a big supportive family in my life. Finally, I would like to honor those loved ones in my family who fought courageously with their cancers: Baby Kaleo Shadron, Aunty Linda Wong, Aunty Janelle "AJ" Taparra, Grandma Severina Charlotte Cachola "Mitch" Tangonan, Uncle William "Boogs" Abe, Uncle Milton "Migs" Abe, Uncle Robert Abe, Uncle Steven Abe, Uncle Andrew Abe, and Uncle Henry Abe. Their courageous battles inspire me to fight on.

TABLE OF CONTENTS

LIST OF FIGURES

Chapter 1: Background and relevant literature

Chapter 2: Investigating the EMT-HBP axis in lung cancer

Chapter 1: Background and relevant literature

1.1 Introduction

The epithelial-mesenchymal transition (EMT) is a highly conserved program necessary for orchestrating distant cell migration during embryonic development. Multiple studies in cancer have demonstrated a critical role for EMT during the initial stages of tumorigenesis and later during tumor invasion. Transcription factors (TFs) such as SNAIL, TWIST, and ZEB are master EMT regulators that are aberrantly overexpressed in many malignancies. Recent evidence correlates EMT-related transcriptomic alterations with metabolic reprogramming in cancer. Metabolic alterations may allow cancer to adapt to environmental stressors, supporting the irregular demand for macromolecules during periods of rapid proliferation. One potential metabolic pathway of increasing importance is the hexosamine biosynthesis pathway (HBP). The HBP utilizes glycolytic intermediates to generate the metabolite UDP-GlcNAc. This and other charged nucleotide sugars serve as the basis for biosynthesis of glycoproteins and other glycoconjugates. Recent reports in the field of glycobiology have cultivated great curiosity within the cancer research community. However, specific mechanistic relationships between the HBP and fundamental pathways of cancer, such as EMT, have yet to be elucidated. Altered protein glycosylation downstream of the HBP is well positioned to mediate many cellular changes associated with EMT including cell-cell adhesion, responsiveness to growth factors, immune system evasion, and signal transduction programs. Here we outline some of the basics of the HBP and putative roles the HBP may have in driving EMT-related cancer processes. With novel appreciation of the connection between HBP and EMT, we hope to illuminate the potential for new

therapeutic targets of cancer.

1.2 Connecting metabolism to epithelial plasticity

1.2.1 History of glucose metabolism in cancer

Since the time of Otto Warburg in the 1930s, scientists have been intrigued by the unique metabolic profile of cancer cells [1,2]. Current research corroborates Warburg's original observation that cancer cells utilize glycolysis over mitochondrial oxidative phosphorylation (OXPHOS) [3], even when oxygen is not limiting. Initially, this metabolic reprogramming appeared paradoxical due to the inefficiencies of glycolysis (*i.e.*, ~38 ATP from OXPHOS versus 2 ATP from glycolysis). Despite early conflicting viewpoints on the Warburg Effect, aerobic glycolysis stands at the center of cancer metabolism demonstrating its importance as an "Emerging Hallmark of Cancer" [4].

Despite decades of research, the molecular advantages of the Warburg effect in cancer are still being interrogated [5]. One popular explanation is the "Glycolytic Intermediate Diversion" hypothesis [6,7]. This hypothesis suggests that glycolysis is well positioned to support anabolic cell growth as it provides the metabolic intermediates (*e.g.*, nucleosides, amino acids, and other carbon compounds) necessary for enzymatic reactions and organelle assembly. A second hypothesis involves the notion of "Cell Subpopulations" [8–10]. This hypothesis posits lactate from "Warburg-effect cells" is sent to neighboring cells, which utilize lactate through the citric acid cycle. The cell subpopulations symbiotically

trade off waste for energy to support cancer progression. Interestingly, both hypotheses demonstrate the ability of the neoplastic state to commandeer normal biological processes observed in development and normal physiology [4].

1.2.2 Cancer metabolism and glycosylation overview

The energetic demand required to survive adverse tumor environments is likely only a fraction of the functional significance underlying cancer metabolic reprogramming. It is likely that glycolytic byproducts reinforce the cancer phenotype by modulating not just metabolic maintenance, but altering other cellular structures and functions. In particular, the role of post-translational modifications (PTM), such as glycosylation, are becoming of increasing appreciation as they provide rapid, reversible adaptations to the stressors that occur during early tumorigenesis. Recent studies have revealed new potential cancer treatment strategies specifically targeting these glycoconjugates [11].

Interestingly, one metabolic pathway with the potential of impacting functional macromolecular structures in cancer is an understudied pathway called the "hexosamine biosynthetic pathway" (HBP) [12–15]. One downstream metabolite of this pathway, Uridine diphosphate *N*-acetylglucosamine (UDP-GlcNAc), serves as an essential building block for glycoconjugate biosynthesis. This pathway is well positioned to not only affect metabolic intermediates, but also functional glycans that accelerate cancer progression [11,16]. The HBP has only recently gained traction in cancer biology and is becoming of increasing importance [17].

1.2.3 Cancer epithelial plasticity overview

The epithelial-mesenchymal transition (EMT) is a conserved epithelial plasticity program capable of impacting cellular morphology, migration, stem cell-ness, among other malignant phenotypes [18]. Moreover, the EMT is involved throughout the natural history of cancer from tumorigenesis to late metastatic progression [19–21]. Master transcriptional regulators of EMT (*i.e.,* TWIST, SNAIL, and ZEB) are elevated in a wide range of primary and metastatic tumors. Recent evidence demonstrates that the expression of key enzymes in the HBP are upregulated in cancer cells with a mesenchymal phenotype [22]. Thus, in this review we will highlight some of the relevant glycoconjugates downstream of the HBP and the implications this has on EMT-mediated cancer programs.

1.3 The epithelial-mesenchymal transition (EMT)

1.3.1 EMT functions and signaling pathways

EMT is an essential epithelial plasticity program deployed during development [23,24], wound healing [25–27], and stem cell maintenance [28–31]. The major characteristics of EMT include loss of cellular adhesion, reorganization of cytoskeleton, loss of cellular polarity, and a switch from epithelial to mesenchymal patterns of gene expression [18]. Many of these EMT pathways are activated by extracellular signaling, highlighting the importance of the tumor microenvironment for the induction of EMT. **Figure 1A** outlines eight critical EMT-activating pathways: TGF-β, Receptor Tyrosine Kinases (RTKs), Integrin, WNT, NOTCH, Hedgehog (HH), Hypoxia Inducible Factor 1α (HIF1α), and JAK/STAT.

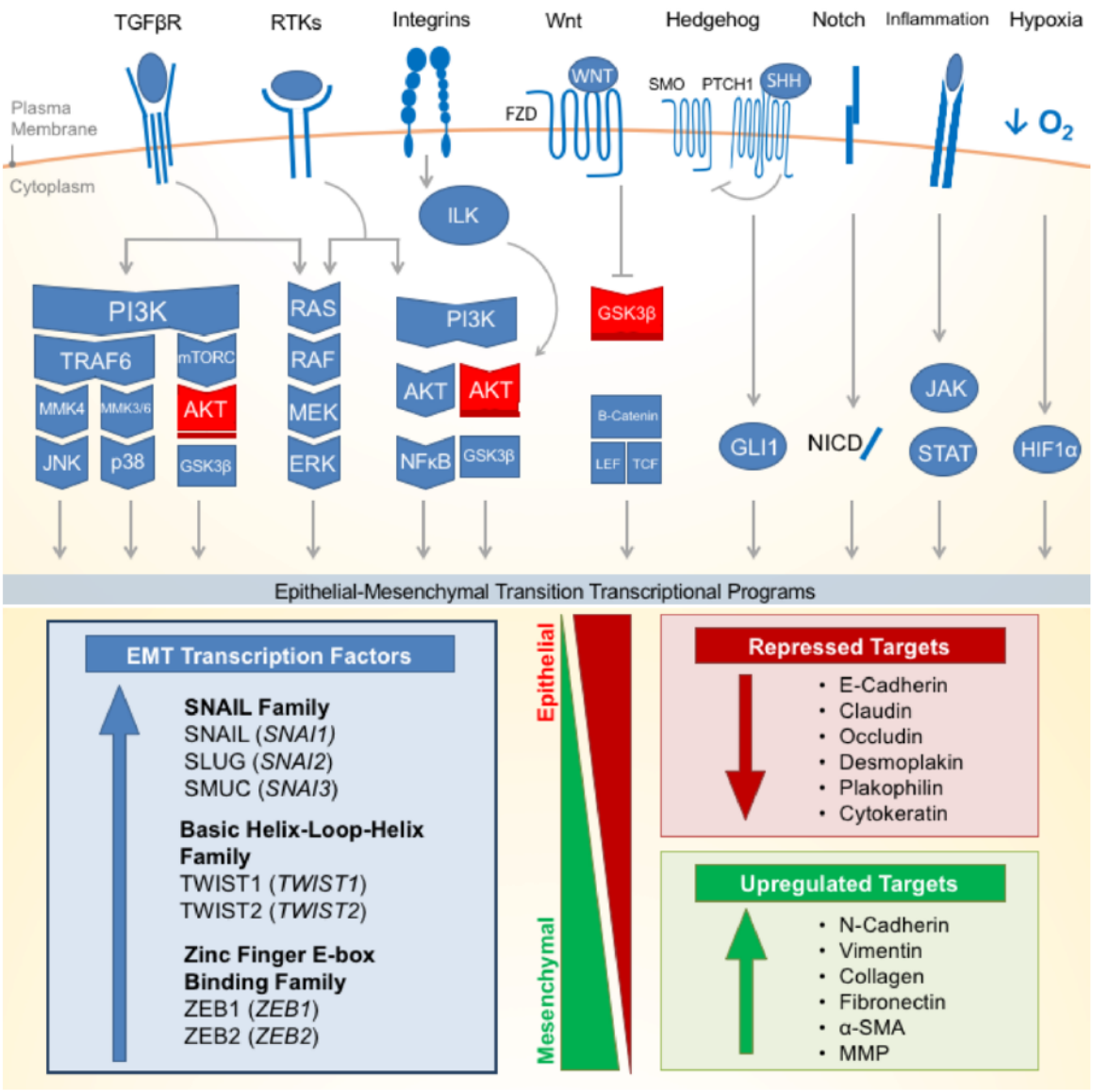

(Taparra, Frontiers in Oncology, 2016)

Figure 1.1 Molecular pathways and targets of the epithelial–mesenchymal transition.

(A) (1) One of the most well characterized EMT-inducing pathways is the transforming growth factor-β (TGF-β) family receptors that activate downstream PI3K–AKT, ERK

MAPK, p38 MAPK, and JUN N-terminal kinase (JNK) pathways (activating pathways in blue; inactivating pathways in red). (2) The RAS–RAF–MEK–ERK MAPK pathway lies downstream of a number of growth factor activated receptor tyrosine kinases (RTKs) and activates a number of major EMT transcription factors (TFs). (3) Integrin signaling can have a multipronged effect on EMT by both interrupting critical epithelial adhesion molecules (e.g., E-cadherin) and antagonizing GSK3-β via the integrin-linked kinase (ILK)-AKT signaling, thus promoting EMT. (4) WNT signaling can also interfere with GSK3-β, thus stabilizing β-catenin to promote EMT transcriptional programs in cooperation with lymphoid enhancer-binding factor 1 (LEF1) and T-cell factor (TCF). (5) The Hedgehog (HH)-glioma 1 (GLI1) and (6) NOTCH pathway both can promote transcription of the EMT regulators. (7) Recently, a number of inflammatory pathways downstream of interleukin (IL) signaling (e.g., IL-6) have demonstrated the activation of the Janus-kinase (JAK)-signal transducer and activator of transcription 3 (STAT3) pathway, which in turn promotes EMT transcription factors. (8) Hypoxia activates a number of key components of EMT through the hypoxia-induced factor 1 (HIF1α). **(B)** Downstream of these signal transduction pathways leading to EMT are a variety of transcription factors that determine the pattern of gene expression. As an epithelial plasticity program, many of the target genes altered include adhesion molecules. Known glycosylated proteins involved with EMT are denoted with an asterisk (*).

1.3.2 EMT transcription factors (TFs)

There are three major families of transcription factors (TFs) that contribute to EMT and may also be general drivers of cancer (**Figure 1B**): 1) the zinc finger protein SNAIL family (*SNAI1*, *SNAI2*, and *SNAI3*) [32], 2) the basic Helix-Loop-Helix (bHLH) proteins TWIST1 and TWIST2 [33], and 3) the zinc-finger E-box binding (ZEB) family of transcription factors [34]. These transcription factors are evolutionarily conserved and critical for development. They bind short DNA segments called Enhancer boxes (E-boxes) with the consensus sequence "CANNTG". Like many transcription factors, they are able to modulate transcription by recruiting a variety of epigenetic regulators to alter the chromatin landscape of epithelial plasticity genes and interactions with transcriptional co-activators and co-repressors [35].

The most well established gene targets of EMT TFs are generally involved in epithelial cell adhesion [36–38]. Cadherins represent a family of calcium-dependent cell-cell adhesion proteins particularly targeted by EMT [39–41]. Loss of epithelial cadherin (E-cadherin) is a major hallmark of EMT [42–44]. Thus, loss of E-cadherin has been used as a biomarker for many cancers. Additionally, loss of tight junctions (e.g., claudin and occludin), desmosomes (e.g., desmoplakin and plakophilin), and cytokeratins (intermediate filaments) are commonly observed during EMT [18]. Conversely, while epithelial markers are repressed, mesenchymal markers are increased during EMT. These markers include N-cadherin, vimentin, and fibronectin [18]. Following the transcriptional alterations of these adhesion molecules, protein degradation and endocytosis aids in recycling epithelial adhesion molecules to promote progress through EMT [45].

1.3.3 EMT transcriptional targets

Altered expression of EMT target genes, such as those involved in cellular adhesion, often facilitate migration and invasion [46–48]. Upon detaching from the basal epithelium, epithelial cells undergoing EMT may alter their extracellular environment by expressing matrix metalloproteinases (MMPs) to promote directional migration [49–51]. During migration, adhesion molecules are disproportionately redistributed between the leading and trailing edge of the cell, which allows the cell to coordinate directed migration leading to tumor dissemination and metastasis [24,52]. Beyond metastasis, EMT has recently been attributed to more fundamental roles in cancer biology including suppressing apoptosis and senescence [53]. The EMT has also been implicated in immune evasion [54] and metabolic reprogramming [22,55] of cancer cells. Together, the data discussed above suggest that the EMT program promotes many cancer cell phenotypes leading to malignancy.

1.4 The hexosamine biosynthetic pathway (HBP)

1.4.1 Enzymatic steps of the HBP

Since the 1950s, cancer has been notorious for its addiction to glucose and glutamine [7,56–58]. Upon depletion of these carbon sources in cancer cell culture media, cellular growth is abrogated. Both glucose and glutamine are essential for the first committed step and rate-limiting step of the HBP, the conversion of fructose-6-phosphate (Fru-6P) to glucosamine-6-phosphate. Approximately 2-5% of glucose (in adipocytes) is shunted

through the HBP [59]. Demonstrating the importance of extracellular glucose concentrations on the HBP, glucose starvation reduces UDP-GlcNAc levels [60,61]. Conversely, elevating extracellular glucose concentrations results in increased flux through the HBP [62]. **Figure 2A** summarizes the four key enzymatic steps of the HBP:

1) Glutamine:fructose-6-phosphate transaminase (GFAT; *GFPT*) utilizes glutamine in a transamination reaction which converts fructose-6-phosphate to glucosamine-6P (GlcN-6P);

2) GlcN-6P is converted to N-acetylglucosamine-6-P (GlcNAc-6P) by Glucosamine-phosphate N-acetyltransferase (GNPNAT; *GNPNAT*) which requires acetyl-CoA;

3) Phosphoglucomutase (PGM; *PGM*) isomerizes GlcNAc-6P to N-acetylglucosamine-1-phosphate (GlcNAc-1P);

4) UDP-N-acetylglucosamine pyrophosphorylase (UAP1; *UAP1*) charges GlcNAc-1P with UDP to form uridine-5'-diphosphate-N-acetylglucosamine (UDP-GlcNAc).

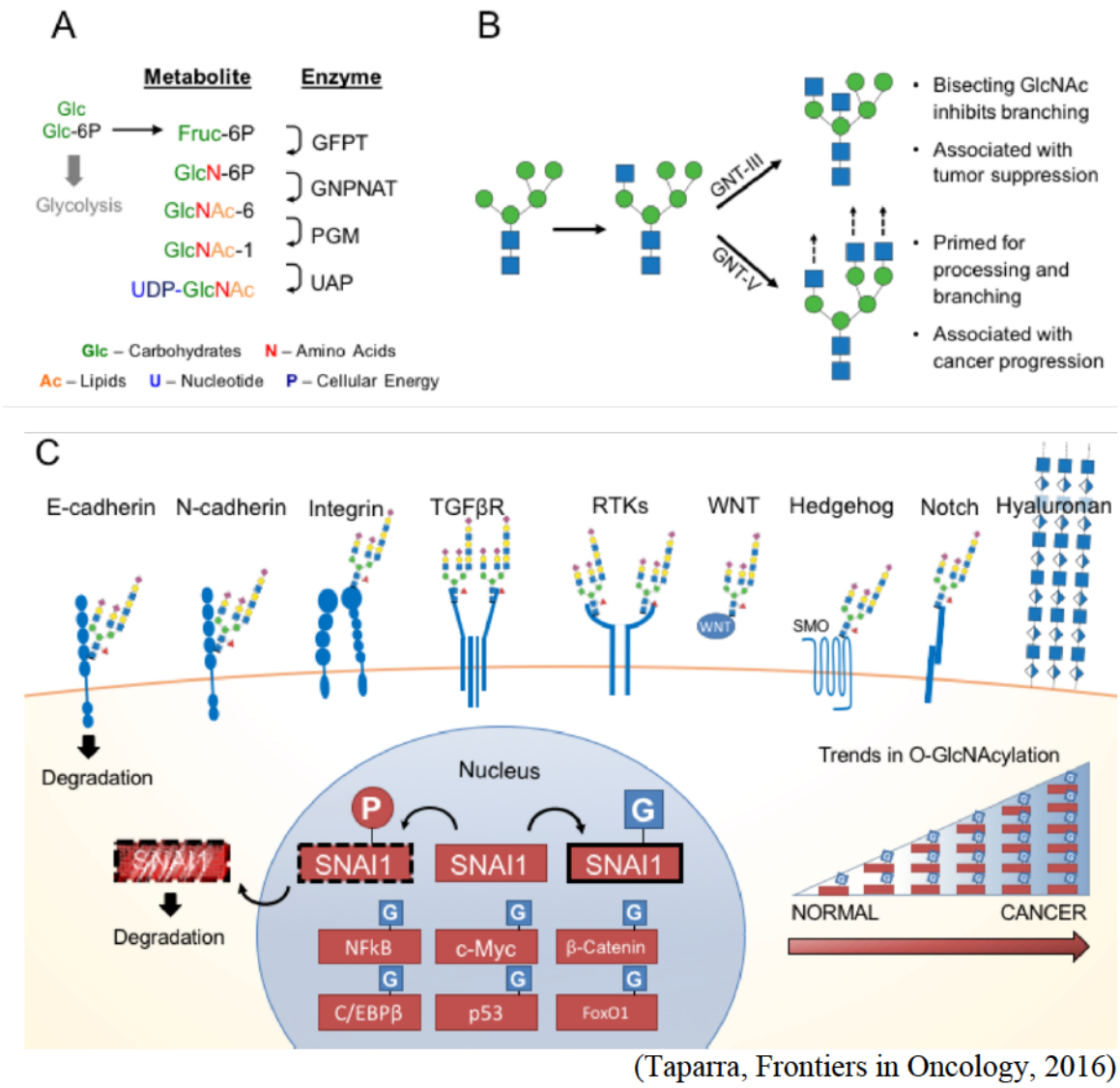

(Taparra, Frontiers in Oncology, 2016)

Figure 1.2 The hexosamine biosynthetic pathway (HBP) and glycosylated EMT targets

(A) First, the rate limiting enzyme of the HBP, glutamine:fructose-6-phosphate transaminase (GFAT), uses glutamine (Gln) as an amine donor to convert Fru-6P into glucosamine-6-P (GlcN-6P). Second, glucosamine-phosphate *N*-acetyltransferase (GNPNAT) *N*-acetylates GlcN-6P in an acetyl-CoA-mediated reaction to form *N*-

acetylglucosamine-6-P (GlcNAc-6P). Third, phosphoglucomutase (*PGM*) isomerizes GlcNAc-6P to the highly active GlcNAc-1P. The final step is catalyzed by UDP–*N*-acetylglucosamine pyrophosphorylase (*UAP1*) and charges GlcNAc-1P with UDP to form uridine-5′-diphosphate-*N*-acetylglucosamine (UDP–GlcNAc). **(B)** UDP–GlcNAc (depicted as a blue square) is essential for N-glycosylation processing and elongation. One critical pivot point includes the branching of complex *N*-glycans. Inhibiting this process with a bisecting GlcNAc is associated with tumor suppressive phenotypes. In contrast, cancers have aberrant expression of glycosyltransferases responsible for branching and elongating complex *N*-glycans. **(C)** Many of the proteins commonly associated with promoting EMT are modified by glycans containing GlcNAc and are found on the cell surface. Hyaluronan, a glycosaminoglycan, is also found extracellularly and is a polymer of glucuronic acid and *N*-acetylglucosamine. Many nuclear, cytoplasmic and mitochondrial proteins are modified by monosaccharides of *O*-linked *N*-acetylglucosamine (*O*-GlcNAc), including many transcription factors, which appear to be stabilized by glycosylation[63]. Numerous studies have identified various cancers with elevated levels of pan-*O*-GlcNAcylation[64].

1.4.2 Functions of the HBP

Together, the four enzymes of the HBP orchestrate the *de novo* biosynthesis of the charged nucleotide sugar UDP-GlcNAc from glucose. This process can be manipulated by endogenous metabolites (*i.e.,* glutamine)[65] as well as exogenous sugars (*i.e.,* glucose, glucosamine, and N-acetylglucosamine)[66]. Interestingly, this pathway is well positioned to sense the four macromolecules of life, coordinating carbohydrate, amino acid, lipid, and nucleotide donors through Fru-6P, Gln, acetyl-CoA, and uridine, respectively [67]. Despite the limited flux through the HBP, cellular UDP-GlcNAc levels can reach over 1 mM making it one of the most abundant high-energy cellular compounds [68]. UDP-GlcNAc is utilized in the synthesis of numerous glycoconjugates and is interconverted into other nucleotide sugars (*e.g.,* UDP-GalNAc, N-acetylmannosamine, CMP-Neuraminic acid), which are incorporated into glycoconjugates [69]. Together, the glycan structures downstream of the HBP metabolite, UDP-GlcNAc, influence a wide range of functional targets highly relevant to cancer and EMT.

1.4.3 Alterations of the HBP and global glycosylations in cancer

Reinforcing the importance of UDP-GlcNAc incorporation, recent data suggest the expression of multiple enzymes of the HBP and glycosyltransferases are altered in cancer, correlating with EMT, cancer progression, and metastasis. In a recent analysis using unsupervised hierarchical clustering of 1,704 metabolic genes and nearly 1,000 cancer cell lines, Shaul and colleagues identified a "Mesenchymal Metabolic Signature" (MMS) [22]. In this MMS, both *GFPT2* and *UAP1*, key enzymes in the HBP, were found to be essential for the mesenchymal phenotype [22,70]. In other studies, metabolites of the HBP

(*e.g.,* UDP-GlcNAc) levels have been reported to be elevated in cancer cells and to promote cancer cell survival [60].

Glycosyltransferases consistently elevated in multiple cancers (*e.g.,* stomach and pancreas cancer) include β-1,4-mannosyl-glycoprotein 4-β-N-acetylglucosaminyltransferase (GNT3), α-1,6-mannosylglycoprotein 6-β-N-acetylglucosaminyltransferase A (GNT5), core 2 β-1,3-galactosyl-O-glycosyl-glycoprotein β-1,6-N-acetylglucosaminyltransferase (Core 2 GNT; GCNT1), N-acetyllactosaminide β-1,6-N-acetylglucosaminyl-transferase-isoform A (GCNT2), and UDP-N-acetylglucosamine-dolichyl-phosphate N-acetylglucosaminephosphotransferase (GPT1), encoded by the genes *MGAT3*, *MGAT5*, *GCNT1*, and *GCNT2*, and *DPAGT1*, respectively [71]. Notably, GNT5 is highly associated with breast, lung, and colon cancer metastasis [72–77], whereas GNT3 is associated with breast, skin, and colon cancer tumor suppression [78–80]. GNT5 and GNT3 have antagonistic roles; GNT5 promotes complex N-linked glycan branching, whereas GNT3 suppresses branching (**Figure 2B**). It is thought that changes in glucose flux through the HBP impacts the function of GNT3 and GNT5 [66]. The rate limiting enzyme that forms the precursor for N-glycosylation, GPT1, has also been shown to drive proliferation, EMT, and cell morphology [81]. As discussed below, flux through the HBP can alter the distribution patterns of glycosylation. To date, this has not been specifically studied in EMT. However, there are a number of glycoconjugates affected by changes in UDP-GlcNAc availability or changes in their biosynthesis. These glycoconjugates and their impact on EMT are discussed below.

1.5 External GlcNAc-containing glycoconjugates observed during EMT

1.5.1 GNT3 and GNT5 mediated N-glycosylation in cancer

Accumulating evidence strongly suggests that changes in protein glycosylation impact numerous cancers including melanoma [82], pancreas [83,84], colon [85], ovarian and breast [86], brain and lung [87], liver [88], and prostate [89] cancers. Generally, alterations in N-glycan structure profoundly affect cellular adhesion and epithelial morphology *in vitro* [90]. **Figures 2B and 2C** show that many glycoproteins utilizing UDP-GlcNAc in their biosynthesis occur on key EMT adhesion molecules (*e.g.,* E- and N-cadherin). E-cadherin has four putative N-linked glycosylation sites [91], which are modified by complex N-linked glycans. The number of "antennae" on these glycans is regulated by the competing activities of GNT3 (*MGAT3*) and GNT5 (*MGAT5*). The introduction of a bisecting GlcNAc by GNT3 (**Figure 2B**) reduces the number of antennae and thus complexity of the N-linked glycan.

1.5.2 Glycosylation of E-cadherin

Epigenetic regulation of the gene encoding GNT3, *MGAT3*, stabilizes E-cadherin and inhibits EMT [92]. In contrast, elevated activity or expression of GNT5 results in more complex N-glycans which impairs E-cadherin localization and cellular aggregation in mice [93]. Additional studies in mice have revealed that *Mgat5* knockdown leads to a reduction of N-glycosylated E-cadherin, which increases E-cadherin cis-dimerization,

catenin recruitment, and cell membrane localization [94,95]. Importantly, aberrantly N-glycosylated E-cadherin is found in gastric cancer patients and correlates with poor patient survival [94].

1.5.3 Glycosylation of N-cadherin

Mesenchymal N-cadherin is also modified by N-linked glycans, and the modification of these glycans with GlcNAc by GNT5 promotes cell migration, MAPK signaling, and reduced adhesion [96,97]. Furthermore, N-cadherin N-glycans attract Galectin-3, forming highly organized lipid rafts on the cell surface, which stabilizes the galectin lattice and enhances cancer cell mobility [98]. This galectin lattice structure also recruits several major signaling receptors such as epidermal growth factor (EGF) receptor (EGFR) and TGF-β to promote oncogenic signaling [99,100].

1.5.4 Glycosylation of integrins

Integrins are heterodimeric glycoproteins responsible for cell-cell and cell-extracellular matrix interactions [101]. The α5β1 integrin serves as the receptor for fibronectin and their interaction is critical for cellular migration in development [102–104]. While both integrin and fibronectin are N-glycosylated, the activity of GNT3 is associated with shorter less complex N-glycans which is thought to result in reduced integrin-mediated EMT signaling [105,106]. Additionally, without N-linked glycans, integrins show significantly decreased heterodimerization, cell surface localization, and promotion of migration *in vitro* [107].

1.5.5 Glycosylation of RTKs

Receptor tyrosine kinases (RTKs) are vital to the transduction of external stimuli into internal signals for induction of EMT in many cancers (*e.g.,* carcinomas). Interestingly, RTKs involved in growth and proliferation (*e.g.,* EGFR) have approximately five-fold more N-glycosylation sites than receptors, which are involved with organogenesis, differentiation, or cell cycle arrest [108]. The HBP has been shown to drive changes in EGFR N-glycosylation; feeding both GNT5 wildtype and GNT5 null tumor cells with N-acetylglucosamine elevated UDP-GlcNAc levels and the number of terminal GlcNAc residues on cell surface proteins. Analysis of the N-linked glycans demonstrated increased flux through the HBP results in increased triantennary structures in GNT5 null cells (2 fold) and a smaller increase in both tri- and tetra-antennary N-glycans in GNT5 wild-type cells. Functionally, increased flux through the HBP altered EGFR plasma membrane retention, active conformation, EGF ligand binding, and inhibition of endocytosis mediated degradation [109,110]. N-glycosylated EGFR recruits N-glycosylated TGF-βR to the galectin lattice thereby promoting TGF-β and SMAD autocrine signaling. TGF-βR with highly branched glycans, a result of increased GNT5 activity, localizes to the plasma membrane, binds galectin-3, inhibits receptor endocytosis, enhances TGF-βR heterodimerization, increases tumor metastasis, and promotes EMT-mediated cell migration [100,111]. TGF-β itself upregulates GCNT1, a critical GlcNAc branching enzyme, producing similar effects in prostate, colorectal, pancreatic, testicular, and breast cancers [112].

1.5.6 Glycosylation of the WNT, NOTCH, and HH pathways

The WNT, NOTCH, and Hedgehog (HH) pathways are also critical for EMT and are modified by glycans that utilize GlcNAc for modulation of pathway activity. All 19 known WNT ligands contain at least one N-linked glycosylation site and these sites are critical for ligand maturation, lipid processing, secretion, and β-catenin signal transduction [113,114]. WNT also regulates transcription of *DPAGT1* to promote EMT through E-cadherin glycosylation [81].

The Notch signaling pathway regulates cell proliferation, survival, and differentiation while glycosylation of components in this pathway are associated with poor prognosis and metastasis in numerous cancers [115,116]. Over two decades of research demonstrates the extracellular domain of Notch receptor is glycosylated with N-linked [117], O-fucose [117,118], O-GlcNAc [119], and O-glucose [117,120] glycans. Extension of O-fucose with GlcNAc (catalyzed by O-fucosylpeptide 3-beta-N-acetylglucosaminyltransferase [Fringe in *Drosophila*]) alters Notch ligand-receptor specificity. In *Drosophila*, extended O-fucose glycans are associated with increase sensitization of Notch to the Delta ligands and reduced sensitivity to the Serrate/Jagged ligands [116]. Little is known about the impact of altered HBP flux on the Notch receptor, although one might postulate that changes in UDP-GlcNAc levels may alter Notch glycosylation and thus signaling downstream of this receptor. In the Sonic HH pathway, the G protein-couple receptor (GPCR), Smoothened (SMO), is activated to promote cell proliferation and migration [121]. Recently, critical N-glycans on SMO were found to abrogate HH induced cell migration due to blunted small heterotrimeric $G_{\alpha i}$ protein signaling [122].

1.5.7 Hyaluronan in cancer

Beyond the suite of GlcNAc-modified adhesion molecules and receptors, hyaluronic acid (hyaluronan or HA) is an oligomer found ubiquitously in the extracellular space particularly of connective, epithelial, and neural tissues [123]. Human HA is a massive (0.5–2 MDa) unbranched glycosaminoglycan composed of the repeating disaccharide consisting of GlcNAc and glucuronic Acid (GlcNAcβ1-4GlcAβ1-3) [124]. It is synthesized by HA synthase (HAS) and is extruded through the plasma membrane as it is synthesized. Recent reports suggest hyaluronan synthesis and catabolism is controlled UDP-GlcNAc concentrations, with hyaluronan serving as a sink for excess UDP-GlcNAc [125]. Recent studies have demonstrated that modulating levels of UDP-GlcNAc and glucuronic acid alter the localization of the HAS enzymes [126]. Low levels of UDP-GlcNAc are associated with an inhibition of HA synthesis, whereas elevated levels of UDP-GlcNAc are associated with HA synthesis and melanoma progression [126]. Consistent with these data, several studies have demonstrated patients with higher-extracellular HA or HAS expression have a worse prognosis and survival with more aggressive and metastatic cancers including breast [127–129], prostate [130,131], lung [132,133], pancreatic [134], colorectal [135], and ovarian [136] cancers. With respect to EMT, high levels of HA are sufficient to induce the EMT in kidney and mammary epithelial cells [137]. Taken together, HA synthesis is in part driven by the HBP, has been associated with EMT and is found at high levels in many cancers.

1.6 Nuclear, cytoplasmic, and mitochondrial glycosylations observed during EMT

1.6.1 O-GlcNAcylation overview

UDP-GlcNAc can also be utilized for the synthesis of O-Linked β-N-acetylglucosamine (O-GlcNAc), an essential PTM of metazoans [138]. O-GlcNAc is found on more than 3,000 cytoplasmic, nuclear, and mitochondrial proteins [67]. O-GlcNAcylation is thought to regulate protein function in a manner analogous to phosphorylation. O-GlcNAc has been demonstrated to regulate cellular processes such as epigenetics, transcription, translation, protein degradation, metabolism, ribosomal bioenergentics and cytokinesis [139].

Unlike N-glycans, the O-GlcNAc modification (or O-GlcNAcylation) consists of a monosaccharide of GlcNAc covalently attached to serine and threonine residues through an O-glycosidic bond [138]. Where N-linked glycan synthesis and processing is regulated by upwards of 18 enzymes (depending on the structure formed), the dynamic cycling of O-GlcNAc on proteins is regulated by just two enzymes: the O-GlcNAc transferase (OGT) and the O-GlcNAcase (OGA), which add and remove O-GlcNAc, respectively [140]. OGT activity and substrate specificity is regulated by changes in UDP-GlcNAc concentrations and this has led many to suggest that OGT may regulate cell function in a manner dependent on extracellular glucose concentrations [140].

1.6.2 O-GlcNAcylation in cancer

Cancer cells which are dependent on glucose and glutamine have been demonstrated to have high UDP-GlcNAc levels (*discussed above*), high O-GlcNAc levels, and in some cases increased expression of OGT [140]. In sum, elevated protein O-GlcNAcylation and

OGT expression have been reported in numerous malignancies including breast [16,63,141,142,64], prostate [143–145], lung [146], pancreas [147], liver [148], and colon [146,149,150] cancers. Importantly, levels of O-GlcNAc, OGT, and OGA have correlated with aggressiveness (e.g. Gleason score for prostate cancer) in a number of patient tumor samples including prostate [144], breast [64], endometrial [151], and bladder [152] cancers.

1.6.3 O-GlcNAcylation of TFs in cancer

One important class of proteins heavily O-GlcNAcylated are TFs (**Figure 2C**). Early analyses suggested that over 25% of known O-GlcNAcylated proteins were TFs [14]. For many of these TFs, O-GlcNAcylation serves as a direct or indirect competitor of key phosphorylation sites [140]. Particularly relevant to EMT is the O-GlcNAcylation and regulation of SNAI1. Upon serial phosphorylation by CK1 and glycogen synthase kinase (GSK)-3β, SNAI1 is primed for nuclear export, β-TrCP ubiquitination, and subsequent proteosomal degradation [153,154]. Interestingly, SNAI1 is O-GlcNAcylated in hyperglycemic conditions preventing GSK-3β phosphorylation which results in SNAI1 stabilization [155]. O-GlcNAcylated SNAI1 is associated with enhanced EMT and migration, which is linked to a repression of E-cadherin. Whether other EMT-inducing TFs are similarly regulated by O-GlcNAcylation is yet to be determined. Beyond SNAI1, O-GlcNAcylation occurs on other transcription factors generally relevant to cancer including c-Myc [156,157], β-catenin [158], C/EBPβ [159], p53 [160], and FoxO1 [161], NFkB [162,163]. Thus, while more experimentation is needed to demonstrate causality between EMT and O-GlcNAcylation, O-GlcNAcylation has demonstrated to be a key regulator of cancer biology.

1.6.4 O-GlcNAcylation and the cell cycle

Previous studies from our lab and others have elucidated the role of the EMT TF, TWIST1, in suppression of oncogene-induced senescence (OIS) [20,21,164]. While normal cells respond to oncogene activation with p53-p19^{ARF}, p16-Rb and Atf4-p27^{KIP}-dependent OIS [165,166], suppression of these pathways through EMT TFs provide an alternative route for cancer to maintain cell cycle progression and proceed along a tumorigenic path. Due to the metabolic regulation of the cell cycle, it is not surprising many of these proteins orchestrating cellular division are also O-GlcNAcylated. Knockdown of OGT results in elevated expression of p27^{Kip} [63], a reduction of cyclin D1 and B1, and diminished PI3K/AKT signaling [167], suggesting that OGT/O-GlcNAc plays key roles during cell cycle progression. Furthermore, OGT is thought to control cytokinesis as it is localized to the mitotic spindle where it interacts with Polo-like kinase. Disrupting O-GlcNAcylation results in defects in cytokinesis and multinucleated cells [168]. Overall, global O-GlcNAc levels have numerous effects on the cell cycle, indicative of yet another link to advancing the neoplastic phenotype.

1.6.5 Bridging the gap

The data discussed here highlight alterations in intracellular and extracellular glycoconjugates that impact different EMT tumorigenic pathways and associated proteins/biomolecules. With recent controversies of EMT transcription programs continuing to unfold [169,170], it is likely that role of EMT may extend beyond cancer development and metastasis, including cancer treatment resistance. Thus, understanding

how changes in metabolic pathways observed in cancer (*e.g.,* the HBP) impact the distribution and composition of glycoconjugates may provide deeper insights into mechanisms of cancer biology. While most of the research discussed here demonstrates the potential for glycoconjugates to regulate EMT, it may be interesting to see in the future how EMT reciprocally promotes metabolic reprogramming and the HBP.

Chapter 2: Investigating the EMT-HBP axis in lung cancer

2.1 Background on EMT and OIS in mutant *KRAS*-driven lung cancer

Non-Small Cell Lung Cancer (NSCLC) mortality remains high with the most frequently observed driver mutation occurring in the small GTPase, *KRAS*[171]. Recent evidence suggest aberrant *KRAS* drives glycolytic flux in lung cancer[172,173], potentially impacting aberrant protein glycosylation. One contributor and proposed target of *KRAS* driven cancers is a developmentally conserved epithelial plasticity program called the epithelial-mesenchymal transition (EMT)[174]. Recently, the EMT has been correlated with aberrant glycosylation to promote neoplastic phenotypes[175]. Despite its prevalence and three decades of research, the KRAS oncoprotein remains difficult to target pharmacologically[176]. A better understanding of metabolic susceptibilities may reveal innovative targets.

Here we show in novel autochthonous mouse models that EMT accelerates $Kras^{G12D}$ lung tumorigenesis by driving expression of hexosamine biosynthetic pathway (HBP) genes to elevate the O-linked β-N-acetylglucosamine post-translational modification (PTM) on intracellular proteins (O-GlcNAcylation)[138]. O-GlcNAcylation promoted suppression of $Kras^{G12D}$ oncogene-induced senescence (OIS) and accelerated lung tumorigenesis. Genetic and pharmacological inhibition of the HBP revealed this metabolic pathway is required for EMT-mediated suppression of OIS. We show that the O-GlcNAcylated proteins SNAI1[155] and c-Myc[157] correlate with the EMT-HBP axis and accelerated lung

tumorigenesis.

Our results demonstrate for the first time that O-GlcNAcylation is sufficient and required to accelerate *Kras*^{G12D} lung tumorigenesis *in vivo*, which is reinforced by EMT programs. These data hold potential as an alternative "metabolic strategy" to target mutant *KRAS* driven lung cancers by activating latent senescence programs. Furthermore, our work provides fundamental new insights into a unique sugar post-translational modification (PTM) that is required for *Kras*^{G12D}-driven lung tumorigenesis.

In the presence of an oncogenic driver, normal primary cells initiate an intrinsic failsafe mechanism, OIS, in response to oncogenic cellular stress, characterized by permanent cell cycle arrest, cytoplasm enlargement, and the senescence-associated secretory phenotype (SASP)[177,178]. To progress towards full-blown malignancy, these pre-malignant cells must initiate programs to suppress OIS. We and others have previously shown the EMT transcription factors (TFs) – commonly associated with cancer aggressiveness, metastasis, and stemness – suppress OIS and accelerate *Kras*^{G1D}–induced tumorigenesis[20,21,179]. This novel EMT function is particularly impactful given recent discoveries suggesting diverse roles of the EMT in cancer beyond metastasis (*e.g.* chemoresistance)[169,170]. Thus, EMT programs hold promise for identifying alternative pathways to target mutant *KRAS*.

2.2 The development of novel mutant *KRAS*-driven EMT mouse models

Two well-characterized EMT TFs are SNAI1 and TWIST1, which are both critical in development, aberrantly expressed in numerous cancers, and correlate with poor patient outcomes[24,174]. We generated novel lung specific inducible mouse models of EMT co-expressing mutant *Kras*^{G12D} and *SNAI1* (CRS) or *TWIST1*[20] (CRT) and compared them to mice expressing *Kras*^{G12D} alone (CR) (Fig. 2.1a, 2.5a, b). Consistent with our previous work on EMT[20], cone-beam computed tomography (CBCT) scans (Fig. 2.1b) revealed EMT expressing CRS and CRT mice developed tumors twice as quickly (median = 16 weeks) as CR mice overexpressing *Kras*^{G12D} alone (median = 32 weeks) and have significantly more tumors (Fig. 2.1c and Fig. 2.5c, d). Furthermore, while CR mice tend to develop adenomas, the EMT CRS and CRT mice developed adenocarcinomas (Fig. 2.1d), which were dependent on the co-expression of *Kras*^{G12D} and an EMT TF for tumor maintenance (Fig. 2.5e). The CRS and CRT tumors also showed high proliferation, activated MAPK signaling, modestly decreased apoptosis, and low senescence relative to CR tumors (Figs. 2.1e, f, 2.5f, g, and Ref. 20). To demonstrate EMT suppression of OIS, we generated SNAI1 and Twist1[20] expressing mouse embryonic fibroblast (MEF) cell lines and found EMT TF expression suppressed mutant *RAS*-induced OIS as shown by activated proliferation and reduced senescence-associated β-galactosidase (SA-βgal) staining (Fig. 2.6). Overall, EMT TFs suppressed OIS, accelerated lung tumorigenesis, and promoted lung tumor progression towards aggressive adenocarcinoma in *Kras*^{G12D}-driven lung cells.

2.3 Identification of EMT associated metabolic gene expression

To identify mechanisms of EMT-mediated suppression of OIS, we used mRNA

microarray analysis to identify differentially expressed genes between CR *vs* CRS and CR *vs* CRT lung tumors. Gene Set Enrichment Analysis (GSEA) revealed a number of gene sets related to the EMT, senescence, and mutant *KRAS*-driven lung cancer (Fig. 2.7). Interestingly, using the PANTHER (Protein ANnotation through Evolutionary Relationship) Gene Ontology (GO) classification system, we identified 1/3 and 1/5 of the differentially expressed genes were involved in "metabolic biological processes", in CR *vs* CRS and CR *vs* CRT models, respectively (Fig. 2.1g, h). Seahorse metabolic analyses indicated that EMT TF expressing NSCLC cells, A549 and PC9, exhibited elevated glucose utilization (Fig. 2.8). As we were interested in mechanisms of glycolytic flux, we then found the EMT mouse lung tumors correlated with increased expression of critical genes in the HBP, a versatile energy-sensing pathway downstream of glycolysis. Specifically, EMT TFs correlated with elevated expression of the rate limiting step (GFPT2) and final enzymatic step (UAP1) of the HBP as confirmed by qPCR and Western blot in both EMT mouse models (Fig. 2.1i-k) and in patient lung adenocarcinoma data from cBIO and The Cancer Genome Atlas (TCGA) (Fig. 2.1l and Fig. 2.8a).

In addition, both the transcriptomic profile of mesenchymal stem cells (Fig. 9b, c) and a recently discovered cancer "Mesenchymal Metabolic Signature" (MMS)[22] showed upregulation of both *GFPT2* and *UAP1*. Interestingly, *GFPT2* was the top metabolism gene significantly overexpressed in tumorigenic $KRAS^{G12D}$-driven human lung epithelial cells[180]. We found GFPT1 and UAP1 were overexpressed in 20 NSCLC gene expression datasets accessed on ONCOMINE (Fig. 2.9d). To verify this EMT-HBP axis, we

overexpressed SNAI1 and TWIST1 in human mutant *KRAS*-driven NSCLC cell lines and found that HBP genes were similarly overexpressed (Fig. 2.1m, n). Additional inducible, knockdown and overexpression models of EMT including NSCLC cells, HeLa cells, non-malignant cells, and CRS mice without DOX induced *SNAI1/KrasG*^{12D} showed direct correlation with HBP genes (Fig. 2.9e-i). Together, these data suggested a novel EMT-HBP in NSCLC cells, patient samples, and our *in vivo* EMT-accelerated *Kras*^{G12D} lung tumorigenesis mouse models.

2.4 The HBP is required for *SNAI1*-mediated suppression of OIS

To determine the requirement of the HBP in senescence, we made use of the non-cancer human bronchial epithelial cell line (HBEC3-KT)[181] that activated an OIS transcriptional phenotype upon *HRAS*^{G12V} transduction (Fig. 2.2a-c). Inhibition of the HBP (Fig. 2.2d) in HBEC3-KTs genetically and pharmacologically induced markers of senescence and decreased cell counts (Fig. 2.2e and 2.10a-e). As the glutamine antagonist 6-Diazo-5-oxo-L-norleucine (DON) is not a specific inhibitor of GFPT2, we also demonstrated that senescence was specific to the HBP with a metabolite rescue experiment: addition of downstream metabolites of the HBP rescued 50 μM DON induced-senescence (Fig. 2.2f and Fig. 2.10f, g), suggesting the HBP is a critical pathway controlling senescence.

We also found SNAI1 could suppress *HRAS*^{G12V}-mediated OIS in HBEC3-KT cells (Fig. 2.2g, h, first two bars), in alignment with our previous work with *TWIST1* expressing MEFs[20]. Genetic (Fig. 2.2g and Fig. 2.10h) and pharmacological (Fig. 2.2h and Fig. 2.10i) inhibition of the HBP abrogated the ability of EMT TF expression to suppress

HRAS^{G12V}-mediated OIS in our *SNAI1* overexpressing HBEC-3KT model.

2.5 A *SNAI1*-inducible, mutant *KRAS*-expressing conditional mouse model

To determine if the EMT TF expression directly impacts the HBP and OIS *in vivo*, we crossed our inducible SNAI1 expressing mouse line (CS) with the conditionally activated *Lox-Stop-Lox-Kras*^{G12D} (LSL)[182] to generate a novel triple transgenic CS-LSL mouse line (Fig. 2.10j and Ref. 20).

In support of our findings in the CRS mouse model (Fig. 2.2), CS-LSL mice generated more rapidly growing, less senescent, and more aggressive tumors compared to LSL mice (Fig. 2.2i). With this model, we were able to inactivate expression of *SNAI1* alone while maintaining expression of *Kras*^{G12D} and found that inactivation of SNAI1 promoted tumor stasis and elevated levels of p53 (Fig. 2.2j-m). Furthermore, without the EMT TF SNAI1, mRNA expression of the HBP genes diminished (Fig 2m). Thus, EMT-mediated suppression of mutant *RAS*-induced OIS required the HBP *in vitro* and SNAI1 directly modulated the HBP *in vivo*.

2.6 Targeting the HBP in NSCLC affects cancer growth

Genetic knockdown of *GFPT2* and *UAP1* in NSCLC cells revealed increased markers of senescence (Fig. 2.3a, b and Fig. 2.11a, b). Pharmacological inhibition of the HBP with low concentrations of DON ($\leq$10 μM) in NSCLC cell lines showed decreased cell viability, decreased clonogenicity, increased senescence morphology, and elevated

molecular markers of senescence and apoptosis, while normal HBEC3-KT cells were seemingly unaffected (Fig. 2.3c-g and Fig. 2.11c-g). To assess the efficacy of targeting NSCLC cells *in vivo*, H358 (Fig. 2.3h-j and Supplementary 12a-d) and A549 (Fig. 2.12e-h) cells were injected into the flanks of athymic nude mice. Mice treated with DON (20 mg/kg/week) resulted in smaller tumors, reduced tumor growth, reduced gross tumor weight, and increased markers of senescence over five weeks without significantly impacting body weight (Fig. 2.12d). DON treatment also inhibited autochthonous lung tumorigenesis in the CS-LSL and CT-LSL mice tumors without impacting body weight (Fig. 2.3k-m and Fig. 2.12i-k). Therefore, targeting the HBP in lung cancer inhibited early lung tumorigenesis and had therapeutic effects on established tumors that resulted in senescence and/or cell death.

2.7 O-GlcNAcylation is upregulated in response to EMT

The HBP produces the nucleotide sugar UDP-GlcNAc which can be utilized in multiple pathways, including both N-linked and O-linked protein glycosylations (Fig. 2.4a), which regulate protein stability and activity[63,70,175]. N-linked glycosylation of proteins occurs in the ER and Golgi and the branching of N-glycans is influenced by flux through the HBP[183]. Interestingly, the O-GlcNAc PTM (O-GlcNAcylation) has previously been shown to stabilize SNAI1 in the nucleus[155]. O-GlcNAcylation is a single sugar modification found on proteins in the nucleus, cytoplasm, and mitochondria[139]. The O-GlcNAc modification[138,139] is added and removed by just two enzymes, O-GlcNAc Transferase (OGT) and O-GlcNAcase (OGA), respectively (Fig. 2.4a). In our models overexpressing EMT TFs, we found that the HBP, OGT, and O-GlcNAcylation were

elevated in both human (Fig. 2.4b, Fig. 2.13a, c and 2.16a) and mouse (Fig. 2.4f-k, Fig. 2.13b and 2.10) NSCLC cells. Analysis with ConA did not reveal a noticeable change in the degree of N-linked glycosylation (Fig. 2.4b and Fig. 2.14a).

To determine which type of glycosylation affected senescence, we used genetic and pharmacologic inhibition of N-linked glycosylation and the O-GlcNAc glycosylation. We found reduction of O-GlcNAcylation in HBEC3-KT cells, via genetic overexpression of OGA (Fig. 2.4c) and pharmacological inhibition with OGT inhibitor TT04 (Fig. 2.4d), promoted senescence while inhibition of N-glycosylation with tunicamycin (TUNI) had no effect on senescence (Fig. 2.15). Reducing O-GlcNAcylation in NSCLC cells *in vitro* with the OGT inhibitor TT04 increased SA-βGal positive staining and promoted senescent cellular morphology in NSCLC cells (Fig. 2.4e and Fig. 2.16b, c). DON treatment also reduced global O-GlcNAcylation *in vitro* and *in vivo* (Fig. 2.16d, e). Genetic knockdown of OGT in A549 cells reduced NSCLC clonogenicity and endogenous levels of SNAI1 (Fig. 2.16f, g). Genetic ablation of OGT reduced cellular number upon conditional OGT knockout in MEFs over 5 days (Fig. 2.16h). These data indicate that EMT and the sugar PTM O-GlcNAcylation promoted each other in a feed-forward loop to regulate senescence.

2.8 Connecting O-GlcNAcylation and mutant *KRAS*-mediated OIS

We next wanted to know the importance of O-GlcNAcyaltion for $Kras^{G12D}$–induced lung tumorigenesis by using established and novel autochthonous mouse models. O-GlcNAcylation was sufficient to significantly accelerate $Kras^{G12D}$–induced lung

tumorigenesis as shown by pharmacological elevation of O-GlcNAcylation with the OGA inhibitor thiamet-G (TMG) in the LSL model (median = 5 weeks; Fig. 2.4l-n, q). Requirement of O-GlcNAcylation was assessed by crossing the LSL mouse line with cre-conditional $OGT^{fl/fl}$ mouse line[184], generating LSL-$OGT^{fl/fl}$ mice that simultaneously express $Kras^{G12D}$ while knocking out OGT specifically in the lung epithelial cells upon intranasal administration of Adeno-CMV-Cre (AdCre) virus (Fig. 2.4o, p). Male LSL-$OGT^{fl/Y}$ mice demonstrated O-GlcNAcylation was required for $Kras^{G12D}$-induced lung tumorigenesis as demonstrated by a significant delay in lung tumor development (medial = 15 weeks; Fig. 2.4q). Overall, data from these autochthonous mouse models revealed O-GlcNAcylation was necessary and sufficient for $Kras^{G12D}$-induced lung tumorigenesis.

Having established that the EMT-HBP axis required O-GlcNAcylation to suppress senescence and accelerate $Kras^{G12D}$-induced lung tumorigenesis, we then focused on O-GlcNAcylated candidates that have been shown to be critical for tumorigenesis. One promising target was the oncoprotein c-Myc based on multiple studies that $Kras^{G12D}$ and *MYC* oncogenes can have collaborative effects during tumorigenesis *in vivo*[185–187] and c-Myc itself is stabilized by O-GlcNAcylation[157]. We found *MYC* gene sets were over-represented by GSEA in our EMT $Kras^{G12D}$ -driven lung cancer mouse models (Fig. 2.16i). We found pharmacological inhibition of O-GlcNAcylation with TT04 or DON (Fig. 2.16c-e, j) or genetic knockdown (Fig. 2.16g) resulted in a reduction of c-Myc in human and mouse NSCLC cells *in vitro* and *in vivo*. Similarly, overexpression of EMT TFs in human and mouse NSCLC cells resulted in increased c-Myc levels *in vitro* (Supplementary 12a, k) and *in vivo* (Fig. 2.4h, i, r, s, Fig. 2.14c, e and 16l). Taken

together, our data suggested the EMT-HBP axis suppressed OIS through stabilizing oncogenes such as c-Myc.

Our work revealed that EMT promotes increased glucose flux through the HBP to increase levels of O-GlcNAcylated proteins in incipient and established lung cancer cells as well as autochthonous lung cancer models. This metabolic sugar pathway and protein O-GlcNAcylation are required to suppress mutant $Kras^{G12D}$-induced OIS and promote $Kras^{G12D}$-induced lung tumorigenesis. Targeting the HBP abrogates EMT-mediated suppression of OIS in normal HBEC3-KTs *in vitro* as well as multiple mouse models of lung cancer *in vivo*. The benefit of these findings are highlighted by recent proposals for senescence programs as an alternative strategy for cancer therapy, especially with the clearance of senescent cells by the immune system[178,188]. Together, our data demonstrate O-GlcNAcylation is a product of EMT-driven metabolic reprogramming that contributes to $Kras^{G12D}$-induced lung tumorigenesis and tumor progression. Modulation of the HBP and specific glycosylations may impact cell death and senescence, providing a novel targetable EMT-HBP axis for *KRAS* driven NSCLC.

2.9 Figures with legends

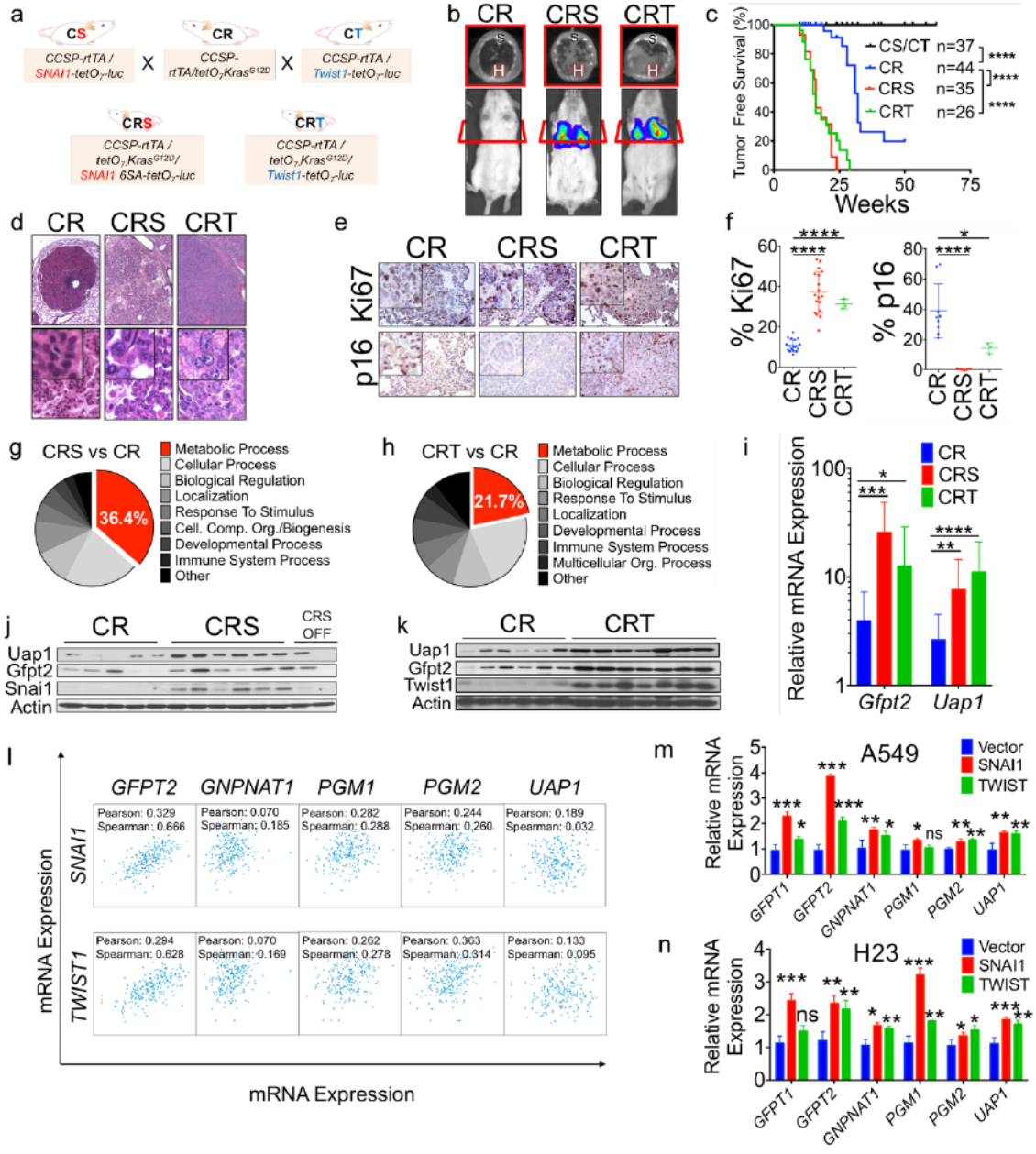

Figure 2.1 The EMT drives the HBP in *KRAS* mutant lung cancer cells

a, Breeding schematic of doxycycline (DOX) inducible Club Cell Specific Promoter (CCSP; C)-driven lung-specific $Kras^{G12D}$ mouse line (CR) crossed with either *SNAI1-6SA*

(CRS) or *Twist1* (CRT) mice with a bidirectional promoter also expressing a *luc* reporter. **b**, Bioluminescence imaging (BLI) and computerized tomography (CBCT) scans of mice (H - heart; S - spine) upon addition of DOX to drinking water. **c,** Kaplan-Meier curve for tumor free survival of EMT TF-$Kras^{G12D}$ mice (median = 16 weeks post-DOX) compared to $Kras^{G12D}$ alone (median = 31 weeks post DOX) (n≥26 mice per genotype; P<0.0001 by log-rank test). **d**, Hematoxylin and eosin (H&E) staining of representative mouse lung tumors in **b** at ~40 weeks. **e, f,** immunohistochemistry (IHC) of Ki67 and p16 in CR, CRS, and CRT tumors with quantification (n≥3 mice per genotype). **g, h,** Enrichment for genes of "Metabolic Process" Gene Ontology of differentially expressed genes between EMT and non-EMT driven mouse tumors. **i-k**, qPCR (**i**) and Western blot (**j, k**) for HBP genes, *Gftp2* and *Uap1,* and corresponding gene products in EMT/$Kras^{G12D}$ CRS/CRT tumors compared to $Kras^{G12D}$ alone CR lung tumors (n≥5 mice per genotype). **l**, Correlation of multiple genes, including *GFPT2* and *UAP1*, in lung adenocarcinoma patient samples from cBIO database (calculated by Pearson and Spearman correlations). **m, n,** HBP gene expression in NSCLC cell lines stably infected with *SNAI1* or *TWIST1*. Unless stated, error bars, mean ± standard deviation (s.d.) P values were derived from an unpaired, two-tailed Student's t-test. (*P<0.05; **P<0.01; ***P<0.001; ****P<0.0001).

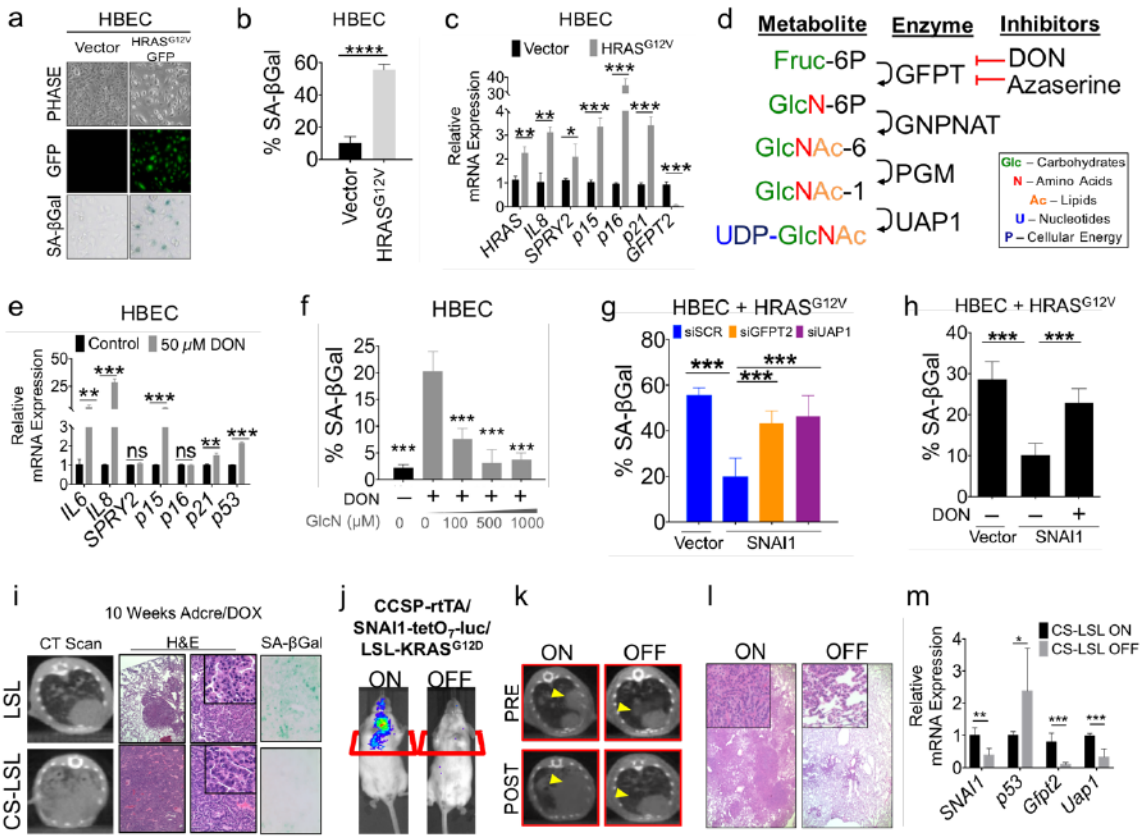

Figure 2.2 The HBP is required for EMT-mediated suppression of OIS

a-c, Human Bronchial Epithelial Cells (HBEC-3KT; HBEC) cells infected with *HRAS*^{G12D} were imaged (phase contrast, GFP fluorescence microscopy, and senescence-associated β-galactosidase (SA-βGal) staining) (**a**), quantified for SA-βGal (**b**), and analyzed for mRNA expression of senescence markers (**c**). **d,** The HBP metabolites, enzymatic steps, and the inhibitors of the pathway. **e,** qPCR of senescence gene expression in HBECs treated with high concentration (50 μM) of 6-diazo-5-oxo-L-norleucine (DON) for 48 hours. **f,** SA-βGal quantification of HBECs for metabolite rescue with glucosamine (GlcN) (P<0.001 by One-way ANOVA with Dunnett's multiple comparison test). **g, h,** SNAI1-mediated OIS suppression was assessed with genetic (**g**) or

pharmacological (**h**) inhibition of the HBP ($P<0.001$ by One-way ANOVA with Dunnett's multiple comparison test). **i,** Representative CBCT scan, H&E, and SA-βGal of lox-stop-lox-$Kras^{G12D}$ (LSL) and LSL crossed with EMT TF SNAI1 (CS-LSL). **j-m**, Representative BLI (j), CBCT (k), H&E (l), and qPCR (m) of CS-LSL mice with and without inactivation of SNAI1 expression by withdrawing DOX from mouse drinking water, while maintain expression of $Kras^{G12D}$ expression. Unless stated, error bars, mean ± s.d. P values were derived from an unpaired, two-tailed Student's t-test. (*$P<0.05$; **$P<0.01$; ***$P<0.001$).

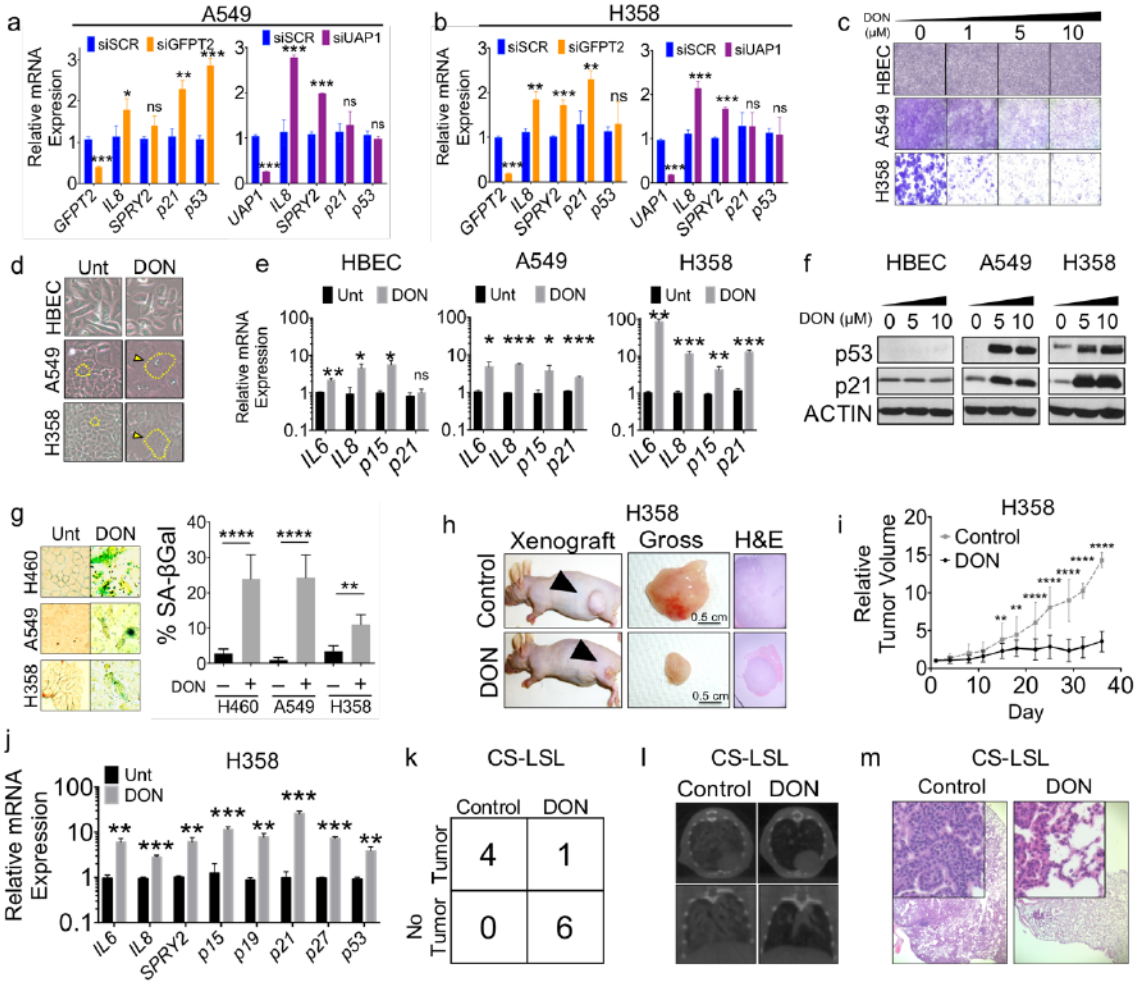

Figure 2.3 Targeting the HBP in mutant *KRAS* lung cancer cells results in senescence

a-b, qPCR for senescence genes in NSCLC cell lines following 48 hours of *GFPT2* and *UAP1* siRNA knockdown. **c-g**, Proliferative capacity (**c**), senescence morphology (**d**), senescence gene expression by mRNA (**e**), senescence protein marker expression (**f**), and SA-βGal staining (**g**) of NSCLC cell lines treated with ≤10 μM DON for 48 hours. **h-j,** Tumor appearance (**h**), quantified tumor volume (n≥10 tumors per arm; $P<0.0001$ by

two-way ANOVA followed by Holm-Sidak's multiple comparisons test) (**i**), and qPCR for senescence gene expression (**j**) of H358 NSCLC cell line xenograft in athymic nude mice treated with 20 mg/kg/week DON versus control for 5 weeks. **k-m**, Contingency table ($P<0.05$ by Fisher's exact test) (**k**), CBCT scan (**l**), and H&E (**m**) of CS-LSL mice treated with DON 20 mg/kg BID. Unless stated, error bars, mean ± s.d. *P* values were derived from an unpaired, two-tailed Student's t-test. (*$P<0.05$; **$P<0.01$; ***$P<0.001$; ****$P<0.0001$).

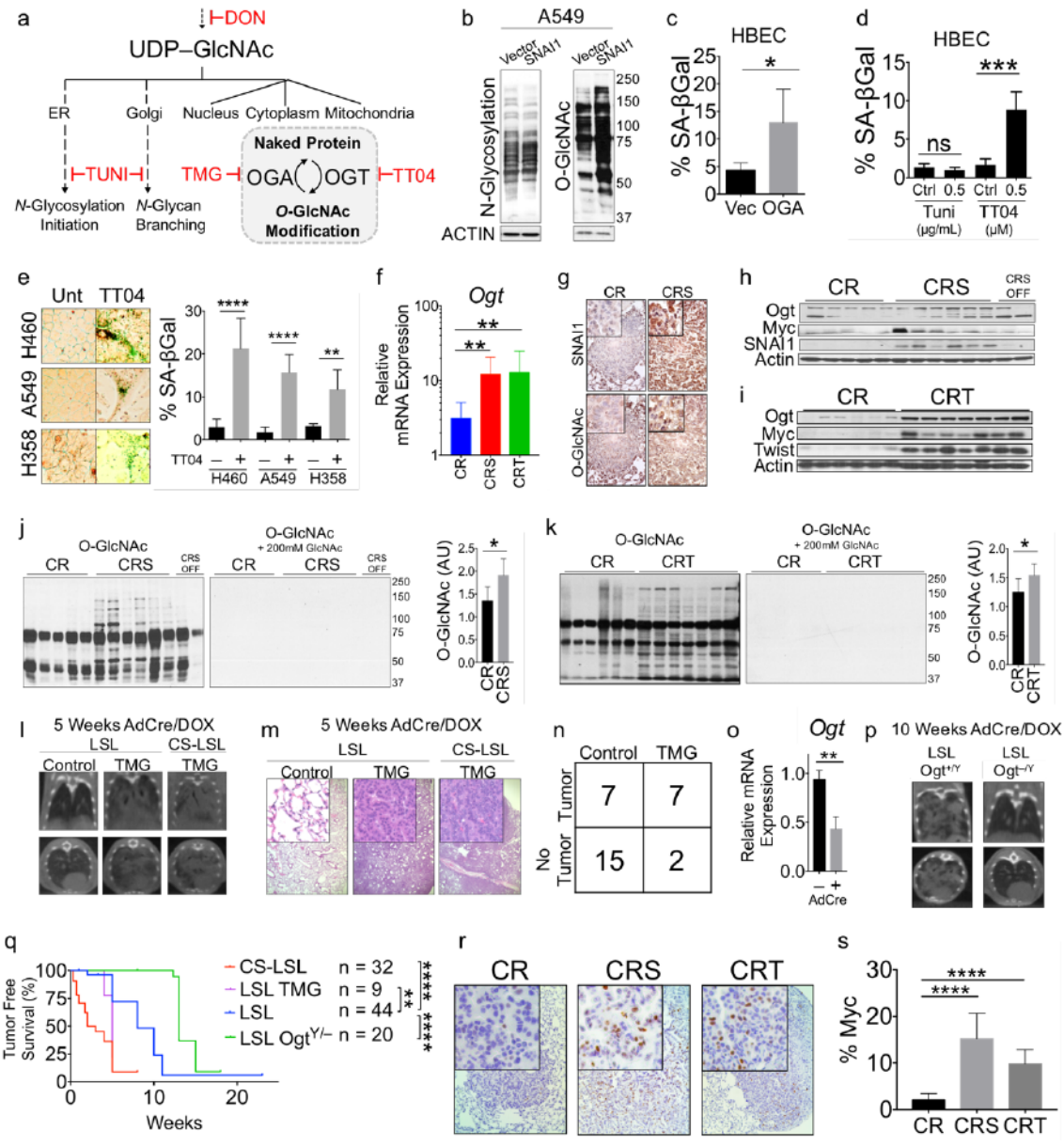

Figure 2.4 O-GlcNAcylation is required to stabilize SNAI1 and c-Myc to suppress senescence

a, Schematic of UDP-GlcNAc incorporation into N-linked and O-linked glycosylation with inhibitors (red). **b**, Effects on N-glycosylation (Concanavalin A) and O-GlcNAcylation (CTD110.6) with 48 hour SNAI1 transient expression in A549 cells. **c**, SA-βGal staining of 48 hour genetic ablation of O-GlcNAcylation via transducing HBECs with OGA overexpression viral construct. **d**, SA-βGal staining following pharmacological inhibition of N-glycosylation (0.5 μg/mL tunicamycin; TUNI) compared to OGT inhibition (0.5 μM TT04). **e**, SA-βGal staining of TT04 treated NSCLC cell lines. **f-k**, SNAI1 (CRS) and TWIST1 (CRT) EMT expressing $Kras^{G12D}$ driven mouse lung tumors mRNA expression of OGT (P<0.01 by One-way ANOVA with Dunnett's multiple comparison test) (**f**), O-GlcNAcylation by IHC (**g**), OGT protein by Western blot (**h, i**), and global O-GlcNAcylation of proteins by Western blot (**j, k**) compared to $Kras^{G12D}$ alone expressing mice (n≥5 mice per genotype). **l-n**, O-GlcNAcylation was elevated pharmacologically with 1.5 mg/mL thiamet-G (TMG) in LSL mouse drinking water and tumor burden was assessed by CBCT scans (**l**), H&E (**m**), and contingency table (P<0.05 by Fisher's exact) (**n**). **o,p,** *Ogt* mRNA expression (**o**) and tumor burden via CBCT (**p**) at 10 weeks post-intranasal administration of Ad-CMV-iCre (AdCre) in mice from $LSL\text{-}Ogt^{+/+}$ females crossed with $Ogt^{Y/fl}$ males. **q**, Tumor free survival Kaplan-Meier curves of $LSL\text{-}Kras^{G12D}$ mice (n=44 mice; median = 8 weeks post-AdCre) compared to EMT/$Kras^{G12D}$ mice (CS-LSL; n=32; median = 2 weeks post-AdCre), elevated O-GlcNAcylation mice (LSL TMG; n=9; median = 5 weeks post-AdCre), and OGT knockout mice (LSL-$OGT^{-/Y}$; n=20; median = 15 weeks) (statistical analysis by log-rank test). **r,s,** IHC for Myc in CR, CRS, and CRT tumors (**r**) with quantification (s). Error bars, mean ± standard deviation (s.d.) Unless stated, P values

were derived from an unpaired, two-tailed Student's t-test. (*P<0.05; **P<0.01; ***P<0.001; ****P<0.0001).

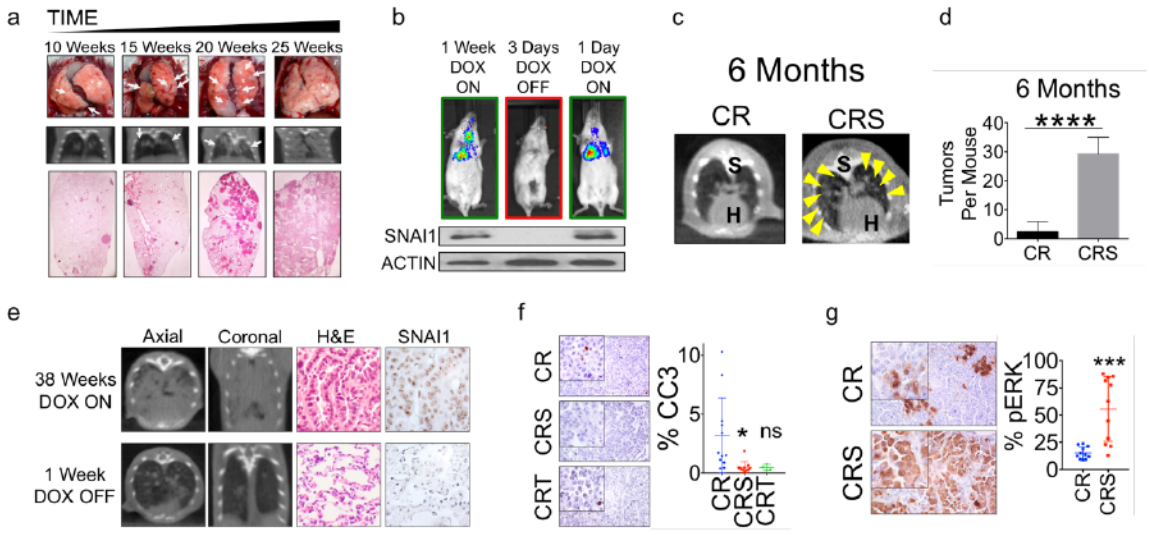

Figure 2.5 Characterizing a novel *Kras*^{G12D} driven EMT mouse model of NSCLC

a, 25 week time course of CRS mouse model with inducible SNAI1 expression monitored by gross anatomy, cone-beam computed tomography (CBCT) scans, and hematoxylin and eosin (H&E) staining. **b**, Doxycycline (DOX) inducible expression of SNAI1 was verified with bioluminescence imaging (BLI) and SNAI Western blotting. **c, d,** CR and CRS mouse tumor CBCT scans (**c**) and quantification (**d**) at 6 months. **e**, Tumor regression of CRS mice 38 weeks post-removal of DOX from mice drinking water as seen by CBCT, H&E, and SNAI1 immunohistochemistry (IHC) staining. **f**, Cleaved-caspase3 (CC3) IHC staining with quantification of EMT CRS and CRT mouse tumors compared to CR mouse lung tumors. **g**, IHC staining of phosphorylated ERK (pERK) IHC in CRS mouse tumors compared to CR mouse tumors. Error bars, mean ± standard deviation (s.d.). P values were derived from an unpaired, two-tailed Student's t-test (*P<0.05; ***P<0.001; ****P<0.0001).

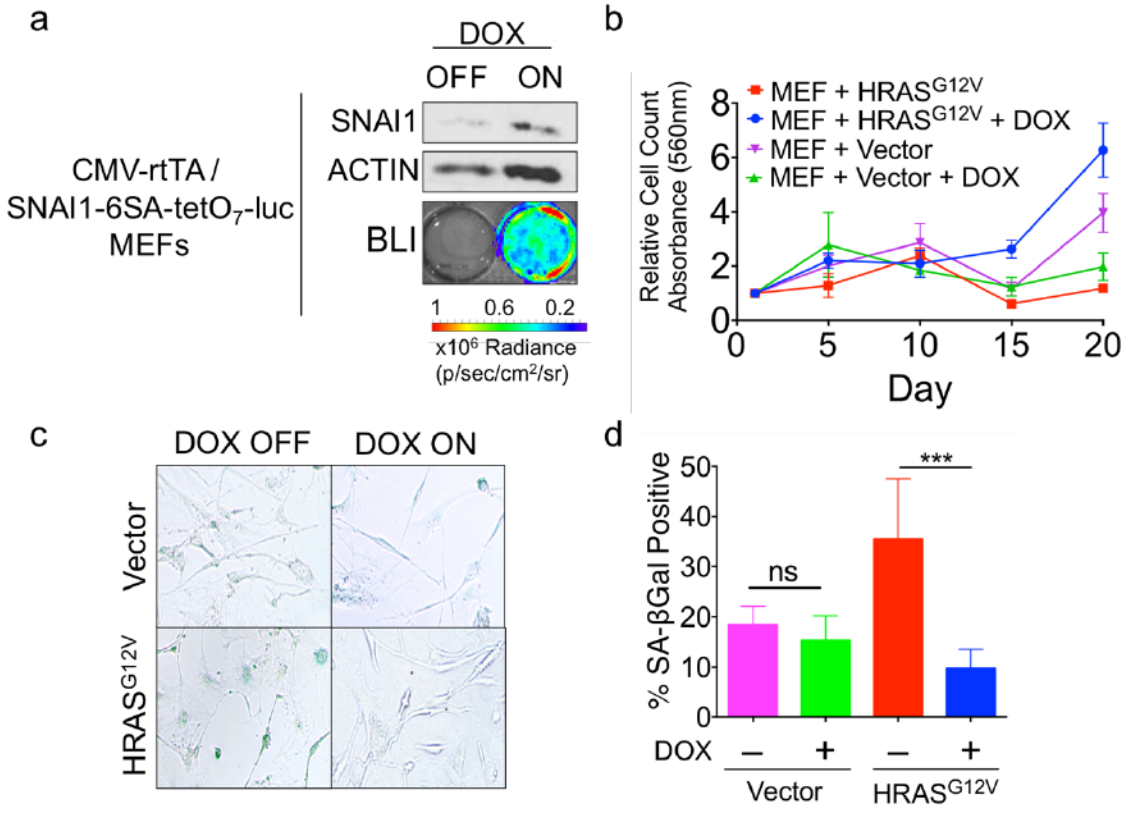

Figure 2.6 Inducible SNAI1 expressing MEFs overcome *HRAS^{G12D}* induced OIS

a, Validation of the DOX inducible SNAI1 expressing MEFs by Western blotting and luciferase reporter (visualized by BLI). **b-d**, Inducible SNAI1 MEFs were transduced with *HRAS^{G12V}* or vector control with or without SNAI1 expression (± 2μg/mL DOX in cell culture media) and relative change in cell number (**b;** *P<0.001* by two-way ANOVA followed by Holm-Sidak's multiple comparisons test), SA-βGal staining (**c, d**) were measured. Unless stated, error bars, mean ± s.d. P values were derived from an unpaired, two-tailed Student's t-test. (*ns* $P \geq 0.05$; ***$P<0.001$; ****$P<0.0001$).

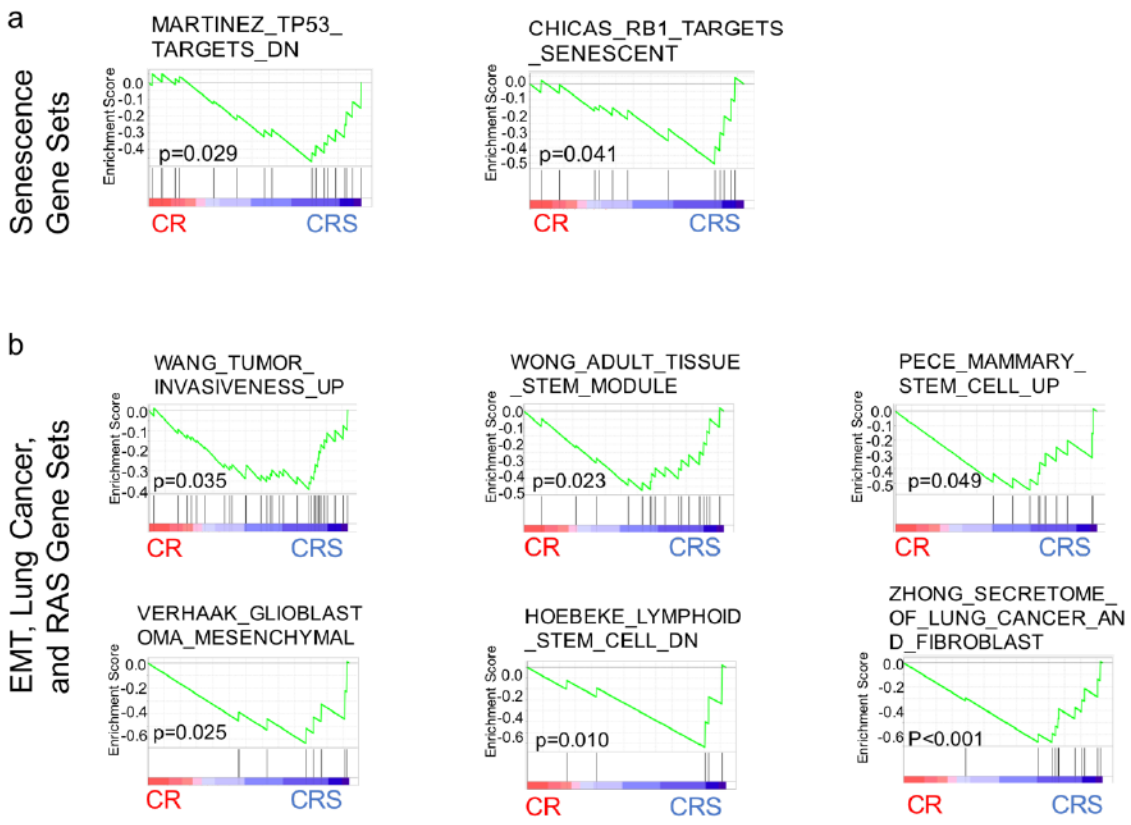

Figure 2.7 Gene expression microarray analysis of EMT NSCLC tumor cells

a, **b,** Gene Set Enrichment Analysis (GSEA) enrichment plots (data sets obtained from the Molecular Signatures Database) were generated using differentially expressed genes between CR and CRS mice and identified significantly matching gene sets involving senescence (**a**) as well as EMT, lung cancer, and RAS (**b**).

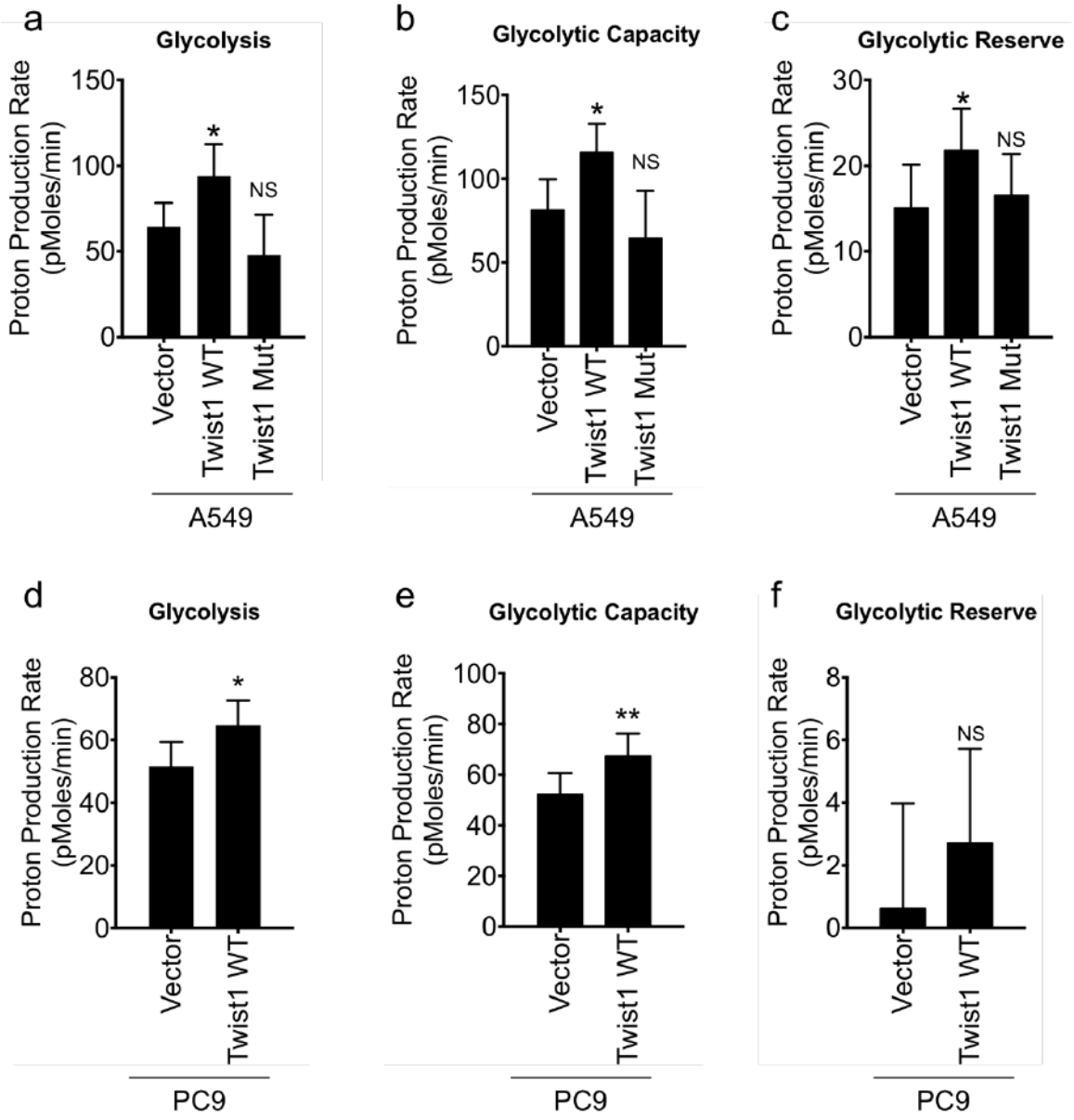

Figure 2.8 Seahorse analysis of glycolytic flux of EMT NSCLC cells

a-f, Glycolytic activity, capacity, and reserve was determined in real-time using the Seahorse extracellular flux analyzer for vector, *Twist1*, and loss of function *Twist1* in

A549 (**a-c**) and PC9 (**d-f**) cells. Error bars, mean ± s.d. P values were derived from an unpaired, two-tailed Student's t-test. (ns $P \geq 0.05$; *$P < 0.05$; **$P < 0.01$).

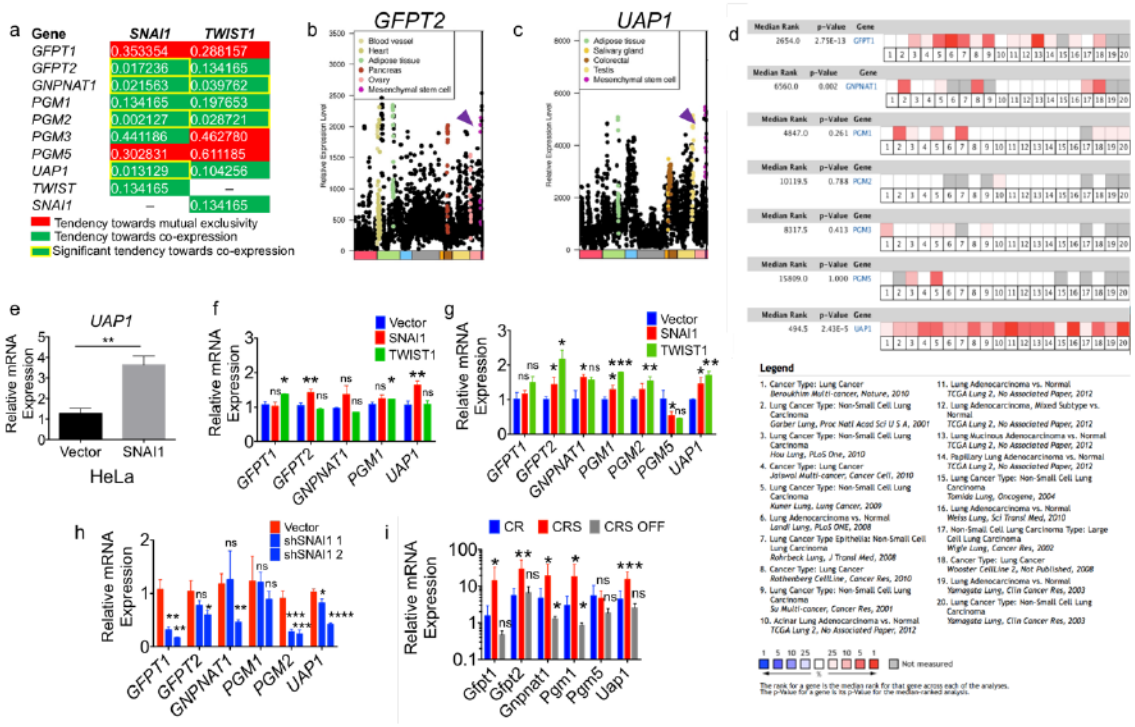

Figure 2.9 The EMT correlates with the HBP and is overexpressed in human NSCLC

a, Gene co-expression data of lung adenocarcinoma patient tumors with co-expression of EMT and HBP genes (Red – tendency towards mutually exclusivity; green – tendency towards co-expression; yellow – significance $P<0.05$). **b, c,** Human tissue gene expression from Medisapiens *In Silico* Transcriptomics (IST) from 60 healthy tissues; significant gene expression of *GFPT2* (**b**) and *UAP1* (**c**) were found in mesenchymal stem cells (purple arrows). **d**, Genes encoding steps of the HBP in lung adenocarcinoma patient tissue samples from 20 individual patient data sets using the Oncomine compendium of cancer transcriptome profiles. **e,** *UAP1* mRNA expression of HeLa cells with or without *SNAI1* DOX induced expression (±2 µg/mL DOX in cell culture media). **f-i**, mRNA expression of the HBP genes by qPCR *in vitro* with EMT expressing non-

cancer HBEC cells (**f**), the NSCLC cell lines H460 (**g**) and H358 NSCLC cell line (**h**), and *in* vivo autochthonous lung tumor mouse models with and without DOX inducible expression of *SNAI1/Kras*^{G12D} (**i**). Error bars, mean ± s.d. P values were derived from an unpaired, two-tailed Student's t-test (ns $P \geq 0.05$; *$P < 0.05$; **$P < 0.01$; ***$P < 0.001$; ****$P < 0.0001$).

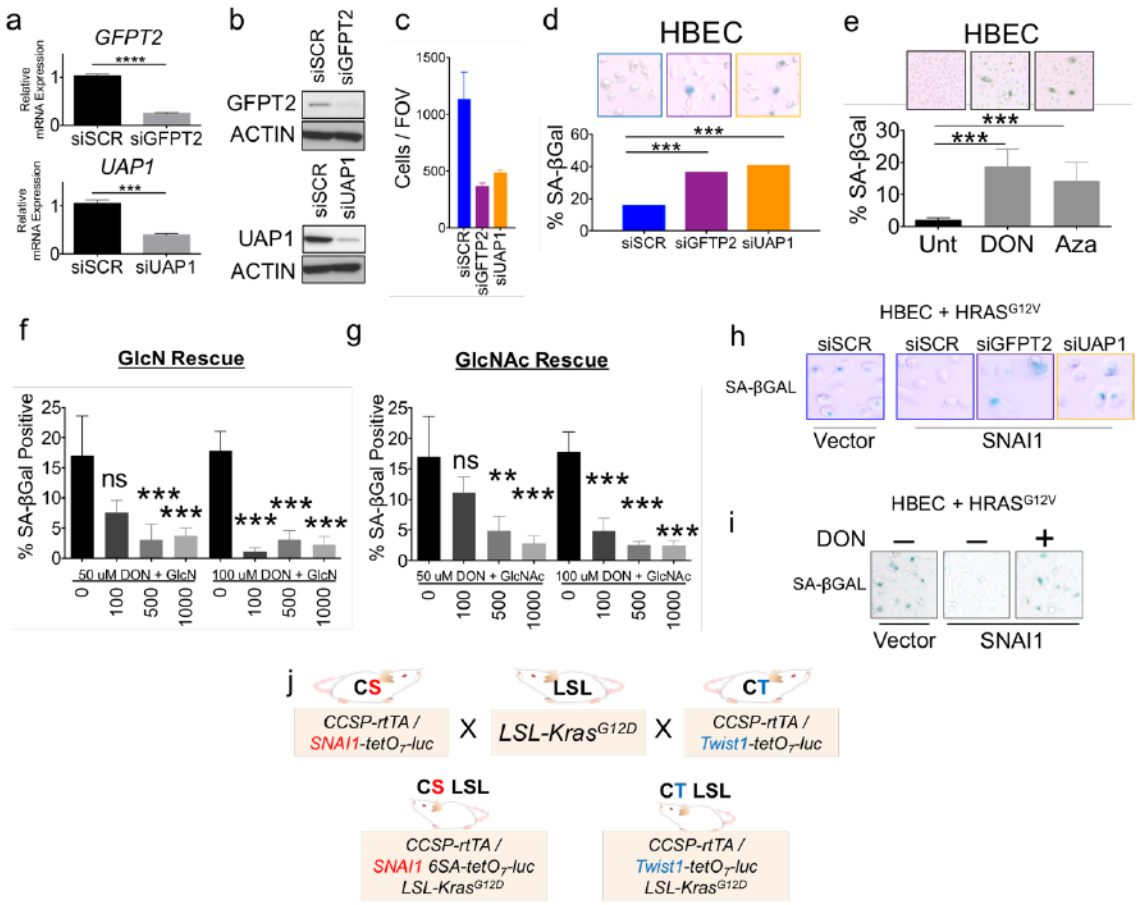

Figure 2.10 The HBP is critical for senescence of normal lung cells and the LSL lung tumor mouse model

a-d, Genetic inhibition of the HBP with knockdown of *GFPT2* and *UAP1* as shown by mRNA(**a**) and protein levels (**b**) and resulting cell number change per field of view (FOV; **c**) and SA-βGal staining (**d**) (statistical analysis by One-way ANOVA with Dunnett's multiple comparison test). **e-g,** SA-βGal staining in HBEC cells upon 48 hour pharmacological inhibition of the HBP with 50μM 6-diazo-5-oxo-L-nor-leucine (DON) and Azaserine (Aza) (**e**) and metabolic rescue by supplementation with glucosamine (GlcN; **f**) or N-acetylglucosamine (GlcNAc; **g**) (statistical analysis by One-way ANOVA

with Dunnett's multiple comparison test). **h, i**, Bright field images of SA-βGal staining using genetic siRNA (**h**) and pharmacological DON (**i**) inhibition of the HBP. **j**, Breeding schematic of the *Lox-Stop-Lox Kras*^{G12D} (LSL) model with DOX inducible lung specific expressing *SNAI1* (CS) and *Twist1* (CT) mouse models to generate DOX inducible EMT models with conditional expression of *Kras*^{G12D} upon intranasal administration of Ad-CMV-iCre (AdCre) virus. Unless stated, error bars, mean ± s.d. P values were derived from an unpaired, two-tailed Student's t-test (***P<0.001; ****P<0.0001).

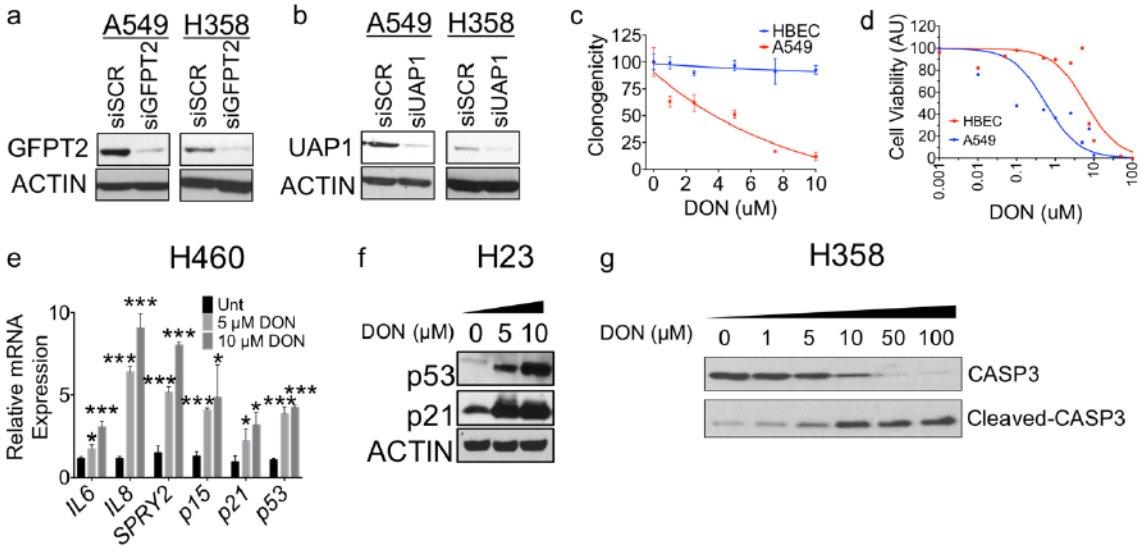

Figure 2.11 Inhibition of the HBP in human NSCLC cell lines reduces cell viability through senescence and/or apoptosis

a, b, Genetic knockdown in A549 and H358 cells with siRNA targeting *GFPT2* (**a**) and *UAP1* (**b**) confirmed on the protein level by Western blot. **c-d**, Clonogenicity measured by crystal violet stained colonies on 10 cm dishes (**c**) and cell viability analyzes by CyQuant Assay (**d**) of A549 cells after 48 hours of pharmacological inhibition of the HBP with DON treatment. **e-f**, qPCR (**e**) Western blot (**f, g**) for markers of senescence in 3 NSCLC cell lines upon 48 hour treatment of DON. Unless stated, error bars, mean ± s.d. P values were derived from an unpaired, two-tailed Student's t-test (**P*<0.05; ****P*<0.001).

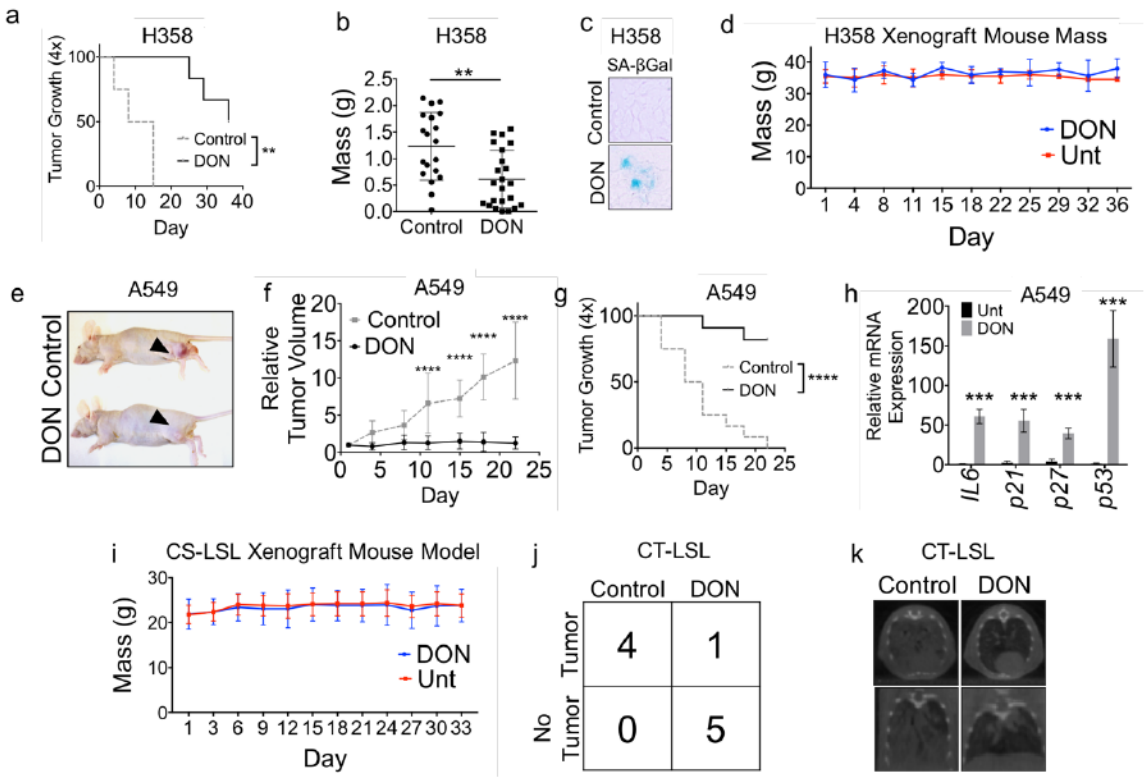

Figure 2.12 Inhibition of the HBP *in vivo* abrogates tumor growth and promotes senescence phenotypes

a-d, H358 NSCLC cells ($8x10^6$) were injected into ~5 week old athymic nude female mice. Within the first week (visible tumors of ~50 mm^3), mice were treated with 20 mg/kg/week DON and were assessed for tumor growth ($P<0.01$ by long-rank test; **a**), tumor mass (**b**), and SA-βGal staining (**c**) with no noticeable toxicities to the mice measured by body mass (**d**) ($P>0.05$ by Two-way ANOVA) over a 5 week period. **e-h**, Likewise, A549 NSCLC cells ($1x10^6$) were injected into ~5 week old athymic nude male mice and within the first week (visible tumors of ~50 mm^3) mice were treated with 20 mg/kg/week DON and were assessed for tumor size (**e**), tumor volume ($n\geq12$ tumors per arm; $P<0.0001$ by two-way ANOVA followed by Holm-Sidak's multiple comparisons

test; **f)**, tumor growth ($P<0.0001$ by log-rank test; **g**), and markers of senescence (**h**) over a 3 week period. **i**, CS-LSL mouse mass with and without DON treatment over 4 weeks ($P>0.05$ by Two-way ANOVA). **j, k**, CT-LSL contingency table ($P<0.05$ by Fisher's test) and CBCT scans (**k**) at 5 weeks post-AdCre. Unless stated, error bars, mean ± s.d. P values were derived from an unpaired, two-tailed Student's t-test. (**$P<0.01$; ***$P<0.001$; ****$P<0.0001$).

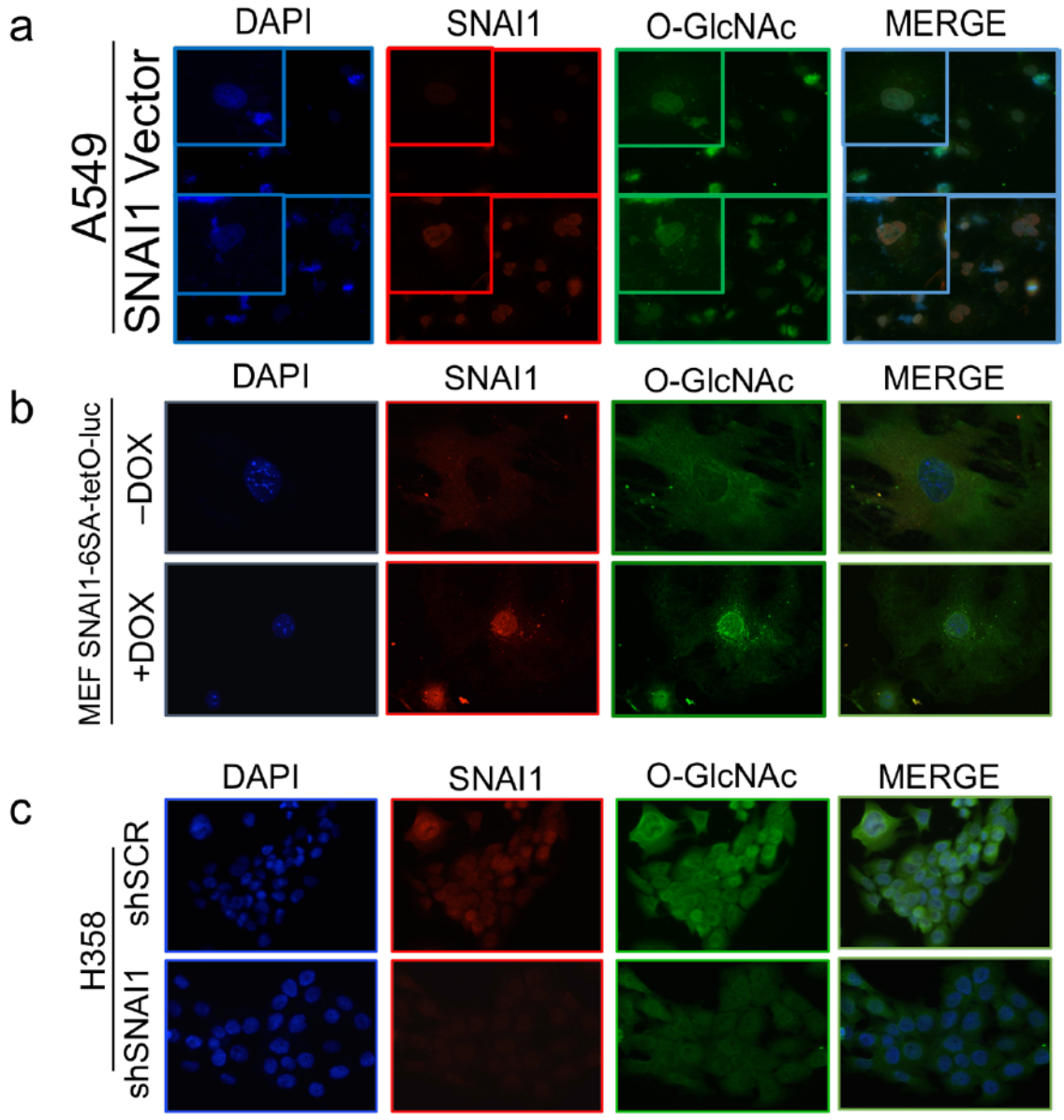

Figure 2.13 SNAI1 expression correlates with O-GlcNAcylation.

a-c, Immununofluoresence (IF) of SNAI1 and O-GlcNAc co-expressing A549 NSCLC cells (with elevated O-GlcNAc cytoplasmic immunopositive foci) (**a**), 48 hour DOX inducible SNAI1 expressing MEFs (**b**), and stable knockdown of *SNAI1* in H358 NSCLC cells (**c**) (blue – DAPI; red – SNAI1; green – O-GlcNAc [RL2]).

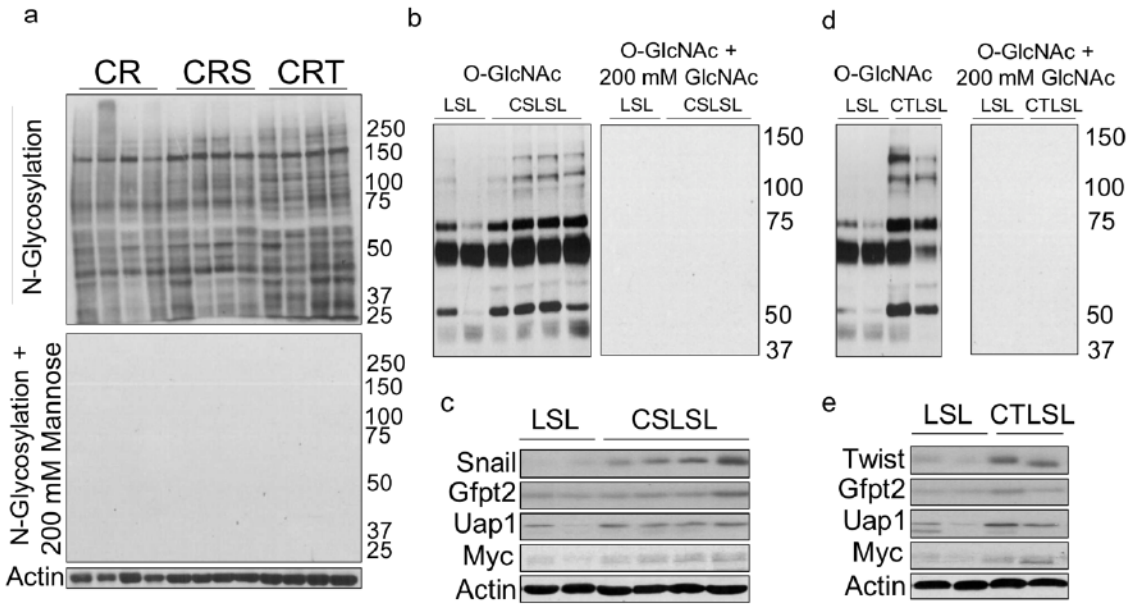

Figure 2.14 N- and O-Linked glycosylation and the HBP in novel EMT mouse models of lung cancer

a, CR, CRS, and CRT mouse tumors were assessed for N-glycosylation with the terminal glycosyl/mannosyl binding lectin (concanavalin A [conA]) and specificity of the conA lectin was assessed by blotting with 200 mM Mannose. **b-e,** LSL mouse tumors were compared to CS-LSL (**b, c**) and CT-LSL (**d, e**) mouse tumors for O-GlcNAcylation, SNAI1/TWIST, and the HBP enzymes Gftp2 and Uap1 by Western blot.

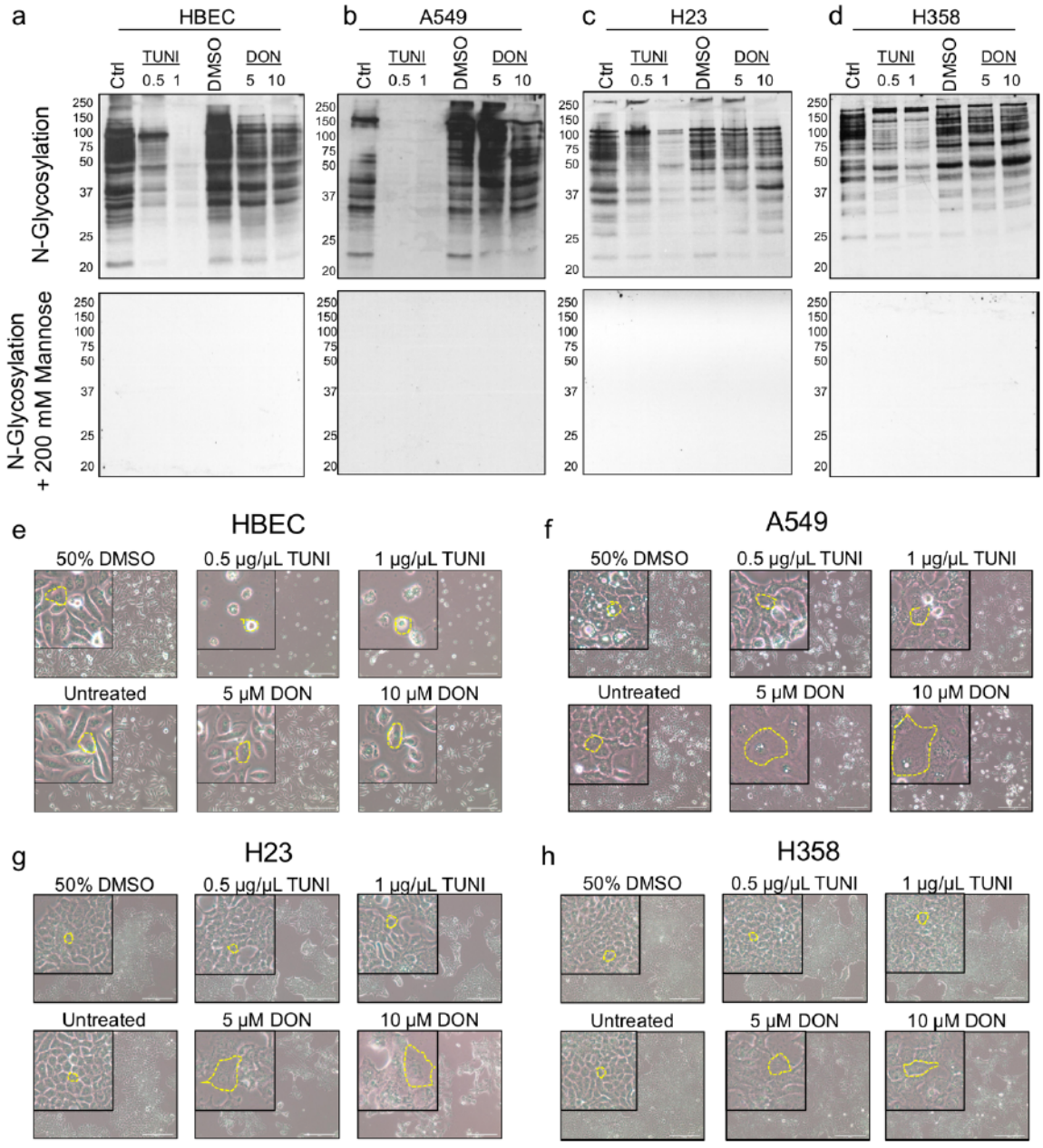

Figure 2.15 Inhibition of N-glycosylation with tunicamycin does not induce senescence phenotype, unlike inhibition of the HBP with DON

a-e, Normal (**a**) and NSCLC cells (**b-d**) were treated with either tunicamycin (TUNI, 0.5 or 1 µg/µL) or DON (5 or 10 µM) and blotted with concanavalin A (ConA) to assess N-

link glycosylation occupancy; ConA was assessed for specificity by competitive blotting with 200 mM mannose. **e-h**, Senescence morphology was seen in DON (5 or 10 μM) treated NSCLC cells, but not with TUNI treatment (0.5 or 1 μg/μL).

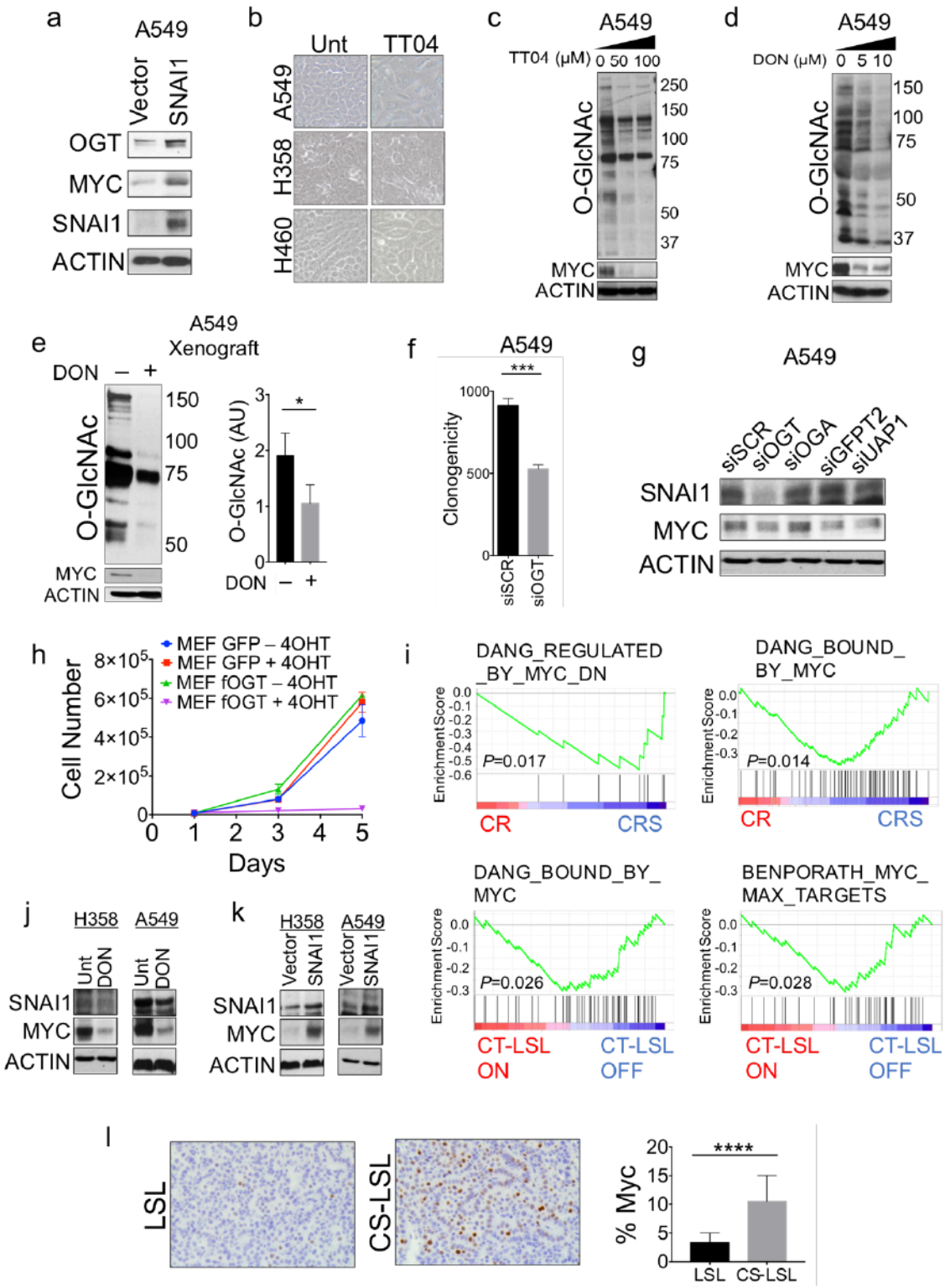

Figure 2.16 EMT elevates O-GlcNAcylation and is required to suppress senescence by stabilizing oncogenes like c-Myc

a, SNAI1 expression A549 cells and the co-expression of O-GlcNAc transferase (OGT) and c-Myc by Western blot. **b, c**, Senescence morphology as seen with phase contrast microscopy (**b**) and destabilization of c-Myc by Western blot (**c**) of in NSCLC cells treated for 48 hours with the OGT inhibitor TT04. **d, e,** O-GlcNAc reduction with treatment DON in NSCLC A549 cells *in vitro* (48 hours; **d**) and A549 xenograft *in vivo* (3 weeks, **e**). **f, g,** Clonogenic assay (**f**) and c-Myc levels by Western blot (**g**) after 48 hour transient genetic ablation of *OGT* in A549 cells. **h,** Cell proliferation over 1 week in inducible tamoxifen *OGT* knockout in MEFs ($P<0.0001$ by Two-way ANOVA). **i**, EMT models of $Kras^{G12D}$ driven lung cancer were enriched for differentially expressed genes related to MYC programs (data sets obtained from the Molecular Signatures Database). **j,k**, Western blots of SNAI1 and c-Myc levels in A549 and H358 NSCLC cell lines treated with pharmacological inhibitor of the HBP (10 μM DON) (**j**) and SNAI1 overexpressing expression cells (**k**). **l**, c-Myc IHC in SNAI1 expressing autochthonous CS-LSL mouse tumors compared to LSL $Kras^{G12D}$ alone SNAI1 increased c-Myc levels *in vivo* assessed with c-Myc. Unless stated, error bars, mean ± s.d. P values were derived from an unpaired, two-tailed Student's t-test. (****$P<0.0001$).

Chapter 3: Materials and methods

3.1 Cell lines and drug treatments

The human non-small cell lung cancer (NSCLC) cell lines (H460 and A549) and embryonic kidney cell lines, (HEK-293T and Gryphon) were obtained from ATCC and grown in media as recommended. The NSCLC cell lines (H358 and H23) and human bronchial epithelial cell (HBEC-3KT) line were gifts from Steve Baylin. $Ogt^{Y/fl}$ MEFs were generated and maintained as previously described[189]. Inducible SNAI1 MEFs were isolated from E13.5 embryos and propagated as described previously[177]. MEFs were grown for two population doublings and then frozen for future experiments. MEFs were grown in DMEM supplemented with 10% fetal calf serum. All cell lines were checked by short tandem repeat profiling and mycoplasma testing services of the Johns Hopkins Medicine Genetic Resources Core Facility. Cells were treated with the appropriate inhibitor for 48 hours prior to analysis using the following compounds: 6-Diazo-5-oxo-L-norleucine (D2141, Sigma), TT04 (ST045849, TimTec), Thiamet-G (4390, Bio-Techne), Tunicamycin (T7765, Sigma), and Azaserine (A4142, Sigma).

3.2 PCR genotyping

DNA was isolated from mouse tails by boiling in 100 µL Solution A (0.5M EDTA pH8 and 10M NaOH in diH_2O) for one hour and then adding Solution B (Tris HCl pH 8 in diH_2O). The *CCSP-rtTA* (C), *tetO7-Kras*^{G12D} (R), *Twist1-tetO7-luc* (T), and *LSL-Kras*^{G12D} (LSL) transgenic lines were screened as described previously[20]. The *SNAI1-tetO7-luc* line was detected with the following primers: SNAI1-Luc.S2 59-

CCTTATGCAGTTGCTCTCCAG -39 and SNAI1-Luc.AS2 59-GCTTGCCTATGTTCTTTTGGA -39. DNA was amplified using PCR and PCR products were resolved on a 2% agarose gel.

3.3 Transgenic mice

The human *SNAI1-6SA* cDNA[153] was PCR cloned into the bidirectional *tetO7* vector S2f-IMCg[190] at *Eco*RI and *Not*I sites, replacing the *eGFP* ORF. The resultant construct, *SNAI1-6SA-tetO7-luc*, was sequence confirmed, digested with *Kpn*I and *Xmn*I to release the bidirectional transgene and then used for injection of FVB/N pronuclei by the Stanford Transgenic Facility. We obtained one founder after screening by tail genotyping using PCR as described below. This founder was mated to *CCSP-rtTA* mice to screen for inducible *SNAI1-tetO7-luc* expression and was used for all the experiments in this study.

We use the *β-actin-rtTA*, *CCSP-rtTA*, *tetO7-Kras^{G12D}*, *Twist1-tetO7-luc*, and *LSL-Kras^{G12D}* single transgenic lines[20,182,191,192] and bred these mouse lines to generate the appropriate double and triple transgenic mouse lines. *SNAI1*, *Twist1*, and/or *Kras^{G12D}* expression was activated in the CS, CT, CR, CRS, CRT, CS-LSL, and CT-LSL lung lines by administering doxycycline (DOX, Sigma) to the drinking water [2 mg/mL] starting at the age of 4-5 weeks and was changed with fresh DOX weekly. The conditional *LSL-Kras^{G12D}* lines were activated by intranasal delivery of Ad-CMV-iCre (no. 1045, Vector Biolabs)[182]. DON (D2141, Sigma) was administered intraperitoneal (I.P.) to mice [20 mg/kg] BID and Thiamet-G (4390, Bio-Techne) was administered [1.5 mg/mL] in mouse drinking water changed every 3 days. All procedures were performed in accordance with

Stanford Administrative Panel on Lab Animal Care (APLAC) and Johns Hopkins Animal Care and Use Committee (ACUC) protocols and animals were housed in a pathogen- free environment.

3.4 *LSL-Kras^{G12D} Ogt* knockout mice

The Cre conditional X-linked *OGT$^{fl/fl}$* mouse line was genotyped and mouse lines were maintained as previously described[189]. Male *LSL-Kras^{G12D}* (LSL) mice with wildtype *OGT$^{Y/+}$* were crossed with female homozygous *OGT$^{fl/fl}$* resulting in all homozygous *OGT$^{Y/fl}$* males. Only male LSL *OGT$^{Y/fl}$* mice were used in experiments, as males were homozygous for the floxed allele compared to hemizygous females. Intranasal administration of Ad-CMV-iCre (no. 1045, Vector Biolabs) was used to infect lung epithelial cells, simultaneously inducing *Kras^{G12D}* expression while knocking out *OGT$^{Y/-}$*. *OGT* knockout was validated by qPCR from frozen lung tissue samples.

3.5 Small animal imaging and quantification

Cone-beam computed tomography (CBCT) were performed on an "in-house standalone system"[193]. The animal was placed in a rotatable animal stage lies between the stationary and parallel opposed x-ray source and the detector panel." Mice were screened serially every 1–5 weeks following doxycycline activation and/or intranasal adenoviral Ad-CMV-iCre (no. 1045, Vector Biolabs) and images were reviewed by a board certified radiation oncologist (PTT). No attenuation correction or partial volume corrections were applied. CBCT images were reviewed by a board certified radiation oncologist (PTT) for quantification at 6 months post-DOX.

3.6 Mouse xenograft model

Female athymic nude mice 4–5 weeks old were purchased from Harlan Laboratories. Mice were maintained under pathogen-free conditions and given food and water *ad libitum* in accordance with guidelines from the Johns Hopkins Animal Care and Use Committee. $1x10^{10}$ A549 cells or $8x10^{10}$ H358 cells in 100 mL of RPMI and Matrigel (BD Biosciences) mixed 1:1 were injected subcutaneously in right and left flank. Mice were split into DON treated and untreated groups ($n \geq 16$ tumors) and tumor measurements were taken every 3 days for 3-5 weeks. DON (D2141, Sigma) was dissolved in sterile diH_2O and was administered once a week intraperitoneal (I.P.) within one week post tumor injection (or when small tumors were first visible,~50 mm^3.) for 3-5 weeks. Mice were euthanized by CO_2 when tumors reached the volume of 500mm^3 (1,000mm^3 per mouse).

3.7 SYBR-green quantitative RT–PCR

Total RNA was isolated from tissue using TRIzol RNA Isolation Reagent (Life Technologies) according to the manufacturer protocol. cDNA was generated from 1 µg of total RNA using the iScript cDNA synthesis kit (Bio-Rad). cDNA was amplified with iTaq™ Universal SYBR® Green Supermix (Bio-Rad) using the CFX384 Touch Real-Time PCR Detection System (Bio-Rad) with the C1000 Touch™Thermal Cycler (Bio-Rad) for up to 40 cycles. PCR reactions were performed in at least triplicate in a final volume of 10 µL.

For every sample, the difference in cycle threshold (ΔCt) values were determined as the difference between the Ct value of a specific transcript and the Ct value of 18s rRNA, serving as the housekeeping control messenger RNA, and relative transcript levels (for example, treated versus untreated) were calculated based on $2^{(-\Delta\Delta Ct)}$ with $\Delta\Delta Ct = \Delta Ct_{treated} - \Delta Ct_{untreated}$. Primers for qPCR are listed below:

HUMAN PRIMERS

ONCOGENE INDUCED SENESENCE GENES

INK4B (*p15*)	F	AAGCTGAGCCCAGGTCTCCTA
	R	CCACCGTTGGCCGTAAACT
INK2A (*p16*)	F	CTAGACGCTGGCTCCTCAGTA
	R	GGGTTTTCGTGGTTCACATCC
CDKN1A (*p21*)	F	CGATGGAACTTCGACTTTGTCA
	R	GCACAAGGGTACAAGACAGTG
CDKN1B (*p27*)	F	ATCACAAACCCCTAGAGGGCA
	R	GGAGCCCCAATTAAAGGCG
TP53 (*p53*)	F	CCAGGGCAGCTACGGTTTC
	R	CTCCGTCATGTGCTGTGACTG
SPRY2	F	CCTACTGTCGTCCCAAGACCT
	R	GGGGCTCGTGCAGAAGAAT
IL6	F	ACTCACCTCTTCAGAACGAATTG
	R	CCATCTTTGGAAGGTTCAGGTTG

IL8	F	ACTGAGAGTGATTGAGAGTGGAC
	R	AACCCTCTGCACCCAGTTTTC

HEXOSAMINE BIOSYNTHESIS PATHWAY GENES

GFPT1	F	ACAATCGGGAAAGTCAAGATACC
	R	CACCAATCAACAGAGGGCTAC
GFPT2	F	AGACACACTTCGGCATTGC
	R	TTGGCGATGGTCTCTGTATCT
GNPNAT1	F	ACTCCTATGTTTGACCCAAGTCT
	R	TCTGTTAGCTGACCCAATACCT
PGM1	F	CCAAACCGACTGAAGATCCGT
	R	CATGTTTCGATCCCCATCTCC
PGM2	F	GAGGCAGTGAAACGACTAATAGC
	R	CTGTCCCAAACTCCATTCGGG
PGM5	F	AGCGACGGCAGGTACTTTAG
	R	CTGTCCAATAATCAGTCGTCCAA
UAP1	F	AATGACCTCAAACTCACGTTGT
	R	GCTCTGCATAAAGTTCTACCTGT

EMT GENE

SNAI1	F	TCTAGGCCCTGGCTGCTACA
	R	CTTGTGGAGCAGGGACATTCG

MOUSE PRIMERS

ONCOGENE INDUCED SENESENCE GENES

Ink4B (*p15*)	F	CCCTGCCACCCTTACCAGA
	R	CAGATACCTCGCAATGTCACG
Ink2a (*p16*)	F	GCTCAACTACGGTGCAGATTC
	R	GCACGATGTCTTGATGTCCC
Cdkn1a (*p21*)	F	CGAGAACGGTGGAACTTTGAC
	R	CCAGGGCTCAGGTAGACCTT
Cdkn1b (*p27*)	F	TCTCTTCGGCCCGGTCAATC
	R	CTCTCCACCTCCTGCCACTC
Trp53 (*p53*)	F	CCCCTGTCATCTTTTGTCCCT
	R	AGCTGGCAGAATAGCTTATTGAG
Spry2	F	TCCAAGAGATGCCCTTACCCA
	R	GCAGACCGTGGAGTCTTTCA
Il6	F	TAGTCCTTCCTACCCCAATTTCC
	R	TTGGTCCTTAGCCACTCCTTC

HEXOSAMINE BIOSYNTHESIS PATHWAY GENES

Gfpt1	F	GCCAACGCCTGCAAAATCC
	R	CCAACGGGTATGAGCTATTCC
Gfpt2	F	ATGTGCGGAATCTTTGCCTAC

	R	AGACCCCTGATAAGGGTTTCG
Gnpnat1	F	TCGTTAGTGACGAGTGCAGAG
	R	TTTGTGGTAGACATTCAAGGGTG
Pgm1	F	CAGAACCCTTTAACCTCTGAGTC
	R	CGAGAAATCCCTGCTCCCATAG
Pgm2	F	CCGCTTCTACATGACCGAGG
	R	GATGATGCAAGATACGGCAGG
Pgm5	F	GGACGGCTACTGAGATCGTG
	R	GGACCTCCATTGGCAACATTAAA
Uap1	F	GGAGTCTCATATCCCAAGGGC
	R	TGTTCTGCCGCTGGTCATTAT

3.8 Immunoblot, immunofluorescence, and lectin blot analysis

Cells were lysed on ice for 60 min in RIPA lysis buffer (R0278, Sigma) supplemented with Protease Inhibitor Cocktail (P8340, Sigma), Phenylmethylsulfonyl fluoride (PMSF; 10837091001, Sigma), β-hexosamindase inhibitor (376820, Millipore), and Thiamet-G (4390, Bio-Techne) inhibitors and clarified by centrifugation. Protein concentrations were determined by Pierce™660nm Protein Assay (Bio-Rad). Equal aliquots corresponding to 20 to 60 µg of protein were resolved on 6-12% SDS-polyacrylamide gels and transferred to PVDF or nitrocellulose membranes. Antigen detection was carried out with the antibodies against the following proteins: Actin (C-11, Santa-Cruz Biotechnology (SCBT), 1:5000), Twist1 (TWIST2C1a, SCBT, 1:100), SNAI1 (NBP1-80022, Novus, 1:2000; H-130, SCBT, 1:500), GFPT2 (EPR19095, Abcam, 1:500), UAP1

(EPR10259, Abcam, 1:500), c-Myc (Y69, Abcam/Epitomics, 1:10000), p21 (12D1, Cell Signaling Technology (CST), 1:1000), p53 (no. 9282, CST, 1:1000), OGT (DM-17, Sigma Aldrich, 1:2000), O-GlcNAc (CTD110.6, 1:2000), and cleaved caspase 3 (9664S, CS). After washing, corresponding anti-mouse IgG (GE Healthcare, 1:2500), anti-rabbit IgG (GE Healthcare, 1:2500), and anti-rabbit IgM (Sigma, 1:2500) peroxidase-conjugated secondary antibodies were used. Antigen-antibody complexes were visualized by Amersham electrochemiluminescence (ECL detection system; GE Healthcare). CTD110.6 specificity for O-GlcNAc was tested by blotting with or without 200mM N-Acetylglucosamine (GlcNAc; Sigma). Relative O-GlcNAcylated protein levels were measured by analyzing the bands density using ImageJ (http://imagej.nih.gov/ij/download.html) then normalized to the density of actin. All experiments were performed in triplicate and average relative fold changes were calculated.

For immunofluorescence, SNAI1 (H-130, SCBT, 1:50) and O-GlcNAc (RL2, Novus, 1:200) were incubated at 4° overnight. After washing, Alexa488-conjugated anti-mouse (green) and Alexa594-conjugated anti-rabbit (red) (Invitrogen, 1:300) were used as secondary antibodies and incubated at room temperature for 30 minutes. DAPI (blue) was used as a nuclear stain and slides were mounted in aqueous mounting media (Vector Laboratories).

For N-glycosylation analysis, membrane was blocked in 3% BSA in TBS, washed in TBS, and incubated at 4° overnight with Concanavalin A-HRP lectin (ConA; L6397,

Sigma, 0.25ug/ml) in high-salt TBST (HS-TBST; 1M NaCl, TBST). The blot was wash extensively in HS-TBST and developed using ECL detection system (GE Healthcare). ConA specificity was tested by blotting with or without 200mM mannose (Sigma).

3.9 Histology and immunohistochemistry

Formalin-fixed paraffin-embedded (FFPE) tissues were processed and stained with hematoxylin & eosin (H&E) according to common procedures. Tissues were prepared on plus slides antigens, antigen were retrieved with Target Retrieval Solution (S1699, Dako) and probed for antigen with the following antibodies: Ki-67 (NCL-Ki67p, Leica, 1:1000), p16 (F-12, SCBT, 1:200), pERK (4370, CST, 1:400), cleaved caspase-3 (9664, CST, 1:2000), SNAI1 (NBP-80022, Novus, 1:200), c-Myc (Y69, Abcam/Epitomics, 1:500), and O-GlcNAc (RL2, Novus, 1:200), as previously described[20,194]. For pathological analysis, a certified veterinarian pathologist (BS) reviewed the disease burden for each mouse. For immunohistochemistry analysis, immunopositive cells were counted and analyzed from at least 5 different fields of view per section from greater ($n \geq 3$ different animals) in total. For SA-β Galactosidase stain, 10μm sections were cut from Tissue-Tek cryo optimal cutting temperature compound (OCT; 14-373-65, Fisher Scientific) infused frozen lung tissue and staining was carried out as previously described[20]. H&E, tissue processing, and c-Myc IHC were performed using the Johns Hopkins Oncology Tissue Services Core Facility.

3.10 Viral transduction and siRNA transfection

Lentivirus was generated by transfecting HEK-293T cells with *SNAI1* shRNA constructs obtained from the Broad RNAi Consortium using *pLKO.1*-shRNA scramble vector (Sigma) as a negative control. H358 NSCLC cell lines were then transduced with virus as previously described[20]. Retrovirus was produced using Gryphon™ Amphotropic Packaging Cell Line (Allele Biotechnology), per company's recommendation. Early passage MEFs, non-cancer HBEC3-KT cells, and NSCLC cell lines (A549, H460, and H23) were transfected with pWZL-Hygro vector (Ador pWZL- Hygro/*SNAI1* constructs, for two successive times over a 36-h period followed by selection, as previously described for Twist1 cell lines[20]. HBEC3-KT cells were infected with OGA or green fluorescent protein (GFP) control adenovirus at a multiplicity of infection (MOI) of 50 for 6 hours, cell lysate were collected 48 hours post-transduction. For siRNA transfection, cells were transfected with ON-TARGETplus Non-targeting siRNA #1, Human *GFPT2* SMARTpool siRNA (L-010390-00-0005, Dharmacon), Human *UAP1* SMARTpool siRNA (L-017160-01-0005, Dharmacon), or Human *OGT* SMARTpool siRNA (L-019111-00-0005, Dharmacon) for a final concentration 50nM. Samples were analyzed 48 hours post-transfection.

3.11 Colony formation and proliferation assays

Cells were transiently transfected with *OGT* siRNA and plated at 500 cells per 10 cm dish. After 2 weeks, colonies were fixed and stained with crystal violet (0.5% in 95% methanol, Sigma) and stained colonies (defined as ≥50 cells) were counted. Quantification of MEFs was performed as previously described[165] by using crystal violet

staining and quantification by spectrophotometer. For all other cell proliferation experiments, CyQUANT® NF Cell Proliferation assay kit (Molecular Probes; Invitrogen Corp., USA) was used to minimize influence of mitochondrial metabolism, according to the manufacture protocol.

3.12 Senescence associated-β-gal staining

After genetic or pharmacological treatment, non-cancer and cancer cells were washed twice with phosphate-buffered saline (PBS) and then fixed with PBS containing 2% formaldehyde and 0.2% glutaraldehyde for 5 min. The cells were then incubated at 37°C overnight with staining solution (no. 9860, Cell Signaling). After incubation, cells were washed twice with PBS and viewed with bright-field microscopy. Cell number was measured by analyzing using the cell count feature of ImageJ (http://imagej.nih.gov/ij/download.html). All experiments were performed in triplicate and average relative fold changes were calculated.

3.13 Microarray data processing and analysis

Total RNA was isolated and purified from cells using TRIzol RNA Isolation Reagent (Life Technologies) as detailed by the manufacture's recommendation with tissue homogenization. Labeled RNA was hybridized to the Illumina Mouse WG-6 Expression Array and scanned as previously described[195]. Gene expression data were normalized using the Robust Multichip Average in the oligo Bioconductor package at the transcript level[196] Genes and gene sets with Benjamini-Hochberg[197] P values below 0.05 were considered statistically significant. Gene set enrichment analysis was performed using the

C2 Curated Gene Sets collection from the Molecular Signature Database 3.0 and statistical comparisons by Fisher exact test. The microarray data will be deposited to the Gene Expression Omnibus.

3.14 Determining differentially expressed genes, enriched gene sets, and gene ontology

Non-specific filtering was used to remove genes with an interquartile range less than 0.05. To find differentially expressed genes between EMT/$Kras^{G12D}$ driven tumors versus $Kras^{G12D}$ alone, Significance Analysis of Microarray28 (''samr'' R package version 2.0) was applied using a two class unpaired comparison, minimal Z-score fold change of 1.2, and median false discovery rate of 0.05[197]. Unannotated transcripts were not considered. To test whether gene sets were enriched in response to different conditions, we used Gene Set Analysis as implemented in the ''GSA'' R package version 1.0329. The ''max mean'' test statistic was used to test enrichment using a two-class comparison. All *p*-values and false discovery rates were based on 500–1,000 permutations. For re-standardization, a method that combines randomization and permutation to correct permutation values of the test statistic and to take into account the overall distribution of individual test statistics, the entire data set was used rather than only the genes in the gene sets tested. Gene Ontology for comprehensive protein evolutionary and functional classification was performed using Protein Analysis THrough Evolutionary Relationships (PANTHER; http://pantherdb.org).

3.15 Measurement of oxygen consumption rate (OCR) and proton production rate (PPR)

Assessment of cellular respiration and aerobic glycolysis was performed by measuring OCR and PPR with a Seahorse Bioscience XF24 Extracellular Flux Analyzer (Seahorse Bioscience, North Billerica, MA) as previously described[198]. Briefly, cell lines were plated in standard growth media at a density of $4x10^4$ cells per well 24 hours prior to metabolic analysis. To measure OCR, 1 hour prior to metabolic analysis the normal growth media was replaced with XF minimal basal medium (Seahorse Bioscience) supplemented with 11 mM glucose, 1 mM sodium pyruvate, and 1X GlutaMax (Life Technologies, Grand Island, NY). To measure PPR, 1 hour prior to metabolic analysis the normal growth media was replaced with XF minimal basal medium (Seahorse Bioscience) supplemented with 11 mM glucose and 1X GlutaMax (Life Technologies). After changing to respective XF media, cells were incubated at 37°C in a humidified atmosphere without CO_2. Oligomycin (1 uM), FCCP (400 nM), rotenone (2 uM) and antimycin A (2 uM), and 2-deoxy-D-glucose (100 mM) were added serially to determine mitochondrial respiration measurements. Oligomycin (1 uM) and 2-deoxy-D-glucose (100 mM) were added serially to determine glycolytic capacity measurements. Data presented are normalized per cell number per well.

3.16 Statistics

Based on previous experience with our *Kras*^{G12D} transgenic lung cancer mouse models, the sample sizes used typically reflect three or more individual primary tumors, each from different mice (that is, biological, not technical replicates). The survival and tumor

latency of mouse cohorts was calculated using Kaplan–Meier estimation and compared with the log-rank (Mantel–Cox) test. Statistical analysis of pharmacological treatments (TMG and DON) and contingency tables were calculated using Fisher's exact test. Statistical analysis of the data was performed using a two-tailed, unpaired Student's t-test. Values are expressed as mean ± standard deviation, where appropriate. Significance is noted as $P<0.05$ unless stated. (*P , 0.05; **P , 0.01; ***P , 0.001).

Chapter 4: Discussion

4.1 Intersection of glycobiology and cancer research

Many of the fundamental discoveries in cancer biology have built upon the field of cancer genetics. These historical discoveries are making a real impact in clinics as physicians strive to implement "precision medicine", that is the specific treatment catered to the genetic drivers in the patient's tumor. Furthermore, our understanding of the human proteome has helped identify the functional components of the cancer cell. Despite these advancements in genomics and proteomics, our understanding of the complete set of carbohydrate modifications of cancer, that is to say glycomics, has lagged behind due to technological challenges. However, as the field of glycobiology is becoming of increasing appreciation and the tools that we can use to study this field are on the rise, we are in an era of great appreciation for how sugar modifications can alter the cellular signaling and behavior of cancer cells. It is not surprising that over half of the literature on O-GlcNAcylation and cancer, for example, has been published just in the past three years. This exponential rate of discovery has been due in part to increasing interest in the field. As discussed in the introduction, many of the key targets in cancer biology are modulated by sugar modifications and these glycosylations provide an additional layer of complexity, shedding new light on the fundamental mechanisms of the cancer cell. By gaining new insights, it is apparent that we will discover new methods of targeting tumors for the benefit of future patients. At the time of this thesis, the field of glycobiology is gaining traction at a time of the revolutionary new cancer immunotherapies. Seeing as many of these immunological receptors are glycosylated, I

envision the field of "glycoimmunology" or "immunoglycobiology" to be a rapidly expanding field in the near future.

4.2 Future Directions

There are many next steps that pertain to the research outlined in this thesis:

1. *How does EMT regulate the HBP?* The precise transcriptional mechanism by which EMT controls the gene expression of the HBP has yet to be elucidated. In data not shown here, preliminary data shows that all of the HBP genes contain consensus sequences for the EMT transcription factors SNAI1 and TWIST1. Preliminary ChIP data did not show direct binding to these predicted binding sites, although much more extensive optimization is required. It is also possible that there is a mechanism beyond direct EMT TF binding to the promoter regions of the genes of the HBP.
2. *Are other EMT TFs O-GlcNAcylated?* This is a question that may be easy to validate. As discussed in the introduction, SNAI1 was identified to be O-GlcNAcylated[155]. This leads to the thought that the EMT-HBP axis discussed in this thesis may serve as a positive feedback loop to stabilize SNAI1. It would be also interesting to see if the TWIST and ZEB family of EMT TFs are also regulated by O-GlcNAcylation.
3. *What is the role of c-Myc O-GlcNAcylation in OIS suppression?* The oncoprotein c-Myc was demonstrated to be elevated via the EMT-HBP axis in this thesis. The conclusion is logical that the EMT-HBP axis is probably leading to the direct O-GlcNAcylation and stabilization of c-Myc. However, it is unclear if this

correlation is necessary for suppression of OIS. Experiments may be done to inhibit the glycosylation or expression of c-Myc to see if O-GlcNAcylated c-Myc is required for acceleration of tumorigenesis.

4. *What are other O-GlcNAcylated targets that are elevated in response to the EMT-HBP axis?* From reviewing the data, it is apparent that there are multiple O-GlcNAcylated proteins/bands that are elevated during EMT. As mentioned in this thesis, c-Myc is one of those targets. However, it will be interesting to identify other EMT-HBP axis specific targets to understand the mechanism better. Mass spectroscopy technology could possibly identify these O-GlcNAcylated targets, as people in the field are currently optimizing this protocol. It would be very appealing to see if immunological receptors such as PD-L1 are also modulated this way to provide cancer some type of immunological resistance.
5. *Does the EMT-HBP axis engender radioresistance?* There is some evidence to suggest the HBP and O-GlcNAcylation have effects on DNA damage response. Thus next step will be to assess if the EMT-HBP axis is sufficient to provide radiation therapy resistance to tumors. These experiments can also be assessed in our *in vivo* mouse models described in this paper. Likewise, it will be of importance to see if the inhibition of the HBP in EMT/mutant *KRAS* lung cancer will sensitize the tumors to radiation therapy.
6. *Do more specific inhibitors of the HBP demonstrate the same effect?* There are currently laboratories synthesizing novel compounds to inhibit the HBP (UAP1 inhibitor). Seeing as UAP1 was one of the significantly altered genes expressed in EMT mice compared to mutant *Kras* expressing mice alone, it may be interesting

to see if targeting UAP1 yields the same effect as the dirty inhibitors DON and Azaserine regarding anti-tumor response and induction of senescence programs.

4.3 Summary

The data presented in this thesis provide novel insight into cancer biology. It uniquely ties together the fields of epithelial plasticity, senescence, glycobiology, and lung cancer. The research outlined demonstrates a novel mechanism by which an epithelial plasticity program alters cancer metabolism to accelerate the formation of lung cancer by suppressing oncogene induced senescence. The novelty of our laboratory definitely comes from our lab's history of working with novel advanced autochthonous mouse models of mutant *KRAS* and EMT. The flexibility of the system allowed us to also cross in the $OGT^{fl/fl}$ mouse model normally utilized in cardio and neuroscience research. This provided a unique opportunity to study the phenomenon not only *in vitro*, but most importantly *in vivo* in a cancer mouse model that closely recapitulates the autochthonous formation of lung tumors in humans. We also demonstrated through this mechanism that inhibition of this pathway leads to stunted tumorigenesis as well as tumor regression *in vivo*. Overall, this thesis provides evidence for a novel EMT-HBP axis that is implicated in mutant *KRAS* lung tumorigenesis and future studies will need to be conducted to fine-tune the precise mechanism and identify key players by which this novel pathway suppresses OIS to facilitate this phenomenon.

References

1. Warburg, O. On the Origin of Cancer Cells. *Science (80-.).* **123,** 309–14 (1956).

2. Warburg, O. Injuring of Respiration the Origin of Cancer Cells. *Science (80-.).* **123,** 309–14 (1956).

3. Koppenol, W. H., Bounds, P. L. & Dang, C. V. Otto Warburg's contributions to current concepts of cancer metabolism. *Nat. Rev. Cancer* **11,** 325–337 (2011).

4. Hanahan, D. & Weinberg, R. A. Hallmarks of cancer: the next generation. *Cell* **144,** 646–74 (2011).

5. Cairns, R. a, Harris, I. S. & Mak, T. W. Regulation of cancer cell metabolism. *Nat. Rev. Cancer* **11,** 85–95 (2011).

6. Potter, V. R. The biochemical approach to the cancer problem. *Fed. Proc.* **17,** 691–7 (1958).

7. Vander Heiden, M. G., Cantley, L. C. & Thompson, C. B. Understanding the Warburg effect: the metabolic requirements of cell proliferation. *Science* **324,** 1029–1033 (2009).

8. Kennedy, K. M. & Dewhirst, M. W. Tumor metabolism of lactate: the influence and therapeutic potential for MCT and CD147 regulation. *Futur. Oncol* **6,** 127–148 (2010).

9. Feron, O. Pyruvate into lactate and back: From the Warburg effect to symbiotic energy fuel exchange in cancer cells. *Radiother. Oncol.* **92,** 329–333 (2009).

10. Semenza, G. L. Tumor metabolism: Cancer cells give and take lactate. *J. Clin. Invest.* **118,** 3835–3837 (2008).

11. Yi, W. *et al.* Phosphofructokinase 1 Glycosylation Regulates Cell Growth and Metabolism. *Science (80-.).* **337,** (2012).

12. Lau, K. S. & Dennis, J. W. N-Glycans in cancer progression. *Glycobiology* **18,** 750–760 (2008).

13. Taniguchi, N. & Kizuka, Y. Glycans and cancer: role of N-glycans in cancer biomarker, progression and metastasis, and therapeutics. *Adv. Cancer Res.* **126,** 11–51 (2015).

14. Love, D. & Hanover, J. The hexosamine signaling pathway: deciphering the 'O-GlcNAc code'. *Sci. STKE* **2005,** re13 (2005).

15. Hanover, J. a., Krause, M. W. & Love, D. C. The hexosamine signaling pathway: O-GlcNAc cycling in feast or famine. *Biochim. Biophys. Acta - Gen. Subj.* **1800,** 80–95 (2010).

16. Ferrer, C. M. *et al.* O-GlcNAcylation Regulates Cancer Metabolism and Survival Stress Signaling via Regulation of the HIF-1 Pathway. *Mol. Cell* **54,** 820–831 (2014).

17. Vasconcelos-dos-Santos, A. *et al.* Biosynthetic Machinery Involved in Aberrant Glycosylation: Promising Targets for Developing of Drugs Against Cancer. *Front. Oncol.* **5,** 1–23 (2015).

18. Lamouille, S., Xu, J. & Derynck, R. Molecular mechanisms of epithelial-mesenchymal transition. *Nat. Rev. Mol. Cell Biol.* **15,** 178–96 (2014).

19. Smit, M. a. & Peeper, D. S. Deregulating EMT and Senescence: Double Impact by a Single Twist. *Cancer Cell* **14,** 5–7 (2008).

20. Tran, P. T. *et al.* Twist1 Suppresses Senescence Programs and Thereby Accelerates and Maintains Mutant Kras-Induced Lung Tumorigenesis. *PLoS Genet.* **8,** e1002650 (2012).

21. Ansieau, S. *et al.* Induction of EMT by twist proteins as a collateral effect of tumor-promoting inactivation of premature senescence. *Cancer Cell* **14,** 79–89 (2008).

22. Shaul, Y. D. *et al.* Dihydropyrimidine Accumulation Is Required for the Epithelial-Mesenchymal Transition. *Cell* **158,** 1094–1109 (2014).

23. Hay, E. D. An overview of epithelio-mesenchymal transformation. *Acta Anat. (Basel).* **154,** 8–20 (1995).

24. Thiery, J. P., Acloque, H., Huang, R. Y. J. & Nieto, M. A. Epithelial-Mesenchymal Transitions in Development and Disease. *Cell* **139,** 871–890 (2009).

25. Schnaper, H. W., Hayashida, T., Hubchak, S. C. & Poncelet, A.-C. TGF-β signal transduction and mesangial cell fibrogenesis. *Am. J. Physiol. - Ren. Physiol.* **284,** F243–F252 (2003).

26. Margadant, C. & Sonnenberg, A. Integrin-TGF-beta crosstalk in fibrosis, cancer and wound healing. *EMBO Rep.* **11,** 97–105 (2010).

27. Yan, C. *et al.* Epithelial to mesenchymal transition in human skin wound healing is induced by tumor necrosis factor-alpha through bone morphogenic protein-2. *Am. J. Pathol.* **176,** 2247–2258 (2010).

28. Brabletz, T. EMT and MET in Metastasis: Where Are the Cancer Stem Cells? *Cancer Cell* **22,** 699–701 (2012).

29. Singh, a & Settleman, J. EMT, cancer stem cells and drug resistance: an emerging axis of evil in the war on cancer. *Oncogene* **29,** 4741–4751 (2010).

30. Mani, S. a *et al.* The epithelial-mesenchymal transition generates cells with properties of stem cells. *Cell* **133,** 704–15 (2008).

31. Fuxe, J., Vincent, T. & De Herreros, A. G. Transcriptional crosstalk between TGFβ and stem cell pathways in tumor cell invasion: Role of EMT promoting Smad complexes. *Cell Cycle* **9,** 2363–2374 (2010).

32. Nieto, M. A. The snail superfamily of zinc-finger transcription factors. *Nat. Rev. Mol. Cell Biol.* **3,** 155–166 (2002).

33. Kang, Y. & Massagué, J. Epithelial-mesenchymal transitions: Twist in development and metastasis. *Cell* **118,** 277–279 (2004).

34. Peinado, H., Olmeda, D. & Cano, A. Snail, Zeb and bHLH factors in tumour progression: an alliance against the epithelial phenotype? *Nat. Rev. Cancer* **7,** 415–428 (2007).

35. Tam, W. L. & Weinberg, R. a. The epigenetics of epithelial-mesenchymal plasticity in cancer. *Nat. Med.* **19,** 1438–49 (2013).

36. Moreno-Bueno, G., Portillo, F. & Cano, a. Transcriptional regulation of cell polarity in EMT and cancer. *Oncogene* **27,** 6958–6969 (2008).

37. Díaz, V., Viñas-Castells, R. & García de Herreros, a. Regulation of the protein stability of EMT transcription factors. *Cell Adh. Migr.* **8,** 418–28 (2014).

38. Yilmaz, M. & Christofori, G. EMT, the cytoskeleton, and cancer cell invasion. *Cancer Metastasis Rev.* **28,** 15–33 (2009).

39. van Roy, F. Beyond E-cadherin: roles of other cadherin superfamily members in cancer. *Nat. Rev. Cancer* **14,** 121–34 (2014).

40. Araki, K. *et al.* E/N-cadherin switch mediates cancer progression via TGF-β-induced epithelial-to-mesenchymal transition in extrahepatic cholangiocarcinoma. *Br. J. Cancer* **105,** 1885–93 (2011).

41. Gheldof, A. & Berx, G. Cadherins and epithelial-to-mesenchymal transition. *Prog. Mol. Biol. Transl. Sci.* **116,** 317–36 (2013).

42. Vesuna, F., van Diest, P., Chen, J. H. & Raman, V. Twist is a transcriptional repressor of E-cadherin gene expression in breast cancer. *Biochem. Biophys. Res. Commun.* **367,** 235–41 (2008).

43. Sánchez-Tilló, E. *et al.* ZEB1 represses E-cadherin and induces an EMT by recruiting the SWI/SNF chromatin-remodeling protein BRG1. *Oncogene* **29,**

3490–3500 (2010).

44. Batlle, E. *et al.* The transcription factor snail is a repressor of E-cadherin gene expression in epithelial tumour cells. *Nat. Cell Biol.* **2,** 84–89 (2000).

45. Corallino, S., Malabarba, M. G., Zobel, M., Di Fiore, P. P. & Scita, G. Epithelial-to-Mesenchymal Plasticity Harnesses Endocytic Circuitries. *Front. Oncol.* **5,** 45 (2015).

46. Nakaya, Y. & Sheng, G. EMT in developmental morphogenesis. *Cancer Lett.* **341,** 9–15 (2013).

47. Revenu, C. & Gilmour, D. EMT 2.0: shaping epithelia through collective migration. *Curr. Opin. Genet. Dev.* **19,** 338–342 (2009).

48. Friedl, P. & Gilmour, D. Collective cell migration in morphogenesis, regeneration and cancer. *Nat. Rev. Mol. Cell Biol.* **10,** 445–457 (2009).

49. Stallings-Mann, M. L. *et al.* Matrix Metalloproteinase Induction of Rac1b, a Key Effector of Lung Cancer Progression. *Sci. Transl. Med.* **4,** 142ra95–142ra95 (2012).

50. Zheng, G. *et al.* Disruption of E-cadherin by matrix metalloproteinase directly mediates epithelial-mesenchymal transition downstream of transforming growth factor-beta1 in renal tubular epithelial cells. *Am. J. Pathol.* **175,** 580–591 (2009).

51. Nelson, C. M., Khauv, D., Bissell, M. J. & Radisky, D. C. Change in cell shape is required for matrix metalloproteinase-induced epithelial-mesenchymal transition of mammary epithelial cells. *J. Cell. Biochem.* **105,** 25–33 (2008).

52. Szabova, L., Chrysovergis, K., Yamada, S. S. & Holmbeck, K. MT1-MMP is required for efficient tumor dissemination in experimental metastatic disease. *Oncogene* **27,** 3274–81 (2008).

53. Wu, Y. & Zhou, B. P. More than EMT. *Cell Adhes. Migr.* **4,** 199–203 (2010).

54. López-Novoa, J. M. & Nieto, M. A. Inflammation and EMT: an alliance towards organ fibrosis and cancer progression. *EMBO Mol. Med.* **1,** 303–14 (2009).

55. Cha, Y. H., Yook, J. I., Kim, H. S. & Kim, N. H. Catabolic metabolism during cancer EMT. *Arch. Pharm. Res.* **38,** 313–20 (2015).

56. Wise, D. R. *et al.* Myc regulates a transcriptional program that stimulates mitochondrial glutaminolysis and leads to glutamine addiction. *Proc. Natl. Acad. Sci. U. S. A.* **105,** 18782–18787 (2008).

57. DeBerardinis, R. J. *et al.* Beyond aerobic glycolysis: transformed cells can engage in glutamine metabolism that exceeds the requirement for protein and nucleotide

synthesis. *Proc Natl Acad Sci U S A* **104,** 19345–19350 (2007).

58. Eagle, H. Nutrition needs of mammalian cells in tissue culture. *Science* **122,** 501–14 (1955).

59. Marshall, S., Bacote, V. & Traxinger, R. R. Discovery of a metabolic pathway mediating glucose-induced desensitization of the glucose transport system: Role of hexosamine biosynthesis in the induction of insulin resistance. *J. Biol. Chem.* **266,** 4706–4712 (1991).

60. Abdel Rahman, A. M., Ryczko, M., Pawling, J. & Dennis, J. W. Probing the Hexosamine Biosynthetic Pathway in Human Tumor Cells by Multitargeted Tandem Mass Spectrometry. *ACS Chem. Biol.* **8,** 2053–2062 (2013).

61. Nakajima, K. *et al.* Simultaneous determination of nucleotide sugars with ion-pair reversed-phase HPLC. *Glycobiology* **20,** 865–71 (2010).

62. Marshall, S., Nadeau, O. & Yamasaki, K. Dynamic actions of glucose and glucosamine on hexosamine biosynthesis in isolated adipocytes: differential effects on glucosamine 6-phosphate, UDP-N-acetylglucosamine, and ATP levels. *J. Biol. Chem.* **279,** 35313–9 (2004).

63. Caldwell, S. a *et al.* Nutrient sensor O-GlcNAc transferase regulates breast cancer tumorigenesis through targeting of the oncogenic transcription factor FoxM1. *Oncogene* **29,** 2831–2842 (2010).

64. Krzeslak, A., Forma, E., Bernaciak, M., Romanowicz, H. & Brys, M. Gene expression of O-GlcNAc cycling enzymes in human breast cancers. *Clin Exp Med* **12,** 61–65 (2012).

65. Broschat, K. O. *et al.* Kinetic characterization of human glutamine-fructose-6-phosphate amidotransferase I. Potent feedback inhibition by glucosamine 6-phosphate. *J. Biol. Chem.* **277,** 14764–14770 (2002).

66. Wellen, K. E. *et al.* The hexosamine biosynthetic pathway couples growth factor-induced glutamine uptake to glucose metabolism. *Genes Dev.* **24,** 2784–2799 (2010).

67. Wells, L., Vosseller, K. & Hart, G. W. A role for N-acetylglucosamine as a nutrient sensor and mediator of insulin resistance. *Cell. Mol. Life Sci.* **60,** 222–8 (2003).

68. Sasai, K., Ikeda, Y., Fujii, T., Tsuda, T. & Taniguchi, N. UDP-GlcNAc concentration is an important factor in the biosynthesis of beta1,6-branched oligosaccharides: regulation based on the kinetic properties of N-acetylglucosaminyltransferase V. *Glycobiology* **12,** 119–127 (2002).

69. Freeze, H. H. & Elbein, A. D. *Glycosylation Precursors*. *Essentials of*

Glycobiology (2009).

70. Itkonen, H. M. *et al.* UAP1 is overexpressed in prostate cancer and is protective against inhibitors of N-linked glycosylation. *Oncogene* 1–7 (2014). doi:10.1038/onc.2014.307

71. Narimatsu, H. Human glycogene cloning: focus on beta 3-glycosyltransferase and beta 4-glycosyltransferase families. *Curr. Opin. Struct. Biol.* **16,** 567–75 (2006).

72. Granovsky, M. *et al.* Suppression of tumor growth and metastasis in Mgat5-deficient mice. *Nat. Med.* **6,** 306–312 (2000).

73. Li, D. *et al.* Knockdown of Mgat5 inhibits breast cancer cell growth with activation of CD4+ T cells and macrophages. *J. Immunol.* **180,** 3158–65 (2008).

74. Zhou, X., Chen, H., Wang, Q., Zhang, L. & Zhao, J. Knockdown of Mgat5 inhibits CD133+ human pulmonary adenocarcinoma cell growth in vitro and in vivo. *Clinical and investigative medicine. Médecine clinique et experimentale* **34,** E155–62 (2011).

75. Fernandes, B., Sagman, U., Auger, M., Demetrio, M. & Dennis, J. W. Beta 1-6 branched oligosaccharides as a marker of tumor progression in human breast and colon neoplasia. *Cancer Res.* **51,** 718–23 (1991).

76. Seelentag, W. K. F., Li, W., Schmitz, S. H. & Carcinoma, C. Prognostic Value of β 1 , 6-Branched Oligosaccharides in Human Colorectal Carcinoma. 5559–5564 (1998).

77. Murata, K. *et al.* Expression of N-acetylglucosaminyltransferase V in colorectal cancer correlates with metastasis and poor prognosis. *Clin. Cancer Res.* **6,** 1772–1777 (2000).

78. Sethi, M. K. *et al.* Comparative N-glycan profiling of colorectal cancer cell lines reveals unique bisecting GlcNAc and α-2,3-linked sialic acid determinants are associated with membrane proteins of the more metastatic/aggressive cell lines. *J. Proteome Res.* **13,** 277–88 (2014).

79. Bubka, M., Link-Lenczowski, P., Janik, M., Pocheć, E. & Lityńska, A. Overexpression of N-acetylglucosaminyltransferases III and V in human melanoma cells. Implications for MCAM N-glycosylation. *Biochimie* **103,** 37–49 (2014).

80. Song, Y., Aglipay, J. A., Bernstein, J. D., Goswami, S. & Stanley, P. The bisecting GlcNAc on N-glycans inhibits growth factor signaling and retards mammary tumor progression. *Cancer Res.* **70,** 3361–71 (2010).

81. Sengupta, P. K., Bouchie, M. P. & Kukuruzinska, M. a. N-glycosylation gene DPAGT1 is a target of the Wnt/??-catenin signaling pathway. *J. Biol. Chem.* **285,**

31164–31173 (2010).

82. Pocheć, E. *et al.* Expression of integrins α3β1 and α5β1 and GlcNAc β1,6 glycan branching influences metastatic melanoma cell migration on fibronectin. *Eur. J. Cell Biol.* **92,** 355–362 (2013).

83. McCarter, C. *et al.* Prediction of glycan motifs using quantitative analysis of multi-lectin binding: Motifs on MUC1 produced by cultured pancreatic cancer cells. *Proteomics. Clin. Appl.* **7,** 632–41 (2013).

84. Tang, H., Hsueh, P., Kletter, D., Bern, M. & Haab, B. in *Glycosylation and Cancer* **126,** 167–202 (2015).

85. Holst, S., Wuhrer, M. & Rombouts, Y. in *Advances in Cancer Research* **126,** 203–256 (2015).

86. Guo, H. & Abbott, K. L. Functional impact of tumor-specific N-linked glycan changes in breast and ovarian cancers. *Adv. Cancer Res.* **126,** 281–303 (2015).

87. Lemjabbar-Alaoui, H., McKinney, A., Yang, Y., Tran, V. & Phillips, J. Glycosylation alterations in lung and brain cancer. *Advances in Cancer Research* **126,** 305–344 (2015).

88. Mehta, A., Herrera, H. & Block, T. Glycosylation and liver cancer. *Adv. Cancer Res.* **126,** 257–79 (2015).

89. Drake, R. R., Jones, E. E., Powers, T. W. & Nyalwidhe, J. O. Altered glycosylation in prostate cancer. *Adv. Cancer Res.* **126,** 345–82 (2015).

90. Liwosz, A., Lei, T. & Kukuruzinska, M. a. N-Glycosylation affects the molecular organization and stability of e-cadherin junctions. *J. Biol. Chem.* **281,** 23138–23149 (2006).

91. Pinho, S. S. *et al.* Modulation of E-cadherin function and dysfunction by N-glycosylation. *Cell. Mol. Life Sci.* **68,** 1011–20 (2011).

92. Pinho, S. S. *et al.* Loss and recovery of Mgat3 and GnT-III mediated E-cadherin N-glycosylation is a mechanism involved in epithelial-Mesenchymal-Epithelial transitions. *PLoS One* **7,** 1–9 (2012).

93. Carvalho, S. *et al.* Preventing E-cadherin aberrant N-glycosylation at Asn-554 improves its critical function in gastric cancer. *Oncogene* 1–13 (2015). doi:10.1038/onc.2015.225

94. Zhou, F. *et al.* Unglycosylation at Asn-633 made extracellular domain of E-cadherin folded incorrectly and arrested in endoplasmic reticulum, then sequentially degraded by ERAD. *Glycoconj. J.* **25,** 727–40 (2008).

95. Pinho, S. S. *et al.* Role of E-cadherin N-glycosylation profile in a mammary tumor model. *Biochem. Biophys. Res. Commun.* **379,** 1091–1096 (2009).

96. Guo, H.-B., Lee, I., Kamar, M. & Pierce, M. N-Acetylglucosaminyltransferase V Expression Levels Regulate Cadherin-associated Homotypic Cell-Cell Adhesion and Intracellular Signaling Pathways. *J. Biol. Chem.* **278,** 52412–52424 (2003).

97. Guo, H. B., Johnson, H., Randolph, M. & Pierce, M. Regulation of homotypic cell-cell adhesion by branched N-glycosylation of N-cadherin extracellular EC2 and EC3 domains. *J. Biol. Chem.* **284,** 34986–34997 (2009).

98. Boscher, C. *et al.* Galectin-3 protein regulates mobility of N-cadherin and GM1 ganglioside at cell-cell junctions of mammary carcinoma cells. *J. Biol. Chem.* **287,** 32940–32952 (2012).

99. Lajoie, P. *et al.* Plasma membrane domain organization regulates EGFR signaling in tumor cells. *J. Cell Biol.* **179,** 341–356 (2007).

100. Partridge, E. a *et al.* Regulation of cytokine receptors by Golgi N-glycan processing and endocytosis. *Science* **306,** 120–124 (2004).

101. Gu, J. G., Isaji, T., Sato, Y., Kariya, Y. & Fukuda, T. Importance of N-Glycosylation on alpha 5 beta 1 Integrin for Its Biological Functions. *Biol. Pharm. Bull.* **32,** 780–785 (2009).

102. Yang, J. T., Rayburn, H. & Hynes, R. O. Embryonic mesodermal defects in alpha 5 integrin-deficient mice. *Development* **119,** 1093–1105 (1993).

103. Goh, K. L., Yang, J. T. & Hynes, R. O. Mesodermal defects and cranial neural crest apoptosis in alpha5 integrin-null embryos. *Development* **124,** 4309–4319 (1997).

104. George, E. L., Georges-Labouesse, E. N., Patel-King, R. S., Rayburn, H. & Hynes, R. O. Defects in mesoderm, neural tube and vascular development in mouse embryos lacking fibronectin. *Development* **119,** 1079–1091 (1993).

105. Sato, Y. *et al.* An N-glycosylation site on the beta-propeller domain of the integrin alpha5 subunit plays key roles in both its function and site-specific modification by beta1,4-N-acetylglucosaminyltransferase III. *J. Biol. Chem.* **284,** 11873–11881 (2009).

106. Isaji, T. *et al.* Introduction of Bisecting GlcNAc into Integrin??5?? 1 Reduces Ligand Binding and Down-regulates Cell Adhesion and Cell Migration. *J. Biol. Chem.* **279,** 19747–19754 (2004).

107. Isaji, T. *et al.* N-glycosylation of the β-propeller domain of the integrin α5 subunit is essential for α5β1 heterodimerization, expression on the cell surface, and its biological function. *J. Biol. Chem.* **281,** 33258–33267 (2006).

108. Nabi, I. R., Shankar, J. & Dennis, J. W. The galectin lattice at a glance. *J. Cell Sci.* (2015). doi:10.1242/jcs.151159

109. Lau, K. S. *et al.* Complex N-Glycan Number and Degree of Branching Cooperate to Regulate Cell Proliferation and Differentiation. *Cell* **129,** 123–134 (2007).

110. Kaszuba, K. *et al.* N-Glycosylation as determinant of epidermal growth factor receptor conformation in membranes. *Proc. Natl. Acad. Sci. U. S. A.* **112,** 2–7 (2015).

111. Kim, Y.-W., Park, J., Lee, H.-J., Lee, S.-Y. & Kim, S.-J. TGF-β sensitivity is determined by N-linked glycosylation of the type II TGF-β receptor. *Biochem. J.* **445,** 403–411 (2012).

112. Zhang, H. *et al.* Engagement of I-branching {beta}-1, 6-N-acetylglucosaminyltransferase 2 in breast cancer metastasis and TGF-{beta} signaling. *Cancer Res.* **71,** 4846–56 (2011).

113. Komekado, H., Yamamoto, H., Chiba, T. & Kikuchi, A. Glycosylation and palmitoylation of Wnt-3a are coupled to produce an active form of Wnt-3a. *Genes Cells* **12,** 521–34 (2007).

114. Anagnostou, S. H. & Shepherd, P. R. Glucose induces an autocrine activation of the Wnt/beta-catenin pathway in macrophage cell lines. *Biochem. J.* **416,** 211–8 (2008).

115. Miele, L. Notch signaling. *Science (80-.).* **12,** 225–232 (2006).

116. Kopan, R. & Ilagan, M. X. G. The Canonical Notch Signaling Pathway: Unfolding the Activation Mechanism. *Cell* **137,** 216–233 (2009).

117. Moloney, D. J. *et al.* Mammalian Notch1 is modified with two unusual forms of O-linked glycosylation found on epidermal growth factor-like modules. *J. Biol. Chem.* **275,** 9604–9611 (2000).

118. Shao, L. Fringe Modifies O-Fucose on Mouse Notch1 at Epidermal Growth Factor-like Repeats within the Ligand-binding Site and the Abruptex Region. *J. Biol. Chem.* **278,** 7775–7782 (2003).

119. Matsuura, A. *et al.* O-linked N-acetylglucosamine is present on the extracellular domain of notch receptors. *J. Biol. Chem.* **283,** 35486–35495 (2008).

120. Rana, N. A. *et al.* O-Glucose Trisaccharide Is Present at High but Variable Stoichiometry at Multiple Sites on Mouse Notch1. *J. Biol. Chem.* **286,** 31623–31637 (2011).

121. Polizio, A. H. *et al.* Heterotrimeric Gi Proteins Link Hedgehog Signaling to Activation of Rho Small GTPases to Promote Fibroblast Migration. *J. Biol. Chem.*

286, 19589–19596 (2011).

122. Marada, S. *et al.* Functional Divergence in the Role of N-Linked Glycosylation in Smoothened Signaling. *PLOS Genet.* **11,** e1005473 (2015).

123. Vigetti, D. *et al.* Hyaluronan: Biosynthesis and signaling. *Biochim. Biophys. Acta - Gen. Subj.* **1840,** 2452–2459 (2014).

124. Holmes, M. W., Bayliss, M. T. & Muir, H. Hyaluronic acid in human articular cartilage. Age-related changes in content and size. *Biochem. J.* **250,** 435–441 (1988).

125. Hascall, V. C. *et al.* The dynamic metabolism of hyaluronan regulates the cytosolic concentration of UDP-GlcNAc. *Matrix Biol.* **35,** 14–7 (2014).

126. Deen, A. J. *et al.* UDP-sugar substrates of HAS3 regulate its O-GlcNAcylation, intracellular traffic, extracellular shedding and correlate with melanoma progression. *Cell. Mol. Life Sci.* (2016). doi:10.1007/s00018-016-2158-5

127. Auvinen, P. *et al.* Hyaluronan in peritumoral stroma and malignant cells associates with breast cancer spreading and predicts survival. *Am. J. Pathol.* **156,** 529–36 (2000).

128. Auvinen, P. *et al.* Increased hyaluronan content and stromal cell CD44 associate with HER2 positivity and poor prognosis in human breast cancer. *Int. J. Cancer* **132,** 531–9 (2013).

129. Auvinen, P. *et al.* Hyaluronan synthases (HAS1-3) in stromal and malignant cells correlate with breast cancer grade and predict patient survival. *Breast Cancer Res. Treat.* **143,** 277–86 (2014).

130. Lipponen, P. *et al.* High stromal hyaluronan level is associated with poor differentiation and metastasis in prostate cancer. *Eur. J. Cancer* **37,** 849–56 (2001).

131. Aaltomaa, S. *et al.* Strong Stromal Hyaluronan Expression Is Associated with PSA Recurrence in Local Prostate Cancer. *Urol. Int.* **69,** 266–72 (2002).

132. Sá, V. K. de *et al.* Hyaluronidases and hyaluronan synthases expression is inversely correlated with malignancy in lung/bronchial pre-neoplastic and neoplastic lesions, affecting prognosis. *Brazilian J. Med. Biol. Res. = Rev. Bras. Pesqui. médicas e biológicas / Soc. Bras. Biofísica ... [et al.]* **48,** 1039–47 (2015).

133. Pirinen, R. *et al.* Versican in nonsmall cell lung cancer: relation to hyaluronan, clinicopathologic factors, and prognosis. *Hum. Pathol.* **36,** 44–50 (2005).

134. Cheng, X.-B., Sato, N., Kohi, S. & Yamaguchi, K. Prognostic impact of hyaluronan and its regulators in pancreatic ductal adenocarcinoma. *PLoS One* **8,** e80765 (2013).

135. Ropponen, K. *et al.* Tumor cell-associated hyaluronan as an unfavorable prognostic factor in colorectal cancer. *Cancer Res.* **58,** 342–7 (1998).

136. Anttila, M. A. *et al.* High levels of stromal hyaluronan predict poor disease outcome in epithelial ovarian cancer. *Cancer Res* **60,** 150–155 (2000).

137. Zoltan-Jones, A., Huang, L., Ghatak, S. & Toole, B. P. Elevated Hyaluronan Production Induces Mesenchymal and Transformed Properties in Epithelial Cells. *J. Biol. Chem.* **278,** 45801–45810 (2003).

138. Torres, C. R. & Hart, G. W. Topography and polypeptide distribution of terminal N-acetylglucosamine residues on the surfaces of intact lymphocytes. Evidence for O-linked GlcNAc. *J. Biol. Chem.* **259,** 3308–3317 (1984).

139. Slawson, C. & Hart, G. W. O-GlcNAc signalling: implications for cancer cell biology. *Nat. Rev. Cancer* **11,** 678–684 (2011).

140. Iyer, S. P. N. & Hart, G. W. Dynamic nuclear and cytoplasmic glycosylation: enzymes of O-GlcNAc cycling. *Biochemistry* **42,** 2493–9 (2003).

141. Champattanachai, V. *et al.* Proteomic analysis and abrogated expression of O-GlcNAcylated proteins associated with primary breast cancer. *Proteomics* **13,** 2088–2099 (2013).

142. Gu, Y. *et al.* GlcNAcylation plays an essential role in breast cancer metastasis. *Cancer Res.* **70,** 6344–6351 (2010).

143. Gu, Y. *et al.* O-GlcNAcylation is increased in prostate cancer tissues and enhances malignancy of prostate cancer cells. *Mol. Med. Rep.* **10,** 897–904 (2014).

144. Kamigaito, T. *et al.* Overexpression of O-GlcNAc by prostate cancer cells is significantly associated with poor prognosis of patients. *Prostate Cancer Prostatic Dis.* **17,** 18–22 (2014).

145. Lynch, T. P. *et al.* Critical role of O-Linked β-N-acetylglucosamine transferase in prostate cancer invasion, angiogenesis, and metastasis. *J. Biol. Chem.* **287,** 11070–81 (2012).

146. Mi, W. *et al.* O-GlcNAcylation is a novel regulator of lung and colon cancer malignancy. *Biochim. Biophys. Acta* **1812,** 514–9 (2011).

147. Ma, Z., Vocadlo, D. J. & Vosseller, K. Hyper-O-GlcNAcylation is anti-apoptotic and maintains constitutive NF-??B activity in pancreatic cancer cells. *J. Biol. Chem.* **288,** 15121–15130 (2013).

148. Zhu, Q. *et al.* O-GlcNAcylation plays a role in tumor recurrence of hepatocellular carcinoma following liver transplantation. *Med. Oncol.* **29,** 985–93 (2012).

149. Phueaouan, T. *et al.* Aberrant O-GlcNAc-modified proteins expressed in primary colorectal cancer. *Oncol. Rep.* **30,** 2929–36 (2013).

150. Yehezkel, G., Cohen, L., Kliger, A., Manor, E. & Khalaila, I. O-linked β-N-acetylglucosaminylation (O-GlcNAcylation) in primary and metastatic colorectal cancer clones and effect of N-acetyl-β-D-glucosaminidase silencing on cell phenotype and transcriptome. *J. Biol. Chem.* **287,** 28755–69 (2012).

151. Krześlak, A., Wójcik-Krowiranda, K., Forma, E., Bieńkiewicz, A. & Bryś, M. Expression of genes encoding for enzymes associated with O-GlcNAcylation in endometrial carcinomas: clinicopathologic correlations. *Ginekol. Pol.* **83,** 22–6 (2012).

152. Rozanski, W. *et al.* Prediction of bladder cancer based on urinary content of MGEA5 and OGT mRNA level. *Clin. Lab.* **58,** 579–83 (2012).

153. Zhou, B. P. *et al.* Dual regulation of Snail by GSK-3beta-mediated phosphorylation in control of epithelial-mesenchymal transition. *Nat. Cell Biol.* **6,** 931–40 (2004).

154. Xu, Y. *et al.* Role of CK1 in GSK3beta-mediated phosphorylation and degradation of snail. *Oncogene* **29,** 3124–33 (2010).

155. Park, S. Y. *et al.* Snail1 is stabilized by O-GlcNAc modification in hyperglycaemic condition. *EMBO J.* **29,** 3787–96 (2010).

156. Chou, T. Y., Dang, C. V & Hart, G. W. Glycosylation of the c-Myc transactivation domain. *Proc. Natl. Acad. Sci. U. S. A.* **92,** 4417–21 (1995).

157. Chou, T. Y., Hart, G. W. & Dang, C. V. c-Myc is glycosylated at threonine 58, a known phosphorylation site and a mutational hot spot in lymphomas. *J. Biol. Chem.* **270,** 18961–5 (1995).

158. Olivier-Van Stichelen, S. *et al.* O-GlcNAcylation stabilizes β-catenin through direct competition with phosphorylation at threonine 41. *FASEB J.* **28,** 3325–38 (2014).

159. Li, X. *et al.* O-linked N-acetylglucosamine modification on CCAAT enhancer-binding protein beta: role during adipocyte differentiation. *J. Biol. Chem.* **284,** 19248–54 (2009).

160. Yang, W. H. *et al.* Modification of p53 with O-linked N-acetylglucosamine regulates p53 activity and stability. *Nat. Cell Biol.* **8,** 1074–83 (2006).

161. Housley, M. P. *et al.* O-GlcNAc regulates FoxO activation in response to glucose. *J. Biol. Chem.* **283,** 16283–92 (2008).

162. Yang, W. H. *et al.* NFkappaB activation is associated with its O-GlcNAcylation

state under hyperglycemic conditions. *Proc. Natl. Acad. Sci. U. S. A.* **105,** 17345–50 (2008).

163. Allison, D. F. *et al.* Modification of RelA by O-linked N-acetylglucosamine links glucose metabolism to NF-κB acetylation and transcription. *Proc. Natl. Acad. Sci. U. S. A.* **109,** 16888–93 (2012).

164. Lee, K. E. & Bar-Sagi, D. Oncogenic KRas suppresses inflammation-associated senescence of pancreatic ductal cells. *Cancer Cell* **18,** 448–58 (2010).

165. Serrano, M., Lin, A. W., McCurrach, M. E., Beach, D. & Lowe, S. W. Oncogenic ras provokes premature cell senescence associated with accumulation of p53 and p16INK4a. *Cell* **88,** 593–602 (1997).

166. Lin, H.-K. *et al.* Skp2 targeting suppresses tumorigenesis by Arf-p53-independent cellular senescence. *Nature* **464,** 374–9 (2010).

167. Olivier-Van Stichelen, S. *et al.* Serum-stimulated cell cycle entry promotes ncOGT synthesis required for cyclin D expression. *Oncogenesis* **1,** e36 (2012).

168. Slawson, C. *et al.* Perturbations in O-linked β-N-acetylglucosamine protein modification cause severe defects in mitotic progression and cytokinesis. *J. Biol. Chem.* **280,** 32944–32956 (2005).

169. Zheng, X. *et al.* Epithelial-to-mesenchymal transition is dispensable for metastasis but induces chemoresistance in pancreatic cancer. *Nature* **527,** 525–530 (2015).

170. Fischer, K. R. *et al.* Epithelial-to-mesenchymal transition is not required for lung metastasis but contributes to chemoresistance. *Nature* **527,** 472–476 (2015).

171. Karachaliou, N. *et al.* KRAS mutations in lung cancer. *Clin. Lung Cancer* **14,** 205–14 (2013).

172. Kerr, E. M., Gaude, E., Turrell, F. K., Frezza, C. & Martins, C. P. Mutant Kras copy number defines metabolic reprogramming and therapeutic susceptibilities. *Nature* **531,** 110–3 (2016).

173. Davidson, S. M. *et al.* Environment Impacts the Metabolic Dependencies of Ras-Driven Non-Small Cell Lung Cancer. *Cell Metab.* **23,** 517–28 (2016).

174. Davis, F. M., Stewart, T. A., Thompson, E. W. & Monteith, G. R. Targeting EMT in cancer: opportunities for pharmacological intervention. *Trends Pharmacol. Sci.* **35,** 479–88 (2014).

175. Taparra, K., Tran, P. T. & Zachara, N. E. Hijacking the Hexosamine Biosynthetic Pathway to Promote EMT-Mediated Neoplastic Phenotypes. *Front. Oncol.* **6,** 85 (2016).

176. Cox, A. D., Fesik, S. W., Kimmelman, A. C., Luo, J. & Der, C. J. Drugging the undruggable RAS: Mission Possible? *Nat. Rev. Drug Discov.* **13,** 828–51 (2014).

177. Serrano, M., Lin, A. W., McCurrach, M. E., Beach, D. & Lowe, S. W. Oncogenic ras provokes premature cell senescence associated with accumulation of p53 and p16(INK4a). *Cell* **88,** 593–602 (1997).

178. Salama, R., Sadaie, M., Hoare, M. & Narita, M. Cellular senescence and its effector programs. *Genes Dev.* **28,** 99–114 (2014).

179. Burns, T. F. *et al.* Inhibition of TWIST1 leads to activation of oncogene-induced senescence in oncogene-driven non-small cell lung cancer. *Mol. Cancer Res.* **11,** 329–38 (2013).

180. Sato, M. *et al.* Human Lung Epithelial Cells Progressed to Malignancy through Specific Oncogenic Manipulations. *Mol. Cancer Res.* **11,** 638–650 (2013).

181. Ramirez, R. D. *et al.* Immortalization of human bronchial epithelial cells in the absence of viral oncoproteins. *Cancer Res.* **64,** 9027–34 (2004).

182. Tuveson, D. A. *et al.* Endogenous oncogenic K-ras(G12D) stimulates proliferation and widespread neoplastic and developmental defects. *Cancer Cell* **5,** 375–87 (2004).

183. Ryczko, M. C. *et al.* Metabolic Reprogramming by Hexosamine Biosynthetic and Golgi N-Glycan Branching Pathways. *Sci. Rep.* **6,** 23043 (2016).

184. Shafi, R. *et al.* The O-GlcNAc transferase gene resides on the X chromosome and is essential for embryonic stem cell viability and mouse ontogeny. *Proc. Natl. Acad. Sci.* **97,** 5735–5739 (2000).

185. Tran, P. T. *et al.* Combined Inactivation of MYC and K-Ras oncogenes reverses tumorigenesis in lung adenocarcinomas and lymphomas. *PLoS One* **3,** e2125 (2008).

186. Podsypanina, K., Politi, K., Beverly, L. J. & Varmus, H. E. Oncogene cooperation in tumor maintenance and tumor recurrence in mouse mammary tumors induced by Myc and mutant Kras. *Proc. Natl. Acad. Sci. U. S. A.* **105,** 5242–7 (2008).

187. Sinn, E. *et al.* Coexpression of MMTV/v-Ha-ras and MMTV/c-myc genes in transgenic mice: synergistic action of oncogenes in vivo. *Cell* **49,** 465–75 (1987).

188. Nardella, C., Clohessy, J. G., Alimonti, A. & Pandolfi, P. P. Pro-senescence therapy for cancer treatment. *Nat. Rev. Cancer* **11,** 503–511 (2011).

189. O'Donnell, N., Zachara, N. E., Hart, G. W. & Marth, J. D. Ogt-dependent X-chromosome-linked protein glycosylation is a requisite modification in somatic cell function and embryo viability. *Mol. Cell. Biol.* **24,** 1680–90 (2004).

190. Loew, R., Vigna, E., Lindemann, D., Naldini, L. & Bujard, H. Retroviral vectors containing Tet-controlled bidirectional transcription units for simultaneous regulation of two gene activities. *J Mol Genet Med* **2,** 107–118 (2006).

191. Fisher, G. H. *et al.* Induction and apoptotic regression of lung adenocarcinomas by regulation of a K-Ras transgene in the presence and absence of tumor suppressor genes. *Genes Dev.* **15,** 3249–62 (2001).

192. Perl, A.-K. T., Tichelaar, J. W. & Whitsett, J. a. Conditional gene expression in the respiratory epithelium of the mouse. *Transgenic Res.* **11,** 21–9 (2002).

193. Yang, Y. *et al.* Systematic calibration of an integrated x-ray and optical tomography system for preclinical radiation research. *Med. Phys.* **42,** 1710–20 (2015).

194. Simons, B. W. *et al.* A human prostatic bacterial isolate alters the prostatic microenvironment and accelerates prostate cancer progression. *J. Pathol.* **235,** 478–89 (2015).

195. Zhou, G. *et al.* Global comparison of gene expression profiles between intramuscular and subcutaneous adipocytes of neonatal landrace pig using microarray. *Meat Sci.* **86,** 440–50 (2010).

196. Carvalho, B. S. & Irizarry, R. A. A framework for oligonucleotide microarray preprocessing. *Bioinformatics* **26,** 2363–7 (2010).

197. Benjamini, Y., Drai, D., Elmer, G., Kafkafi, N. & Golani, I. Controlling the false discovery rate in behavior genetics research. *Behav. Brain Res.* **125,** 279–84 (2001).

198. Shiraishi, T. *et al.* Glycolysis is the primary bioenergetic pathway for cell motility and cytoskeletal remodeling in human prostate and breast cancer cells. *Oncotarget* **6,** 130–43 (2015).

Curriculum Vitae

Kekoa A. Taparra

ktaparra@jhmi.edu
Cell (808) 551-9401

Work Address
1550 Orleans St, Rm 416
Baltimore MD, 21231

Home Address
101 N. Wolfe St., Apt 363
Baltimore MD, 21231

EDUCATION:

Mayo Clinic College of Medicine - Mayo Medical School (Rochester, MN)
Class of 2020
M.D. Program

The Johns Hopkins University School of Medicine (Baltimore, MD)
Start *2012* **Graduated** *2016*
Cellular and Molecular Medicine Ph.D. Program
Thesis Advisor: Dr. Phuoc Tran M.D., Ph.D.
Department of Radiation Oncology & Molecular and Radiation Sciences
NIH NRSA F31 Pre-doctoral Training Fellow

Fairfield University (Fairfield, CT)
Summa Cum Laude, Valedictorian
Phi Beta Kappa
GPA: 3.93
Class of 2008
Major 1. Biology (Concentration: Cellular and Molecular Biology)
Major 2. Psychology (Concentration: Cognitive and Behavioral Neuroscience)
Minor 1. Asian Studies
Minor 2. Mathematics
Minor 3. Philosophy

The Kamehameha Schools (Honolulu, HI)
Class Rank: 16/442 Academic Honors Diploma GPA: 4.053 2004-2008
Schools' Mission: to create educational opportunities to improve the capability and well-being of Native Hawaiian people

PUBLICATIONS:

1. **Taparra K**, Tran PT, Zachara NE. Hijacking the Hexosamine Biosynthetic Pathway to Promote EMT-Mediated Neoplastic Phenotypes. ***Frontiers in Oncology*** 2016 Apr 18;6(85). PMID: 26980196
2. Chettiar ST, Malek R, Annadanam A, Nugent KM, Kato Y, Wang H, Cades JA, **Taparra K**, Belcaid Z, Ballew M, Manmiller S, Proia D, Lim M, Anders RA, Herman JM, Tran PT. Ganetespib radiosensitization for liver cancer therapy. ***Cancer Biology and Therapy*** 2016 Apr 2;17(4):457-66. PMID: 26980196
3. Gajula RP, Chettiar ST, Williams RD, Nugent K, Kato Y, Wang H, Malek R, **Taparra K**, Cades J, Annadanam A, Yoon AR, Fertig E, Firulli BA, Mazzacurati L, Burns TF, Firulli AB, An SS, Tran PT. Structure-function studies of the bHLH phosphorylation domain of TWIST1 in prostate cancer cells. ***Neoplasia*** 2015 Jan;17(1):16-31. PMID: 25622896
4. McDonald C, Muhlbauer J, Perlmutter G, **Taparra K**, Phelan SA. Peroxiredoxin proteins protect MCF-7 breast cancer cells from doxorubicin-induced toxicity. ***International Journal of Oncology*** 2014 Jul;45(1):219-26. PMID: 24789097
5. Tehan L, **Taparra K,** Phelan S. Peroxiredoxin overexpression in MCF-7 breast cancer cells and regulation by cell proliferation and oxidative stress. ***Cancer Investigation*** 2013 Jul;31(6):374-84. PMID: 23758190
6. Wild AT, Gandhi N, Chettiar ST, Aziz K, Gajula RP, Williams RD, Kumar R, **Taparra K**, Zeng J, Cades JA, Velarde E, Menon S, Geschwind JF, Cosgrove D, Pawlik TM, Maitra A, Wong J, Hales RK, Torbenson MS, Herman JM, Tran PT. Concurrent versus sequential sorafenib therapy in combination with radiation for hepatocellular carcinoma. ***PLoS ONE*** 2013 Jun 6;8(6). PMID: 23762417
7. Humphreys T, Sasaki A, Uenishi G, **Taparra K**, Arimoto A, Tagawa, K. Regeneration in the Hemichordate, *Ptychodera flava*. ***Zoological Science*** 2010 Feb;27(2):91-5. PMID: 20141413

BOOK CHAPTER REVIEWER

1. Freeze H, Schachter H, Kinoshita T. *Essentials of Glycobiology, Third Edition*. Chapter 45: Genetic Disorders of Glycosylation (Reviewer).

2. Hascall V, Esko JD. *Essentials of Glycobiology, Third Edition*. Chapter 16: Hyaluronan (Reviewer).

AWARDS & ACHIEVEMENTS:

2016 American Association for Cancer Research-Takeda Oncology Scholar in Training Award
2016 First Place Johns Hopkins Radiation Oncology and Molecular Radiation Sciences Scientific Presentation Award
2015 Johns Hopkins University, Hospital, and Health System Martin Luther King, Jr. Award for Community Service
2015 Thermo Pierce Biotechnology Fisher Scientific Scholarship Award
2015 American Association for Cancer Research Minority Scholar in Cancer Research Award
2015 Johns Hopkins Alumni Association Student Grant Awardee - Science Health and Research Partnership
2014 NIH Predoctoral Individual National Research Service Award (NRSA), Johns Hopkins University School of Medicine
2014 Cold Spring Harbor Models and Mechanisms of Cancer Graduate Student Travel Award
2014 National Cancer Institute CURE Scholar
2013 Selected Speaker at the Annual Johns Hopkins University Radiation Oncology Retreat
2012 Fairfield University Class of 2012 Academic Achievement Award for Excellence in Biology
2012 Fairfield University Class of 2012 Academic Achievement Award in Asian Studies
2009-2012 Fairfield University Magis Scholar (Highest Institution Academic Scholarship)
2012 Fairfield University *Cura Personalis* Mentor of the Year Award
2011 Gladys Brooks Prize Scholarship in Asian Studies
2009 Fairfield University Christopher Blake Love Minority Student Achievement Award
2008 Fairfield University Campus Heroes Project Award - Award for Demonstrating Excellence in Teamwork
2008 USA Swimming National Scholastic All American

DISTINGUISHED ACADEMIC SOCIETY HONORS & AFFILIATIONS:

American Association for Cancer Research (AACR) - Associate Member
American Association for the Advancement of Science (AAAS) - Excellence in Science program
Phi Beta Kappa Zeta Chapter of Connecticut National Honor Society Inductee - *Junior Inductee*
Sigma Xi The Scientific Research Society Inductee
Psi Chi International Honor Society in Psychology Inductee
Phi Sigma Tau International Honor Society in Philosophy Inductee
Alpha Sigma Nu National Jesuit Academic Honor Society

RESEARCH & WORK EXPERIENCE:

➢ ***Johns Hopkins University School of Medicine Cellular and Molecular Medicine***
(Baltimore, MD) *2012-2013*

- *Dr. Sara Sukumar Lab:* Cellular signaling in the tumor microenvironment; induction of angiogenesis in breast cancer
- *Dr. William Nelson:* Novel function, localization, and expression of the epigenetic Methyl Binding Domain 3 (MBD3),
- **Dr. Phuoc Tran*: Studied Epithelial-Mesenchymal Transition transcription factors TWIST1 and SNAI1 in both *in vitro* cell and *in vivo* autochthonous murine tumor model settings (*current laboratory for doctoral thesis)

➢ ***Millennium: The Takeda Oncology Company - Global Medical Affairs***
(Boston, MA) *Summer 2012*

- Analyzed and contributed edits to multiple publications for pharmaceutical scientists and physicians
- Worked with design team and physicians to create a more intuitive/artistic rendition of Orteronel (TAK-700) drug MOA

➢ ***Fairfield University - Cancer Biology Research, Dr. Shelley Phelan***
(Fairfield, CT) *Summer 2011-2012*

- Aim was to determine upstream effects of growth factors, MAP kinases, PKC, and H_2O_2 on Peroxiredoxin expression
- Researched breast cancer's relationship to Peroxiredoxin (PRDX) antioxidant gene family
- This research is important because oxidative stress is associated with cell death, cancer, and other degenerative diseases

➢ ***Fairfield University - Molecular Biology Research, Dr. Anita Fernandez***
(Fairfield, CT) *Fall 2010*

- Aim was to identify gene segment and sequence related to *Piwi-2*, *Beta-Catenin*, *Sine Oculus* in *Dugesia tigrina*
- Identified sequences for *β-catenin* and *Sine oculis* in *D. tigrina* by developing PCR primers

➢ ***University of Hawai'i Hilo - Life Sciences C. elegans Researcher***
(Hilo, HI) *Summer 2010*

- Researched protocol for inducing male *C. elegans* and gender differences related to heat shock proteins
- Worked with the United States Department of Agriculture to test medical compound on male cultures

➢ ***University of Hawai'i Mānoa - Biomedical Research Associate***
(Honolulu, HI) *Summer 2009*

- Worked under the mentorship of the late Dr. Tom Humphreys, School of Medicine Institute for Biogenesis Research
- Mapped hemichordate regeneration in *P. flava* in its application to chordate neurogenesis, POU domain, and stem cells
- Determined localized *PfSoxB1* gene expression in regenerating blastema tissue post decapitation

SELECT MEETING POSTERS/CONFERENCE TALKS:

Taparra K, Wang H, Nugent K, Malek R, Groves J, Yildirir G, Simons B, Nelkin B, Zachara B, Felsher D, Tran P. SNAI1 regulates the hexosamine biosynthesis pathway to promote tumorigenesis in lung cancer. In: Proceedings of the 107th Annual Meeting of the American Association for Cancer Research. April 2016; New Orleans, LA.

Taparra K, Wang H, Nugent K, Malek R, Groves J, Yildirir G, Simons B, Nelkin B, Zachara B, Tran P. SNAI1 Regulates the Hexosamine Biosynthesis Pathway in Lung Cancer. 7th Biennial TEMTIA Meeting 2015.

Taparra K, Wang H, Nugent K, Malek R, Cades J, Gajula R, Felsher D, Tran P. Snai1 accelerates $Kras^{g12d}$ driven lung tumorigenesis by overcoming oncogene-induced senescence. In: Proceedings of the 106th Annual Meeting of the American Association for Cancer Research. April 2015; Philadelphia, PA . Abstract no. 2291.

Taparra K, Wang H, Nugent K, Williams R, Malek R, Cades J, Gajula R, Felsher D, Tran P. Snai1 accelerates $Kras^{g12d}$ driven lung tumorigenesis by overcoming oncogene-induced senescence. In: Cold Spring Harbor Laboratory 9th Biennial Mechanisms & Models of Cancer. August 2014; Cold Spring Harbor, NY.

Taparra K, Wild AT, Bellovin DI, Williams RD, Gandhi N, Chettiar ST, Gajula RP, Cades JA, Herman JM, Felsher DW, Wang XW, Torbenson M, Tran PT**.** Modeling EMT-Induced Sorafenib Treatment Resistance in Liver Cancer. In: 2013 Sidney Kimmel Comprehensive Cancer Center Fellow Research Day. May 2013; Baltimore, MD.

McDonald C, Perlmutter G, **Taparra K**, Muhlbauer J, Passarelli J, Phelan SA. Function and regulation of peroxiredoxin proteins in doxorubicin-treated MCF-7 breast cancer cells. In: Proceedings of the 104th Annual Meeting of the American Association for Cancer Research. April 2013; Washington, D.C. Abstract no. 2908.

Taparra K, Nugent K, Aziz K, Ghandi N, Wang H, Williams R, Malek R, Cades J, Gajula R, Chettiar S, Hales R, Herman J, Felsher D, Tran P. SNAI1 Collaborates with Kras to Promote Accelerated Lung Tumorigenesis. In: 2014 Scientific Retreat of the Department of Radiation Oncology and Molecular Radiation Sciences. October 2013; Mt. Washington Conference Center, MD.

Taparra K, Tehan L, Rodriguez B, Phelan S. Overexpression of the peroxiredoxin family of antioxidant proteins in MCF7 breast cancer cells and investigation of possible regulatory mechanisms [abstract]. In: Proceedings of the 103rd Annual Meeting of the American Association for Cancer Research. April 2012; Chicago, IL. Abstract no. 2075.

GRANTS & RESEARCH SUPPORT:

NIH F31 Predoctoral Individual National Research Service Award
(Over 3 Years: **$128,028**) **2013-2016**

"Mechanisms of TWIST1-induced sorafenib resistance in liver cancer" Predoctoral Fellow

- Youngest PhD student in program 20 year history to receive F31 grant, First Native Hawaiian at Johns Hopkins School of Medicine
- Ruth L. Kirschstein NRSA for Individual Predoctoral Fellowships to Promote Diversity in Health-Related Research
- Received this F31 from the National Cancer Institute of the National Institutes of Health; Award Number F31CA189588.

American Association for Cancer Research-Takeda Oncology Scholar in Training Award
($1,500) 2016

- Selected by the AACR Awards committee, competing against over 1,200 applicants from around the world
- AACR Scholar-in-Training Awards are highly competitive and are presented to fewer than 10 percent of applicants
- "Recognizes outstanding young cancer investigators presenting meritorious papers at the AACR Annual Meeting"

American Association for Cancer Research MICR Minority Scholar in Cancer Research Award
($1,500) 2015

- Selected by AACR's Minorities in Cancer Research (MICR) Council to receive this Research Award
- Sponsored by the National Cancer Institute to support my attendance at the 2015 AACR Annual Meeting
- I competed against graduate students, medical students, residents, clinical/postdoctoral fellows, and junior faculty

Cold Spring Harbor Laboratory - National Cancer Institute Travel Award
(Travel Grant: **$150**) **2014**

"Snai1 accelerates Kras^{g12d} driven lung tumorigenesis by overcoming oncogene-induced senescence"

- This travel award was made possible by a NCI grant awarded to the Cold Spring Harbor Laboratory
- This grant provided financial assistance for graduate students in the life sciences to attend this CSHL conference

Johns Hopkins Alumni Association Grant for the Biomedical Scholars Association
(Grant: **$1,500**) **2014**

"A SHaRP Way to Engage Early Baltimore Biomedical Scholars"

- Selected for a competitive grant to provide interactive laboratories to underrepresented minority high school students
- Students in the MERIT program are prepared for their dreams of becoming biomedical researchers and physicians
- Grant was selected for "holding the most promise for enhancing academics, extracurricular activities, student life, and/or community involvement at JHU"

Fairfield University Magis Scholar - Highest Institutional Scholarship
(Scholarship: **$66,000** Grant: **$1,500**) **2009-2012**

"Overexpression of the Peroxiredoxin Family of Antioxidant Proteins in Breast Cancer"

- The grant portion of this scholarship allowed me to conduct summer research and provided financial assistance to attend the 103rd Annual Meeting of the American Association for Cancer Research (AACR) in April 2012 (Chicago, IL).

TEACHING EXPERIENCE:

➢ ***Peer Learning Group (PLG) Instructor at Fairfield University*** *(Fairfield, CT) 2010-2012*

- Prepared lessons for general biology (BI 171, 172) to complement weekly lectures conducted by biology faculty
- Mentored first year biology students, guiding them along their adjustment to college life

➢ ***Fairfield University Peer Tutoring Program Tutor*** *(Fairfield, CT) 2009 - 2012*

- Provided one-on-one tutoring sessions from Department of Academic and Disability Support Services
- Tutored Japanese 110, 111, 210, & 211 as well as Chemistry 11 &12

➢ ***Modern Languages Oral Practice Sessions Instructor*** *(Fairfield, CT) 2009 - 2010*

- Trained in and learned to implement the Dartmouth Method of language acquisition
- Prepared three weekly hour-long Japanese lessons to supplement material covered in JPN 110, 111, 210, & 211 courses

COMMUNITY SERVICE / VOLUNTEERING / EXTRACURRICULARS:

➢ ***American Association for Cancer Research (AACR) - Associate Member Council*** *(USA) 2015-2018*

- Selected among ~100 graduate and medical students, residents, clinical and postdoctoral fellows from across the world
- Advocates for and represents over 15,000 Associate Members of the AACR for a 3 year leadership position

➢ ***National Rally for Medical Research Hill Day and Early Career Scientist Hill Day*** *(Washington, D.C.) 2015-2016*

- Invited twice to Washington, D.C. to meet with United States Senators and Representatives to advocate future of NIH funding
- Advocated alongside survivors, scientists, and health care professionals to discuss the importance of biomedical research

➢ ***Volunteer at The Hackerman-Patz Patient and Family Pavilion at Johns Hopkins*** *(Baltimore, MD) 2014-2016*

- Volunteered at the Johns Hopkins Hospital Sidney Kimmel Comprehensive Cancer Center affiliated patient housing
- Provided hospitality and support to patients and families enhancing the Pavilion's welcoming, home-like environment
- Assisted with weekly programming including hosting, setting up, and cleaning up weekly dinners for cancer patients

➢ ***Johns Hopkins University Biomedical Scholars Association - Executive Board***
(Baltimore, MD) 2014-2016
- Served as the BSA Executive Board Community Service and Outreach Officer
- Director of the Science, Health, and Research Partnership (*SHaRP*) Initiative engaging high school biomedical scholars

➢ ***Medical Education Resources Initiative for Teens (MERIT) Mentoring Program***
(Baltimore, MD) 2014-2016
- Served on the 2015 MERIT Education Curriculum Development team as a biomedical content coordinator
- Assisted in developing biomedical curriculum and research experience for Baltimore County high school students

➢ ***Embajadores de Salud Volunteer***
(Baltimore, MD) Summer 2014
- Participated in weekly work out sessions with minority latino community members to promote health and well being
- Communicated with 15+ hispanic members of the community while training for 5K run despite having no Spanish language training

➢ ***The Maryland School for the Blind Outreach Volunteer***
(Baltimore, MD) 2012-2014
- Aided in arts and crafts with middle school to college level students with visual and/or hearing impairments
- Designed lessons to promote enhancement of tactile and auditory sensation in an engaging manner through the arts

➢ ***Mentoring at Fairfield University***
(Fairfield, CT) 2009-2012
- First Year Student Mentor (FYE Program), taught a formal class helping new students adjust to college life
- Mentored first year minority and first generation students as a *Cura Personalis* Mentor; Mentor of the Year Award

➢ ***Leader of Ignatian Solidarity Corps International Service and Immersion Program*** *(Kingston, Jamaica) 2011-2012*
- Missionaries of the Poor Bethlehem Center: Helped feed, bathe, and care for mentally and physically impaired children
- The Home for the Destitute and Dying: Worked at home for the elderly run by Mother Teresa's Missionaries of Charity
- Served as teachers' aide for Pre-Primary School/Health Clinic located in an economically poor area built on a city dump
- Selected to lead the 2011-2012 Ignatian Solidarity Corps International Service Trip to Kingston, Jamaica

➢ ***Ignatian Solidarity Corps International Service and Immersion Program***
(Punta Gorda & Delores, Belize) 2010-2011
- Participated in a 3 month program in preparation for service trip learning Belizian culture, politics, economics, etc.

- Filmed, directed, and edited a 30 minute documentary on the 2011 International Service Trip to Belize
- Built a Hurricane shelter, renovated an HIV/AIDS Children Center, engaged with locals, worked in Mayan village
- Lived in solidarity with Mayan villagers and presented English and Mathematics lessons at village elementary school

➢ ***Hui ʻOhana ʻO Hawaiʻi Founder and President***
(Fairfield, CT) 2010-2012
- Led an organization that welcomed members from all cultures to learn about the local and Native traditions of Hawaiʻi
- Worked with Hawaiian Tropic Sunscreen and Colleges Against Cancer to distribute hundreds of free sunscreen samples
- Organized a culturally authentic Lūʻau with hula lessons, authentic Hawaiʻi cuisine, and self-produced educational video

➢ ***Office of Residence Life - Resident Assistant***
(Fairfield, CT) 2010-2012
- Responsible for >200 sophomore college students and promoted healthy living with weekly yoga sessions, group morning jogs, etc.
- 2011 Residence Life Programer of the Year for planning numerous intellectually and socially engaging programs

➢ ***USA Swimming National Athlete Representative/State Athlete Representative***
(USA) 2006 - 2010
- Selected Nationally to represent the swimmer athletes on the Convention Education Committee for USA Swimming
- Planned, moderated, and led national convention sessions on technology safety, social media, sports energy drinks, etc.

➢ ***Fairfield University Rotaract Club***
(Fairfield, CT) 2010 - 2012
- Helped with the on campus blood drive in sponsorship with the American Red Cross
- Was involved with the Purple Pinky Project fundraiser to raise money to eradicate polio around the world

➢ ***Fairfield University Varsity Swimming and Diving Team***
(Fairfield, CT) 2008 - 2009
- Set 6 individual and 2 relay Fairfield University Program Records; MAAC Conference Swimmer of the Week
- Multiple Time Conference Championship Medalist, Won 19 out of 24 dual meet races